

DEVELOPING KINEMATIC SYNTHESIS SOFTWARE FOR LANDING GEAR
RETRACTION MOTION INVOLVING PLANAR AND SPATIAL
MECHANISMS

A THESIS SUBMITTED TO
THE GRADUATE SCHOOL OF NATURAL AND APPLIED SCIENCES
OF
MIDDLE EAST TECHNICAL UNIVERSITY

BY

ALİYE BİHTER VAROL

IN PARTIAL FULFILLMENT OF THE REQUIREMENTS
FOR
THE DEGREE OF MASTER OF SCIENCE
IN
MECHANICAL ENGINEERING

SEPTEMBER 2023

Approval of the thesis:

**DEVELOPING KINEMATIC SYNTHESIS SOFTWARE FOR LANDING
GEAR RETRACTION MOTION INVOLVING PLANAR AND SPATIAL
MECHANISMS**

submitted by **ALİYE BİHTER VAROL** in partial fulfillment of the requirements
for the degree of **Master of Science in Mechanical Engineering, Middle East
Technical University** by,

Prof. Dr. Halil Kalıpçılar
Dean, Graduate School of **Natural and Applied Sciences**

Prof. Dr. M. A. Sahir Arıkan
Head of the Department, **Mechanical Engineering**

Assoc. Prof. Dr. Ergin Tönük
Supervisor, **Mechanical Engineering, METU**

Examining Committee Members:

Assoc. Prof. Dr. Ulaş Yaman
Mechanical Engineering, METU

Assoc. Prof. Dr. Ergin Tönük
Mechanical Engineering, METU

Assoc. Prof. Dr. Mehmet Bülent Özer
Mechanical Engineering, METU

Assist. Prof. Dr. Hüseyin Enes Salman
Mechanical Engineering, TOBB ETU

Assoc. Prof. Dr. Kıvanç Azgın
Mechanical Engineering, METU

Date: 11.09.2023

I hereby declare that all information in this document has been obtained and presented in accordance with academic rules and ethical conduct. I also declare that, as required by these rules and conduct, I have fully cited and referenced all material and results that are not original to this work.

Name Last name: Aliye Bihter Varol

Signature:

ABSTRACT

DEVELOPING KINEMATIC SYNTHESIS SOFTWARE FOR LANDING GEAR RETRACTION MOTION INVOLVING PLANAR AND SPATIAL MECHANISMS

Varol, Aliye Bihter
Master of Science, Mechanical Engineering
Supervisor : Assoc. Prof. Dr. Ergin Tönük

September 2023, 123 pages

A computer program is developed for the kinematic synthesis of a landing gear retraction four-bar mechanism. The software incorporates a graphical user interface and generates various four-bar linkages that fulfill the required wheel position on the ground and in the bay, ensuring they fit within the available aircraft stowage volume. To accommodate configurations where retracting landing gear around a single axis is insufficient, the system introduces secondary motion, such as additional translation or rotation. For design cases necessitating wheel rotation, the program performs retraction involving motion in two planes. The computer software, integrated with Siemens NX, creates potential four-bar retraction mechanism linkages, allowing users to visualize the resulting mechanism and assess its design and manufacturability aspects.

Keywords: Mechanism Synthesis, Landing Gear Retraction, Spatial Mechanisms, Computer Aided Design Integration

ÖZ

DÜZLEMSEL VE UZAYSAL MEKANİZMALARI İÇEREN İNİŞ TAKIMI KATLANMA HAREKETİ İÇİN KİNEMATİK SENTEZ YAZILIMI GELİŞTİRİLMESİ

Varol, Aliye Bihter
Yüksek Lisans, Makina Mühendisliği
Tez Yöneticisi: Doç. Dr. Ergin Tönük

Eylül 2023, 123 sayfa

İniş takımı katlanma hareketini gerçekleştiren dört çubuk mekanizmasının kinematik sentezi için bir bilgisayar yazılımı geliştirilmiştir. Yazılım, bir kullanıcı arayüzü (GUI) içerir ve iniş takımının hem yerdeki hem bölmedeki gerekli tekerlek konumunu karşılayan çeşitli dört çubuk mekanizmaları oluşturarak bunların mevcut hava taşıtı depolama hacmine sığmasını sağlar. İniş takımlarının tek bir eksen etrafında katlanmasının yetersiz olduğu konfigürasyonlara uyum sağlamak için sistem, öteleme veya döndürme gibi ikincil hareketler sunar. Tekerlek dönüşünü gerektiren tasarım durumları için, program iki düzlemde hareket içeren katlanma gerçekleştirir. Siemens NX ile entegre edilen bilgisayar yazılımı, potansiyel dört çubuklu katlanma mekanizması bağlantıları oluşturarak kullanıcıların ortaya çıkan mekanizmayı görselleştirmesine, tasarım ve üretilebilirlik yönlerinin değerlendirmesine olanak tanır.

Anahtar Kelimeler: Mekanizma Sentezi, İniş Takımı Katlanması, Uzaysal Mekanizma, Bilgisayar Destekli Tasarım Entegrasyonu

To my pure serendipity

ACKNOWLEDGMENTS

First and foremost, I would like to express my gratitude to my thesis supervisor, Assoc. Prof. Dr. Ergin Tönük, for his guidance and unconditional support not only during this thesis project but throughout my career.

I am grateful to my parents and my brother, Sevgi, Ahmet, and Türker Günal, for providing me with everything I could have wished for, as well as to my extended family for their meritorious support and encouragement.

I would like to thank my wonderful colleagues in the landing gear system design team for their assistance, patience, and understanding throughout my journey.

Most of all, a heartfelt thank you to my outstanding spouse, Alperen Varol, for always taking me to the top with his love, comfort, and unwavering support. When we stand together, there is nothing we cannot overcome.

TABLE OF CONTENTS

| | |
|---|------|
| ABSTRACT..... | v |
| ÖZ..... | vi |
| ACKNOWLEDGMENTS | viii |
| TABLE OF CONTENTS..... | ix |
| LIST OF TABLES | xiii |
| LIST OF FIGURES | xvi |
| LIST OF ABBREVIATIONS..... | xx |
| LIST OF SYMBOLS | xxi |
| CHAPTERS | |
| 1 INTRODUCTION | 1 |
| 1.1 General Definition of a Landing Gear..... | 1 |
| 1.2 Landing Gear Main Parts | 1 |
| 1.3 Landing Gear Retraction Mechanisms | 2 |
| 1.4 Scope of This Study | 3 |
| 2 LITERATURE REVIEW | 5 |
| 3 THEORY AND FORMULATION..... | 9 |
| 3.1 General | 9 |
| 3.1.1 Degree of Freedom of Space, Kinematic Pairs | 9 |
| 3.1.2 Reference Frame Definition..... | 10 |
| 3.1.3 Representation of a Vector in a Selected Reference Frame..... | 12 |
| 3.1.4 Denavit–Hartenberg’s Convention | 13 |
| 3.1.5 Relative Positioning of Consecutive Links..... | 14 |

| | | |
|---------|---|----|
| 3.1.6 | Loop Closure Equations | 15 |
| 3.1.7 | Path Generation Synthesis | 17 |
| 3.2 | Landing Gear Retraction Mechanism Synthesis Tasks | 18 |
| 3.2.1 | Reference Frame Assignment..... | 18 |
| 4 | LANDING GEAR MECHANISMS INVOLVING PLANAR MOTION | 21 |
| 4.1 | The Constrained RRCR Mechanism..... | 21 |
| 4.1.1 | Degree of Freedom of the Constrained RRCR Mechanism | 21 |
| 4.1.2 | General Displacement Equation | 22 |
| 4.1.2.1 | Numerical Example | 26 |
| 4.1.3 | Path Generation Synthesis of the Constrained RRCR Mechanism ... | 28 |
| 4.1.3.1 | Prescribed Orientations of Fixed Joints | 33 |
| 4.1.3.2 | Unprescribed Positions of the Ground Pivots..... | 35 |
| 4.2 | The RRRR Mechanism with Shock Absorber as the Output Link..... | 39 |
| 4.2.1 | Degree of Freedom | 39 |
| 4.2.2 | General Displacement Equation | 39 |
| 4.2.2.1 | Numerical Example | 46 |
| 4.2.3 | Path Generation Synthesis of the RRRR Mechanism with Shock Absorber as the Output Link | 47 |
| 4.2.3.1 | Prescribed Orientations of Fixed Joints | 52 |
| 4.2.3.2 | Unprescribed Positions of the Ground Pivots..... | 54 |
| 5 | LANDING GEAR MECHANISMS INVOLVING SPATIAL MOTION | 59 |
| 5.1 | The SSRR Mechanism..... | 59 |
| 5.1.1 | Degree of Freedom of the Constrained SSRR Mechanism | 59 |
| 5.1.2 | General Displacement Equation | 60 |
| 5.1.2.1 | Numerical Example | 65 |

| | | |
|---------|---|-----|
| 5.1.3 | Path Generation Synthesis of the SSRR Mechanism..... | 67 |
| 5.1.3.1 | Prescribed Orientations of Fixed Joints | 73 |
| 5.1.3.2 | Unprescribed Positions of the Ground Pivots | 76 |
| 6 | LANDING GEAR RETRACTION MECHANISM DESIGN COMPUTER PROGRAM AND PARAMETRIC MASTER GEOMETRY MODELS | 81 |
| 6.1 | Program Interface | 82 |
| 6.2 | NX Models and Journal Running..... | 84 |
| 7 | RESULTS AND DISCUSSION | 87 |
| 7.1 | Numerical Examples for the Landing Gear Retraction Mechanism Synthesis Tasks | 88 |
| 7.1.1 | Constrained RRCR (RRPR) Mechanism Synthesis Tasks | 88 |
| 7.1.1.1 | RRPR Mechanism Synthesis with Prescribed Positions of the Fixed Joints | 89 |
| 7.1.1.2 | RRPR Mechanism Synthesis with Unprescribed Positions of the Fixed Joints | 92 |
| 7.1.2 | RRRR Mechanism Synthesis Task | 94 |
| 7.1.2.1 | RRRR Mechanism Synthesis with Prescribed Positions of the Fixed Joints | 96 |
| 7.1.2.2 | RRRR Mechanism Synthesis with Unprescribed Positions of the Ground Pivots | 99 |
| 7.1.3 | SSRR Mechanism Synthesis Task | 102 |
| 7.1.3.1 | SSRR Mechanism Synthesis with Prescribed Positions of the Fixed Joints | 103 |
| 7.1.3.2 | SSRR Mechanism Synthesis with Unprescribed Positions of the Ground Pivots | 106 |

| | | |
|-----|---|-----|
| 7.2 | Model Verification Test Case: SSRR Mechanism Synthesis with Prescribed Positions of the Fixed Joints..... | 108 |
| 7.3 | Discussion on Free Parameter Choices..... | 112 |
| 8 | CONCLUSION | 113 |
| | REFERENCES | 117 |
| | APPENDICES | 121 |
| | NX Journal for Expression Integration on CAD Model..... | 121 |

LIST OF TABLES

TABLES

| | |
|--|----|
| Table 3.1 Some Kinematic Pairs with Independent Rotational and Translational Motion [21], [22] | 10 |
| Table 3.2 Link Parameters based on Denavit – Hartenberg’s Convention | 14 |
| Table 4.1 Point Coordinates at Extended Position..... | 26 |
| Table 4.2 Components of Position Vectors V and W | 29 |
| Table 4.3 Components of Equation (4-43) for the Initial Position P_0 | 31 |
| Table 4.4 Components of Equation (4-45) for the Initial Position P_0 | 31 |
| Table 4.5 Components of Equation (4-43) for the In-Between Position P_1 | 31 |
| Table 4.6 Components of Equation (4-45) for the In-Between Position P_1 | 32 |
| Table 4.7 Components of Equation (4-43) for the Final Position P_2 | 32 |
| Table 4.8 Components of Equation (4-45) for the Final Position P_2 | 32 |
| Table 4.9 The Number of Unknown Parameters and Free Parameters for the Three Positions of RRPR (Constrained RRCR) Mechanism, for the Synthesis Task When Orientations of Fixed Joints are Prescribed | 33 |
| Table 4.10 Equation Set to be Used for the RRPR (Constrained RRCR) Mechanism Synthesis Task When Orientations of Fixed Joints are Prescribed..... | 33 |
| Table 4.11 Components of Equation (4-66)..... | 36 |
| Table 4.12 The Number of Unknown Parameters and Free Parameters for The Three Positions of RRPR (Constrained RRCR) Mechanism, for the Synthesis Task When Orientations of Fixed Joints are Unprescribed..... | 36 |
| Table 4.13 Equation Set to be Used for The RRPR (Constrained RRCR) Mechanism Synthesis Task When Orientations of Fixed Joints are Unprescribed | 37 |
| Table 4.14 Point Coordinates at Extended Position..... | 46 |
| Table 4.15 Components of Equation (4-107) for the Initial Position P_0 | 49 |
| Table 4.16 Components of Equation (4-107) for the In-Between Position P_1 | 50 |
| Table 4.17 Components of Equation (4-107) for the Final Position P_2 | 51 |

| | |
|---|----|
| Table 4.18 The Number of Unknown Parameters and Free Parameters for the Three Positions of RRRR Mechanism with Shock Absorber as the Output Link, for the Synthesis Task When Orientations of Fixed Joints are Prescribed | 52 |
| Table 4.19 Equation Set to be Used for the RRRR Mechanism (with Shock Absorber as the Output Link) Synthesis Task When Orientations of Fixed Joints are Prescribed | 53 |
| Table 4.20 The Number of Unknown Parameters and Free Parameters for the Three Positions of RRRR Mechanism with Shock Absorber as the Output Link, for the Synthesis Task When Orientations of Fixed Joints are Unprescribed | 56 |
| Table 4.21 Equation Set to be Used for the RRRR Mechanism (with Shock Absorber as the Output Link) Synthesis Task When Orientations of Fixed Joints are Unprescribed..... | 56 |
| Table 5.1 Point Coordinates at Extended Position | 65 |
| Table 5.2 Components of Position Vectors V and W | 68 |
| Table 5.3 Components of Equation (5-42) for the Initial Position P_0 | 70 |
| Table 5.4 Components of Equation (5-44) for the Initial Position P_0 | 70 |
| Table 5.5 Components of Equation (5-42) for the In-Between Position P_1 | 71 |
| Table 5.6 Components of Equation (5-44) for the In-Between Position P_1 | 71 |
| Table 5.7 Components of Equation (5-42) for the Final Position P_2 | 72 |
| Table 5.8 Components of Equation (5-44) for the Final Position P_2 | 72 |
| Table 5.9 The Number of Unknown Parameters and Free Parameters for the Three Positions of SSRR Mechanism with Shock Absorber as the Output Link, for the Synthesis Task When Orientations of Fixed Joints are Prescribed | 73 |
| Table 5.10 Equation Set to be Used for the SSRR Mechanism (with Shock Absorber as the Output Link) Synthesis Task When Orientations of Fixed Joints are Prescribed | 74 |
| Table 5.11 The Number of Unknown Parameters and Free Parameters for the Three Positions of SSRR Mechanism with Shock Absorber as the Output Link, for the Synthesis Task When Orientations of Fixed Joints are Unprescribed | 77 |

| | |
|--|-----|
| Table 5.12 Equation Set to be Used for the SSRR Mechanism (with Shock Absorber as the Output Link) Synthesis Task When Orientations of Fixed Joints are Unprescribed | 78 |
| Table 7.1 Synthesis Tasks and Their Corresponding Design Conditions..... | 87 |
| Table 7.2 Free Parameter Classification for the Three-Position Synthesis | 112 |

LIST OF FIGURES

FIGURES

| | |
|---|----|
| Figure 1.1. Common Landing Gear Retraction Mechanisms [3] | 3 |
| Figure 3.1. Reference Frame Representation | 11 |
| Figure 3.2. Circle Rule and Cross – Products | 11 |
| Figure 3.3. Reference Frame Installation According to Denavit-Hartenberg’s Convention | 13 |
| Figure 3.4 Path Tracer Point and Vector Installation According to D-H Convention | 17 |
| Figure 3.5. Earth Frame and Global Reference Frame Allocation..... | 19 |
| Figure 4.1. RRPR (Constrained RRCR) Linkage Landing Gear Hardpoint Definitions [26] | 21 |
| Figure 4.2. Isometric View of RRPR Mechanism..... | 23 |
| Figure 4.3. Required Actuator Length with-respect-to the Change of Landing Gear Position..... | 27 |
| Figure 4.4. Isometric View of RRPR Mechanism for Path Generation | 28 |
| Figure 4.5. Landing Gear Hardpoint Definitions for RRRR Linkage with Shock Absorber as the Output Link [26]..... | 39 |
| Figure 4.6. Isometric View of RRRR Mechanism with Shock Absorber as the Output Link..... | 40 |
| Figure 4.7. Angle Definitions of the RRRR Linkage with Shock Absorber as the Output Link | 41 |
| Figure 4.8. The Correlation of Input angle θ_1 with Output Angle θ_4 | 46 |
| Figure 4.9. Isometric View of RRRR Mechanism with S/A as the Output Link for Path Generation | 47 |
| Figure 4.10. Side View of The Mechanism at Extended Dead Center Position | 49 |
| Figure 4.11. Side View of The Mechanism at Folded Dead Center Position | 51 |
| Figure 5.1. SSRR Linkage Landing Gear Hardpoint Definitions [3]..... | 59 |
| Figure 5.2. Isometric View of SSRR Mechanism with the Shock Absorber as the Output Link | 60 |

| | |
|--|----|
| Figure 5.3. Joint Angle and Axis Definitions for the SSRR Mechanism | 61 |
| Figure 5.4. The Correlation Between Output Angle θ_1 and Swing Angle θ_2 | 65 |
| Figure 5.5. Mobility Classification for five types of RRSS Linkages [28] (a) Crank- Rocker, (b) Rocker-Crank, (c) Grashof Double Rocker, (d) Non-Grashof Double Rocker, (e) Double Crank | 66 |
| Figure 5.6. Isometric View of SSRR Mechanism with S/A as the Output Link for Path Generation..... | 67 |
| Figure 6.1. Mechanism Synthesis and Design Process..... | 81 |
| Figure 6.2. Graphical User Interface..... | 82 |
| Figure 6.3. Steps to be Followed on the GUI | 83 |
| Figure 6.4. Helicopter CAD Model with SSRR Mechanism, Side View | 84 |
| Figure 6.5. Helicopter CAD Model with RRPR Mechanism, Front View | 85 |
| Figure 6.6. Developer Tab on NX 1855 Ribbon..... | 85 |
| Figure 6.7. Journal Manager on NX 1855 | 86 |
| Figure 6.8. Journal Editor | 86 |
| Figure 7.1. RRPR Mechanism Parametric CAD Model | 88 |
| Figure 7.2. Parameter definitions for the RRPR Synthesis Tasks | 89 |
| Figure 7.3. User Inputs and Solver Outputs for the RRPR Synthesis Task with Prescribed Ground Pivots | 90 |
| Figure 7.4. Expression File Parameters for the RRPR Synthesis Task with Prescribed Ground Pivots | 91 |
| Figure 7.5. Resulting CAD Model at the Three Positions for RRPR Synthesis Task with Prescribed Ground Pivots | 91 |
| Figure 7.6. User Inputs and Solver Outputs for the RRPR Synthesis Task with Unprescribed Ground Pivots..... | 92 |
| Figure 7.7. Expression File Parameters for the RRPR Synthesis Task with Unprescribed Ground Pivots..... | 93 |
| Figure 7.8. Resulting CAD Model at the Three Positions for RRPR Synthesis Task with Unprescribed Ground Pivots..... | 93 |

| | |
|---|-----|
| Figure 7.9. RRRR Mechanism Parametric CAD Model for the Synthesis Task with Prescribed Ground Pivots | 94 |
| Figure 7.10. RRRR Mechanism Parametric CAD Model for the Synthesis Task with Unprescribed Ground Pivots | 95 |
| Figure 7.11. Parameter definitions for the RRRR Synthesis Task with Prescribed Ground Pivots | 96 |
| Figure 7.12. User Inputs and Solver Outputs for the RRRR Synthesis Task with Prescribed Ground Pivots | 97 |
| Figure 7.13. Expression File Parameters for the RRRR Synthesis Task with Prescribed Ground Pivots | 98 |
| Figure 7.14. Resulting CAD Model at the Three Positions for RRRR Synthesis Task with Prescribed Ground Pivots | 98 |
| Figure 7.15. Parameter definitions for the RRRR Synthesis Task with Unprescribed Ground Pivots | 99 |
| Figure 7.16. User Inputs and Solver Outputs for the RRRR Synthesis Task with Unprescribed Ground Pivots | 100 |
| Figure 7.17. Expression File Parameters for the RRRR Synthesis Task with Unprescribed Ground Pivots | 101 |
| Figure 7.18. Resulting CAD Model at the Three Positions for RRRR Synthesis Task with Unprescribed Ground Pivots | 101 |
| Figure 7.19. SSRR Mechanism Parametric CAD Model | 102 |
| Figure 7.20. Parameter definitions for the SSRR Synthesis Tasks | 103 |
| Figure 7.21. User Inputs and Solver Outputs for the SSRR Synthesis Task with Prescribed Ground Pivots | 104 |
| Figure 7.22. Expression File Parameters for the SSRR Synthesis Task with Prescribed Ground Pivots | 105 |
| Figure 7.23. Resulting CAD Model at Three Positions for SSRR Synthesis Task with Prescribed Ground Pivots | 105 |
| Figure 7.24. User Inputs and Solver Outputs for the SSRR Synthesis Task with Unprescribed Ground Pivots | 106 |

| | |
|---|-----|
| Figure 7.25. Expression File Parameters for the SSRR Synthesis Task with Prescribed Ground Pivots | 107 |
| Figure 7.26. Resulting CAD Model at Three Positions for SSRR Synthesis Task with Unprescribed Ground Pivots, Front View | 107 |
| Figure 7.27. NX Motion Model, Motion Body Definitions..... | 108 |
| Figure 7.28. Swept Volume (Motion Envelope) Generated by NX Motion..... | 109 |
| Figure 7.29. θ_2 with respect to θ_1 Graph, Plotted by NX Motion XY Result View | 110 |
| Figure 7.30. θ_7 with respect to θ_1 Graph, Plotted by NX Motion XY Result View | 110 |
| Figure 7.31. θ_8 with respect to θ_1 Graph, Plotted by NX Motion XY Result View | 111 |

LIST OF ABBREVIATIONS

ABBREVIATIONS

| | |
|------|---------------------------------------|
| 3D | Three Dimensional |
| ARP | Aerospace Recommended Practice |
| AW | AgustaWestland |
| C | Cylindrical |
| CAD | Computer Aided Design |
| D-H | Denavit-Hartenberg's |
| DOF | Degree of Freedom |
| EASA | European Union Aviation Safety Agency |
| GUI | Graphical User Interface |
| jv | Joint Variable |
| LG | Landing Gear |
| LMLG | Left Main Landing Gear |
| MLG | Main Landing Gear |
| N/A | Not Applicable |
| P | Prismatic |
| R | Revolute |
| RMLG | Right Main Landing Gear |
| S | Spherical |
| S/A | Shock Absorber |
| SAE | Society of Automotive Engineers |

LIST OF SYMBOLS

SYMBOLS

| | |
|---------------------|---|
| O_k | The k^{th} origin |
| F_k | Reference frame based on origin O_k |
| U_k | Basis vector triad of Frame F_k |
| $\vec{u}_i^{(k)}$ | Basis vector, $i=1,2,3$ |
| \bar{u}_i | The i^{th} basic column matrix |
| $\bar{u}_i^{(k/k)}$ | The i^{th} basic column matrix of frame F_k represented in its own frame F_k |
| δ_{ij} | Kronecker delta function of indices i and j |
| \vec{r} | Vector |
| $\bar{r}^{(k)}$ | Column matrix representation of vector \vec{r} |
| $r_i^{(k)}$ | The i^{th} component of \vec{r} in the direction of basis vector $\vec{u}_i^{(k)}$ |
| L_k | The k^{th} link |
| J_k | The joint that connects link L_k to L_{k-1} |
| $\vec{u}_3^{(k)}$ | Axis of the joint J_k |
| $\vec{u}_1^{(k)}$ | Common normal N_k between axes of J_k and J_{k+1} |
| $\vec{u}_2^{(k)}$ | $\vec{u}_2^{(k)} = \vec{u}_3^{(k)} \times \vec{u}_1^{(k)}$ |
| O_k | Origin located at the intersection of N_k with J_k |
| B_k | Auxiliary point, intersection of N_k with J_{k+1} |
| β_k | Twist angle between J_{k-1} and J_k about N_{k-1} |
| θ_k | Rotation angle between N_{k-1} and N_k about J_k |
| δ_k | Deflection angle |
| s_k | Offset between N_{k-1} and N_k along J_k |
| b_k | Effective link length of L_k between J_k and J_{k+1} along N_k |
| $\hat{C}^{(k-1,k)}$ | Transformation matrix of $k-1^{\text{th}}$ reference frame to k^{th} reference frame |

| | |
|-----------------|---|
| N | Number of links of a mechanism |
| $\#$ | Number |
| P_i | i^{th} Precision point |
| \vec{U} | Vector directed from the origin of the proximal joint to the auxiliary point on the distal joint |
| \vec{V} | Vector directed from the origin of the proximal joint to the tracer point |
| \vec{W} | Vector directed from the origin of the tracer point to the auxiliary point on the distal one |
| \vec{R} | Vectors that originate from the origin of global frame towards the precision points |
| F | DOF |
| λ_s | Degree of freedom of space |
| n | Number of links including the fixed link |
| j | Number of joints in the mechanism |
| f_k | Number of freedoms for k^{th} joint |
| γ_i | Crank rotation at the i^{th} position |
| μ_i | Transmission angle at the i^{th} position |
| α | Angle between the projected line connecting the two ends of the stationary link and the output link |
| ϕ | Crank rotation |
| ψ | Swing angle |
| λ | Ratio of coupler link to the crank length |
| λ_{opt} | Optimum coupler-to-crank ratio |

CHAPTER 1

INTRODUCTION

1.1 General Definition of a Landing Gear

The landing gear of a helicopter is a critical component, serving as a complex and dynamic interface between the aircraft and the terrain during takeoff, landing, and ground operations. The importance of landing gear design lies in its role in ensuring overall safety, performance, and functionality by distributing the aircraft's weight effectively, absorbing kinetic energy upon touchdown to prevent structural damage, and providing controlled damping of vibrations. Furthermore, the design must ensure the helicopter's intended mission profile, whether it be civilian transport, military operations, or specialized tasks like search and rescue.

Landing gear systems for helicopters are mainly of two types: skid type and wheel type, each designed to fulfill specific operational requirements. This study focuses on the retraction motion of wheel type landing gears whereas skid type landing gear, being non-retractable, is not within the scope.

1.2 Landing Gear Main Parts

Main parts of a wheel type landing gear system used in this study includes: structural attachment, shock absorber, piston, axle, brake, wheel, tire, toggle link, drag stay and retraction / extension actuators [1]. The structural attachment, alternatively named as trunnion or barrel, is the connecting part between the helicopter fuselage and the landing gear. The shock absorber incorporates a piston and a cylinder, whose cylinder is on the barrel side and piston is connected to the wheel axle. In this study,

torque links (toggle links) and the brakes are not included in the system for the sake of simplifying the CAD models. The wheel and tire are taken as a simplified assembly. The retraction / extension mechanisms are located between the fuselage and the shock absorber. Drag stay (drag beam) is a strut that is incorporated into the system when excessive drag loads are seen. If the Landing Gear is retractable, in many cases the retraction actuator itself will also do the function of drag stay [2].

1.3 Landing Gear Retraction Mechanisms

The meticulous design and functionality of landing gear retraction mechanisms contribute profoundly to the overall performance and mission capabilities of helicopters. The importance of these mechanisms lies in their role in reducing drag and improving aerodynamic efficiency during flight. The retraction mechanism enables helicopters to transition from takeoff and landing configurations to in-flight, where reduced drag leads to decreased fuel consumption and enhanced maneuverability. While design, considerations of weight, structural integrity, and ease of maintenance are primary factors that must be optimized to provide effective gear retraction operations.

The majority of landing gear retraction mechanisms solutions are derived from four bar linkages. Most of the mechanisms employed in helicopters are planar type by motion involving only one plane but as a necessity from structural design, have offsets in three dimensions between joint locations. The straightforward variations of the common four bar type retraction mechanisms are given in Figure 1.1. Mechanism A, actuated directly by the jack, has a single hinge connected to the fuselage and is often used for the smaller retraction bays. Resembling mechanism A, mechanism B is the most common type of main landing gear retraction system for helicopters with cantilevered landing gear. Mechanisms C and D behave similarly to mechanism B, with an advantage in maintaining up-lock and down-locked positions of the landing gear without a complicated locking system. Mechanism E provides retraction involving two planes by placing rotation axes in a skew configuration,

whereas mechanism F provides similar motion by involvement of a radius link into mechanism [3]. In this study, types B and C, RRPR and RRRR mechanisms respectively, are selected as planar mechanisms, whereas type F, the SSRR mechanism is chosen as the spatial mechanism.

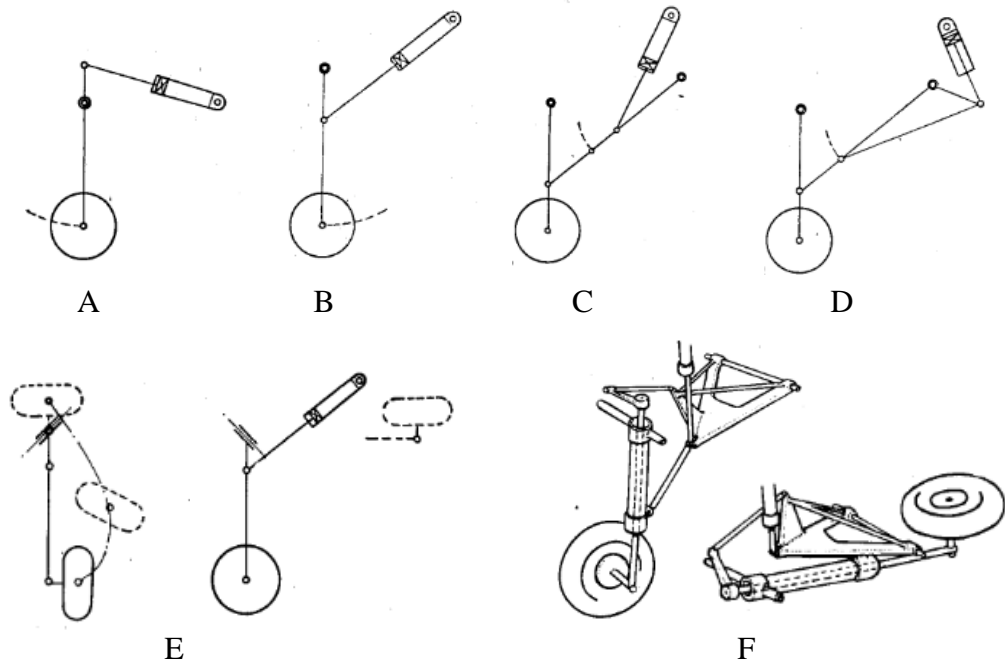


Figure 1.1. Common Landing Gear Retraction Mechanisms [3]

Smaller helicopters, like light utility or training models, often utilize planar retraction for its design simplicity and reliability. In contrast, larger and more advanced helicopters, where aerodynamic performance is critical, may opt for spatial retraction to achieve better performance. The spatial retraction system allows more flexibility in the placement and configuration of the landing gear.

1.4 Scope of This Study

The objective of this study is to develop a user-friendly tool to synthesize and visualize helicopter landing gear retraction mechanisms that fulfill the required wheel position on the ground and in the bay.

The initial step of the project is to create a MATLAB-based user interface tailored for the synthesis of landing gear retraction mechanisms. This interface takes separate positions of the landing gear and generates an expression file including design parameters for the CAD models.

The development process of kinematic synthesis software for landing gear retraction motion introduced in this study starts with the selection of the linkage type amongst the RRPR, RRRR, and SSRR options. Then, based on the design and operational needs, the type of kinematic synthesis task is determined regarding whether the ground pivots are prescribed or not. In cases where the connection of the retraction mechanism to the fuselage is pre-determined by the fuselage designers, mechanism synthesis with prescribed ground pivots is required. If the position of the ground pivot between the retraction mechanism and the fuselage is provided as a free parameter, opportunities to improve the performance of the landing gear retraction mechanism, such as minimizing the deviation of the transmission angle from 90° , are introduced to the system. Using Denavit-Hartenberg's convention and the rotational matrices to define loop closure equations and the relative positioning of the consecutive links, equation sets for the path generation synthesis tasks are constructed. These equations are used to develop a solver that utilizes inputs provided from the user interface and outputs the calculated parameters and joint variables on the same user interface screen and to the expression file.

The expression files are integrated with Siemens NX to automatically update CAD models based on user inputs. The user can visualize and evaluate the results and rapidly incorporate the changes into the overall helicopter model.

This study streamlines the design process, improves efficiency, and enhances the accuracy of landing gear design by developing a user interface for landing gear retraction mechanism synthesis, integrating it with the CAD environment, and enabling numerous design iterations with minimum effort.

CHAPTER 2

LITERATURE REVIEW

Unlike many military helicopters that feature non-retractable landing gear to facilitate emergency landings on uneven terrains, utility helicopters often employ retractable landing gear to minimize drag and fuel consumption. The design of these retractable mechanisms, however, is constrained by the specific wheel positions required in both extended and retracted states and the available stowage volume in the bay.

Historically, until the 1950s, various solutions for landing gear retraction mechanisms have been categorized and documented [3]. These solutions include fundamental mechanisms, practical geometries, linkages with shock absorber movements affecting the geometry, multi-link mechanisms, deformable quadrilateral mechanisms, retraction involving motion in two planes, hinged wheels, contracting (shortening) shock absorbers, and self-breaking strut linkages. Among these categories, the spatial retraction mechanism involving motion in two planes is commonly utilized, where the input and output links move in different planes, resulting in the landing gear sweeping through an arc that is not parallel to the aircraft's longitudinal axis [2].

The selection of the appropriate linkage type marks the beginning of the kinematic synthesis process, determining whether motion generation or function generation is employed for the mechanism [1].

The evolution of kinematic synthesis techniques starts from the usage of graphical methods [4], which have limitations on a systematic framework for the synthesis of complex mechanisms, [5]. Subsequently, studies on the analysis on the four-bar linkages kinematic behavior in terms of trigonometric relations and mathematical

equations became prevalent [6]. As the technological capabilities are enhanced, a shift from graphical methods to algebraic methods, which marked the introduction of complex numbers and matrices into the kinematic synthesis process enabled usage of mathematical modeling of mechanism [7]. While complex numbers are mostly used for representing the motion quantities, matrices are employed to represent relative positional relationships between components of the mechanism.

As the most significant shift in the methodology, usage of dyads, pairs of connected links featuring joints, and triads are formulated for the planar mechanisms [8]. Various kinematic synthesis procedures for the synthesis of planar mechanisms using RR, RP and PR dyads, are developed for exact [9] and approximate [10] positions.

A planar slider-crank and four-bar generating computer program called “MECSYN” [11] has been developed in Fortran[®]. The program employs a dyad vector approach to provide center and circle point locations for a given motion. Another software named “Quad-Link” [12], written in Delphi and Pascal, offers graphical outputs for synthesis tasks such as motion generation and path generation. Unlike “MECSYN”, “Quad-Link” boasts an enhanced user interface but does not communicate with a CAD environment.

For the synthesis tasks based on three and four infinitesimally and finitely separated approximate positions, “CADSYN”, a Visual Basic application integrated with AutoCad 2004, is designed [13]. Similar to “MECSYN” and “Quad-Link”, “CADSYN” employs a dyadic approach to perform motion, path, and function generation, but with increased number of solutions by usage of approximate position inputs. On the other hand, “SynCAT” [9], another Visual Basic application operating with CATIA V5, which handles motion, path, and function generation problems using inputs from a graphical user interface. The program has been tested on aerospace mechanism synthesis problems such as nose landing gear retraction. Both “CADSYN” and “SynCAT” are tailored for planar mechanisms.

Retraction mechanisms involving motion in two planes are commonly used in aerospace applications due to the constraints posed by the stowage volume of landing gear mechanisms. Spatial mechanisms can be used for path and motion generation synthesis by employing exponential rotation matrices [14], [15]. Spatial mechanisms applied to multi-loop linkages are suitable for the integration of secondary motion into the retraction system. In this study, SSRR linkage, by R-R link being the output, is taken as the case study for the synthesis of a spatial mechanism.

Several methodologies are introduced to synthesize the RRSS mechanisms. An RRSS mechanism synthesis methodology for multiple phase motion generation involving that the coupler passes through distinct positions called phases, is developed by constructing S-S and R-R dyad constraint equations [16]. The position of the coupler is defined by four separate marker points located on the S-R link on AutoCAD 2000 software [17]. Another technique using Euler parameters combined with quaternion algebra to define motion generation synthesis equations of RRSS mechanism is shown to be efficient in two position and three position synthesis tasks due to not including non-linear trigonometric equations [18].

For the derivation of input-output relation equations of a RSSR linkage, Denavit-Hartenberg's convention is used to define linkage parameters together with reordering of closure equations such that the mechanism is composed of two R-S links. The derived equations are visualized and verified using GeoGebra [19].

In this study, a software with a graphical user interface (GUI) interacting with Siemens NX, NX Open Journal [20], is developed for the path generation synthesis of both planar and spatial landing gear retraction four-link mechanism. While accomplishing this, the capability of state-of-the-art planar mechanism synthesis programs is enhanced by expanding the system into three-dimensional space.

CHAPTER 3

THEORY AND FORMULATION

3.1 General

In order to define the motion of four-link mechanisms, orthonormal, right-handed reference frames, Denavit-Hartenberg's convention and exponential rotation matrices are used to generate loop closure equations, displacement equations and path generation synthesis.

3.1.1 Degree of Freedom of Space, Kinematic Pairs

Degree of Freedom (DOF) in space refers to the count of independent parameters necessary to define the position or motion of a rigid body within that space. In spatial motion, the DOF is 6, while for planar motion, the DOF reduces to 3.

DOF of kinematic pair is defined as the number of independent parameters that are required to determine the relative position of one rigid body with respect to the other connected by the kinematic pair. The kinematic pairs are classified by this characteristic. For this study, only lower kinematic pairs are used as joints.

The general degree of freedom equation is [21]:



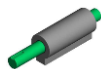

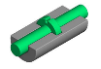

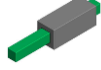

$$DOF = \lambda_s(n - j - 1) + \sum_{k=1}^j f_k \quad (3-1)$$

where DOF is the degree of freedom of the mechanism, λ_s is degree of freedom of space, n is number of links including the fixed link, j number of joints in the

mechanism, f_k number of freedoms for k^{th} joint. Rotational and translational freedoms of the joint types being used in this study are presented in Table 3.1

In case the movement of all links within a kinematic chain occurs in a plane or within parallel planes, the kinematic chain is considered planar. Conversely, if the motion of the links takes place in three dimensions, the kinematic chain is termed spatial.

Table 3.1 Some Kinematic Pairs with Independent Rotational and Translational Motion [21], [22]

| DOF (f) | Rotational Freedom | Translational Freedom | Name | Form Closed | Force Closed |
|-------------|--------------------|-----------------------|--------------------------------------|--|---|
| 3 | 3 | 0 | Spherical pair (S, Ball Joint) |  |  |
| 2 | 1 | 1 | Cylindrical joint (C) |  |  |
| 1 | 1 | 0 | Revolute pair (R, turning joint) |  |  |
| | 1 | 0 | Prismatic pair (P, sliding joint) |  |  |

Concerning the landing gear systems, the first link of the kinematic chain is fixed to the rotorcraft structure; thus, the retraction system is called a mechanism. In this study, all the retraction mechanisms are four-link mechanisms, and they are classified by their topological characteristics such as type, number, and distribution of joints. All joints used in this study are form-closed kinematic pairs.

3.1.2 Reference Frame Definition

All reference frames being used in this study are defined in three-dimensional Euclidean space, consisting of a specified origin being O_k , and three non-coplanar

axes emanating from the origin. All reference frames are orthonormal and right-handed. Reference frames will be identified by their basis vectors, which are orthogonal unit vectors such as:

$$F_k = F_k(O_k)[O_k; \vec{u}_1^{(k)}, \vec{u}_2^{(k)}, \vec{u}_3^{(k)}] \quad (3-2)$$

As shown in reference frame representation given by Figure 3.1, the coordinate axes of the frame are aligned with the basis vector triad of:

$$U_k = \{\vec{u}_i^{(k)} : i = 1, 2, 3\} \quad (3-3)$$

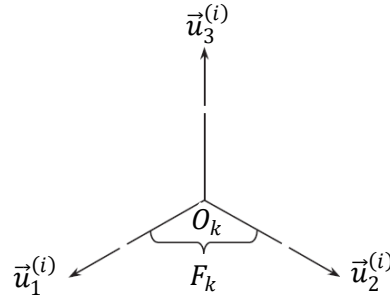


Figure 3.1. Reference Frame Representation

Due to the right-handedness of the reference frame, the cross product of basis vectors obeys the circle rule based on the Levi-Civita epsilon function ϵ_{ijk} , as illustrated in Figure 3.2.

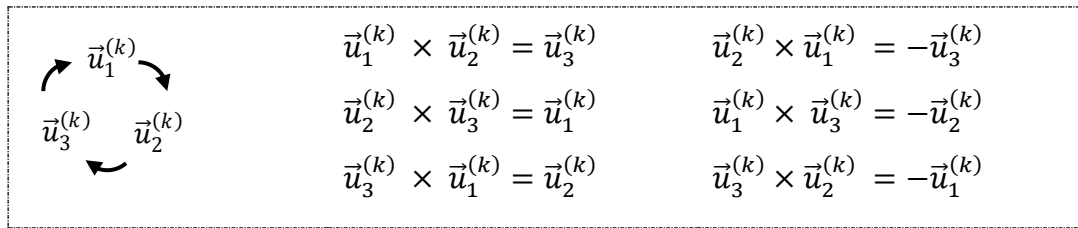


Figure 3.2. Circle Rule and Cross – Products

Due to the orthonormality of basis vectors, the dot product of any two basis vectors can be defined by the Kronecker delta function δ_{jk} as equation (3-4).

$$\vec{u}_i^{(i)} \cdot \vec{u}_j^{(i)} = \delta_{ij} = \begin{cases} 1 & \text{if } i = j \\ 0 & \text{if } i \neq j \end{cases} \quad (3-4)$$

Any basis vector $\vec{u}_i^{(k)}$ of reference frame F_k can be represented by the following basic column matrix \bar{u}_i defined in F_i :

$$\left[\vec{u}_i^{(k)} \right]^{(k)} = \bar{u}_i^{(k/k)} = \bar{u}_i \quad (3-5)$$

Basic column matrix is an entity that is independent from the reference frame. Basic column matrices are the primary basis of the space R^3 of 3×1 column matrices. \bar{u}_i is represented as the i^{th} row of each 3×1 matrix being 1 whereas other rows are 0 as given below. Any column matrix can be expressed as linear combinations of \bar{u}_1 , \bar{u}_2 and \bar{u}_3 .

$$\bar{u}_1 = \begin{bmatrix} 1 \\ 0 \\ 0 \end{bmatrix}, \quad \bar{u}_2 = \begin{bmatrix} 0 \\ 1 \\ 0 \end{bmatrix}, \quad \bar{u}_3 = \begin{bmatrix} 0 \\ 0 \\ 1 \end{bmatrix} \quad (3-6)$$

3.1.3 Representation of a Vector in a Selected Reference Frame

A vector \vec{r} can be resolved in a selected reference frame F_i by the components of \vec{r} in basis vectors:

$$\vec{r} = r_1^{(k)} \vec{u}_1^{(k)} + r_2^{(k)} \vec{u}_2^{(k)} + r_3^{(k)} \vec{u}_3^{(k)} \quad (3-7)$$

The components of \vec{r} can be represented in column matrix as:

$$\bar{r}^{(k)} = \begin{bmatrix} r_1^{(k)} \\ r_2^{(k)} \\ r_3^{(k)} \end{bmatrix} \quad (3-8)$$

Since any column matrix can be expressed as linear combinations of \bar{u}_1 , \bar{u}_2 and \bar{u}_3 , $\bar{r}^{(k)}$ can be re-written as:

$$\bar{r}^{(k)} = r_1^{(k)} \bar{u}_1^{(k/k)} + r_2^{(k)} \bar{u}_2^{(k/k)} + r_3^{(k)} \bar{u}_3^{(k/k)} \quad (3-9)$$

3.1.4 Denavit–Hartenberg’s Convention

Denavit-Hartenberg’s Convention is used to express kinematic relations of the four-link linkages according to following definitions [14], [23]:

Figure 3.3 defines a sketch that involves four successive intermediate links L_{k-2} , L_{k-1} , L_k and L_{k+1} where L_{k-2} is the proximal and L_{k+1} is the distal one. The joint that connects link L_k to L_{k-1} is designated as J_k . The right-handed reference frame is located on link L_k where O_k is the origin and $\vec{u}_1^{(k)}$, $\vec{u}_2^{(k)}$, $\vec{u}_3^{(k)}$ are the basis vectors of the reference frame.

If the axes of joints are not intersecting, the common normal N_k is directed from the proximal joint to the distal joint. If there is an intersection of axes, the sense of common normal can be selected arbitrarily.

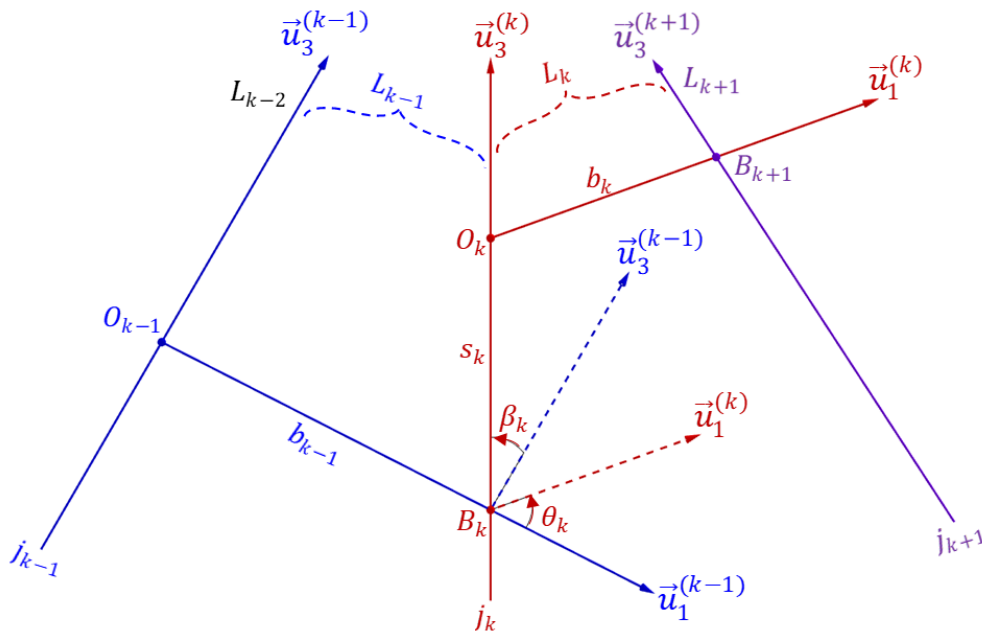


Figure 3.3. Reference Frame Installation According to Denavit-Hartenberg’s Convention

The joint variables and link parameters based on D-H Convention are given in Table 3.2. It shall be noted that the twist angle β_k and effective link length b_k are constant for both revolute and prismatic joints.

Table 3.2 Link Parameters based on Denavit – Hartenberg’s Convention

| D-H Parameter Definition | $J_k = \text{Revolute}$ Joint | $J_k = \text{Prismatic}$ Joint |
|--|----------------------------------|---|
| $\beta_k = \angle [\vec{u}_3^{(k-1)} \rightarrow \vec{u}_3^{(k)}]$ about $\vec{u}_1^{(k-1)}$ | Constant | Constant |
| $\theta_k = \angle [\vec{u}_1^{(k-1)} \rightarrow \vec{u}_1^{(k)}]$ about $\vec{u}_3^{(k)}$ | Joint variable | Constant, Notation: δ_k (deflection angle) |
| $s_k = B_k O_k$ along $\vec{u}_3^{(k)}$ | Constant, notation: d_k | Joint variable (sliding distance) |
| $b_k = O_k B_{k+1}$ along $\vec{u}_1^{(k)}$ | Constant | Constant |

3.1.5 Relative Positioning of Consecutive Links

Relative orientation $F_k(O_k)$ with respect to $F_{k-1}(O_{k-1})$ can be expressed by the following formulae:

$$\hat{C}^{(k-1,k)} = \hat{R}_1(\beta_k)\hat{R}_2(\theta_k) = e^{\tilde{u}_1\beta_k}e^{\tilde{u}_3\theta_k} \quad (3-10)$$

Relative position of $F_k(O_k)$ with respect to $F_{k-1}(O_{k-1})$:

$$\vec{r}_{k-1,k} = \vec{r}_{O_{k-1}O_k} = \vec{r}_{O_{k-1}B_k} + \vec{r}_{B_kO_k} = b_{k-1}\vec{u}_1^{(k-1)} + s_k\vec{u}_3^{(k)} \quad (3-11)$$

$\vec{r}_{k-1,k}$ can be written in column matrix form as:

$$\vec{r}_{k-1,k}^{(k-1)} = b_{k-1}\vec{u}_1^{(k-1/k-1)} + s_k\vec{u}_3^{(k/k)} \quad (3-12)$$

$$\vec{r}_{k-1,k}^{(k-1)} = b_{k-1}\vec{u}_1^{(k-1/k-1)} + s_k\hat{C}^{(k-1,k)}\vec{u}_3^{(k/k)} \quad (3-13)$$

$$\vec{r}_{k-1,k}^{(k-1)} = b_{k-1}\vec{u}_1 + s_k e^{\tilde{u}_1\beta_k}e^{\tilde{u}_3\theta_k}\vec{u}_3 = b_{k-1}\vec{u}_1 + s_k e^{\tilde{u}_1\beta_k}\vec{u}_3 \quad (3-14)$$

$$\vec{r}_{k-1,k}^{(k-1)} = b_{k-1}\vec{u}_1 - \vec{u}_2 s_k \sin(\beta_k) + \vec{u}_3 s_k \cos(\beta_k) \quad (3-15)$$

3.1.6 Loop Closure Equations

For this study, a single loop spatial mechanism with n links is considered, where both the zeroth and the last (n^{th}) link address the fixed link.

Since the zeroth and the last link are the same link, the orientation matrix loop closure equation indicates a 3×3 identity matrix:

$$\hat{C}^{(0,1)}\hat{C}^{(1,2)}\hat{C}^{(2,3)}\hat{C}^{(3,4)} \dots \hat{C}^{(n-1,n)} = \hat{C}^{(0,n)} = \hat{I} \quad (3-16)$$

Therefore, by considering that the orientation of the fixed link is always constant, the orientation loop closure equation is written as:

$$e^{\tilde{u}_1\beta_1}e^{\tilde{u}_3\theta_1}e^{\tilde{u}_1\beta_2}e^{\tilde{u}_3\theta_2}e^{\tilde{u}_1\beta_3}e^{\tilde{u}_3\theta_3}e^{\tilde{u}_1\beta_4}e^{\tilde{u}_3\theta_4} \dots e^{\tilde{u}_1\beta_n}e^{\tilde{u}_3\theta_n} = \hat{I} \quad (3-17)$$

The position vector $\vec{r}_{k-1,k}$ of the k^{th} link is directed from the origin of the previous frame O_{k-1} to k^{th} link reference frame origin O_k .

Again, the following vector loop can be written by using the zeroth and n^{th} links as the fixed frames.

$$\vec{r}_{0,1} + \vec{r}_{1,2} + \vec{r}_{2,3} + \vec{r}_{3,4} + \dots + \vec{r}_{n-1,n} = \vec{0} \quad (3-18)$$

By defining each position vector in the zeroth (fixed) frame, the column matrix form of the position loop closure equation is written as follows:

$$\begin{aligned} b_0\bar{u}_1^{(0)} + s_1\hat{C}^{(0,1)}\bar{u}_3^{(1)} + b_1\hat{C}^{(0,1)}\bar{u}_1^{(1)} + s_2\hat{C}^{(0,2)}\bar{u}_3^{(2)} + b_2\hat{C}^{(0,2)}\bar{u}_1^{(2)} \\ + s_3\hat{C}^{(0,3)}\bar{u}_3^{(3)} + b_3\hat{C}^{(0,3)}\bar{u}_1^{(3)} + s_4\hat{C}^{(0,4)}\bar{u}_3^{(4)} + \dots \\ + b_{n-1}\hat{C}^{(0,n-1)}\bar{u}_1^{(n-1)} + s_n\hat{C}^{(0,n)}\bar{u}_3^{(n)} = \vec{0} \end{aligned} \quad (3-19)$$

The orientation and position loop closure equations are the two fundamental matrix equations that define the displacement equation of any spatial linkage.

The position loop closure equation can be written with respect to the global frame as:

$$\begin{aligned}
\bar{r} + b_0 \hat{C}^{(g,0)} \bar{u}_1^{(0)} + s_1 \hat{C}^{(g,1)} \bar{u}_3^{(1)} + b_1 \hat{C}^{(g,1)} \bar{u}_1^{(1)} + s_2 \hat{C}^{(g,2)} \bar{u}_3^{(2)} \\
+ b_2 \hat{C}^{(g,2)} \bar{u}_1^{(2)} + s_3 \hat{C}^{(g,3)} \bar{u}_3^{(3)} + b_3 \hat{C}^{(g,3)} \bar{u}_1^{(3)} \\
+ s_4 \hat{C}^{(g,4)} \bar{u}_3^{(4)} + b_{n-1} \hat{C}^{(g,n-1)} \bar{u}_1^{(n-1)} + \dots \\
+ s_n \hat{C}^{(g,n)} \bar{u}_3^{(n)} - \bar{r} = \bar{0}
\end{aligned} \tag{3-20}$$

Where $\hat{C}^{(g,0)}$ is the orientation of the zeroth frame with respect to the global frame. Since both frames are fixed, the components of the orientation matrix are constant values.

$$\hat{C}^{(g,0)} = e^{\tilde{u}_1 \alpha_1} e^{\tilde{u}_2 \alpha_2} e^{\tilde{u}_3 \alpha_3} \tag{3-21}$$

where $\bar{r}^{(k)}$ is the position of zeroth frame origin based on the global frame.

3.1.7 Path Generation Synthesis

Modified reference frame installation for path generation synthesis is provided in the Figure 3.4.

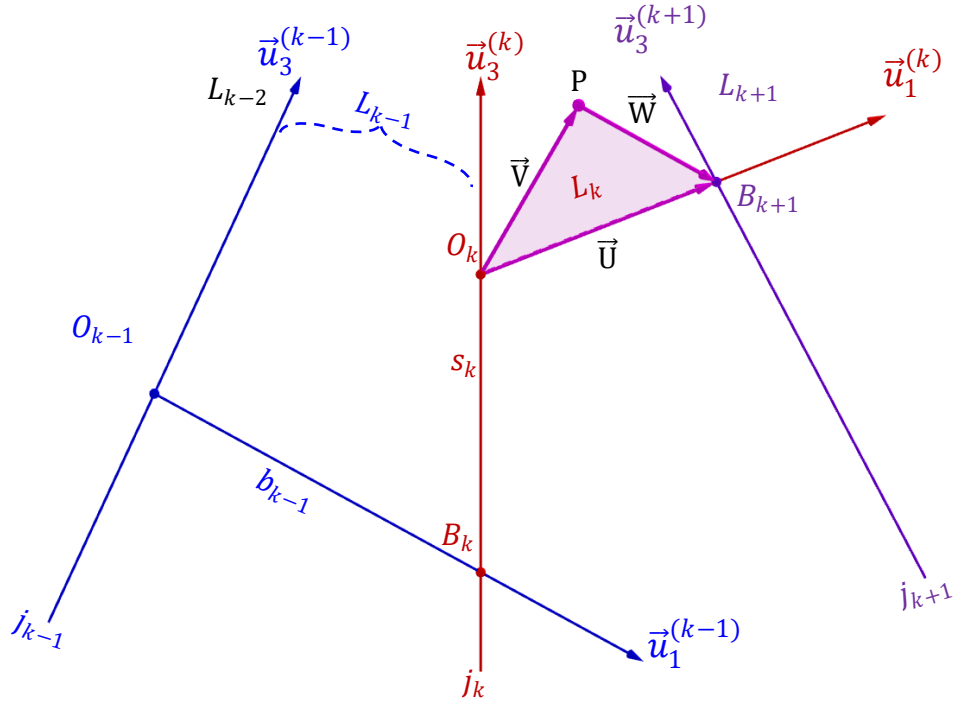


Figure 3.4 Path Tracer Point and Vector Installation According to D-H Convention

Link k is a binary link, to which the path tracer point P is attached on. The vector \vec{U} is directed from the origin of the proximal joint to the auxiliary point on the distal joint, through the common normal between the joint pair. The vector \vec{V} is directed from the origin of the proximal joint to the tracer point, whereas the vector \vec{W} is directed from the origin of the tracer point to the auxiliary point on the distal one [24]. Therefore:

$$\vec{U} = \vec{V} + \vec{W} \quad \text{and} \quad \vec{V}^{(k)} + \vec{W}^{(k)} = \vec{U}^{(k)} \quad (3-22)$$

The linkage including the precision point can be divided into left and right dyads at point P . The vectors that originate from the origin of global frame towards the precision points P_0, P_1, \dots, P_{j-1} can be represented as $\vec{R}_0, \vec{R}_1, \dots, \vec{R}_{j-1}$ respectively.

The following two left and right dyad loop closure equations for any vector \vec{R}_i can be written as:

$$\begin{aligned} \vec{r} + b_0 \hat{C}^{(g,0)} \bar{u}_1 + s_1 \hat{C}^{(g,1)} \bar{u}_3 + b_1 \hat{C}^{(g,1)} \bar{u}_1 + s_2 \hat{C}^{(g,2)} \bar{u}_3 + \dots \\ + b_{k-1} \hat{C}^{(g,k-1)} \bar{u}_1 + s_k \hat{C}^{(g,k)} \bar{u}_3 + \hat{C}^{(g,k)} \bar{V}^{(k)} = \vec{R}_i \end{aligned} \quad (3-23)$$

$$\begin{aligned} \hat{C}^{(g,k)} \bar{W}^{(k)} + s_{k+1} \hat{C}^{(g,k+1)} \bar{u}_3 + b_{k+1} \hat{C}^{(g,k+1)} \bar{u}_1 + s_{k+2} \hat{C}^{(g,k+2)} \bar{u}_3 + \dots \\ + b_{n-1} \hat{C}^{(g,n-1)} \bar{u}_1^{(n-1)} + s_n \hat{C}^{(g,n)} \bar{u}_3^{(n)} - \vec{r} = -\vec{R}_i \end{aligned} \quad (3-24)$$

\vec{r} represents the vector starting from the origin of the global frame and moving towards the origin of the zeroth frame, in matrix form. The fixed frame of linkage is assumed to be attached to the linkage as both the zeroth and the last link.

3.2 Landing Gear Retraction Mechanism Synthesis Tasks

3.2.1 Reference Frame Assignment

The body axes coordinate system for helicopter is assigned as [25]:

- x axis as the longitudinal axis along the fuselage along aft to fore of helicopter,
- y axis as the lateral axis directing from port side to the starboard side and
- z axis as the vertical axis directing from center of gravity to waterline level through the bottom of fuselage.

The three angular rate components along the x, y, z axis in the body axes system define the Euler angle representation as roll, pitch, and yaw respectively.

The Body Frame is used for the placement of the landing gears wheels based on the rollover and turnover stability angles at static position. Therefore, the fully extended position of the helicopter wheel, and the attachment point between the shock absorber and fuselage is determined based on the location of the Body Frame.

The Hub-Axes coordinate system for helicopter is assigned as [25]:

- x axis as the longitudinal axis along the fuselage along fore to aft of helicopter,
- y axis as the lateral axis directing from port side to the starboard side and
- z axis as the vertical axis directing outwards the fuselage body from hub center.

The Earth Frame used in CAD modelling lays parallel to the three main planes of the Hub-Axes coordinate system.

A representative utility helicopter model based on AgustaWestland AW169 is modelled on Siemens NX. The right-handed absolute coordinate system represents the Earth Frame, located on the coordinates of $(x, y, z) = (0,0,0)$. The helicopter is placed on the CAD screen at flying position.

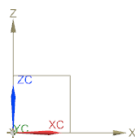
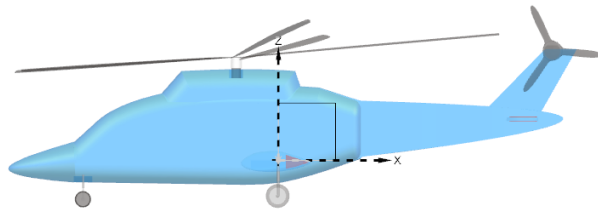


Figure 3.5. Earth Frame and Global Reference Frame Allocation

In this study, Left Main Landing Gear (MLG) is chosen as the landing gear that the retraction mechanism will be designed for.

The Left MLG Reference Frame is generated by translating the Earth Frame to the center of the shock absorber joint with the helicopter fuselage. The Left MLG Reference Frame will be used as the global frame.

CHAPTER 4

LANDING GEAR MECHANISMS INVOLVING PLANAR MOTION

Retraction mechanisms with planar motion are primarily composed of four-link mechanisms designed for rotation around a single axis. These mechanisms may incorporate a piston-cylinder actuator, such as hydraulic pistons, as two links of the four-link. In some cases, the four-bar is used for down-locking and is actuated by an external actuator connected to the crank. Exponential rotation matrices are used for the planar retraction mechanisms to include structural joint offsets.

4.1 The Constrained RRCR Mechanism

4.1.1 Degree of Freedom of the Constrained RRCR Mechanism

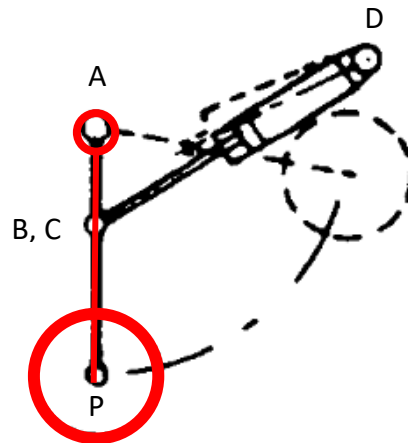


Figure 4.1. RRPR (Constrained RRCR) Linkage Landing Gear Hardpoint Definitions [26]

For the RRCR mechanism, $\lambda_s = 3$, $n = j = 4$, $f_1 = f_2 = f_4 = 1$, $f_3 = 2$ and $DOF = 2$.

The links 2 and 3 represent hydraulic actuator piston and cylinder. The rotation of piston inside cylinder is undesired to minimize the wear of sealing elements. Even when the rotation is not constrained, due to high pressure inside the actuator and the friction between adjacent elements, the rotation gets minimized and the mechanism acts as a RRPR linkage.

For RRPR mechanism, $f_1 = f_2 = f_3 = f_4 = 1$, degree of freedom reduces to one, where the only freedom of motion is the translation between the second and the third links.

4.1.2 General Displacement Equation

Utilizing D-H convention, the reference frames are placed on the mechanism. Frames 0, 4 and 5 are located on the fixed link, which is the structural frame of helicopter for the given case study. 5th reference frame is defined to facilitate transformation from the 0th reference frame to the 4th one.

The Loop Closure Equation starting from and ending at the zeroth link is:

$$\begin{aligned}
 |AB|\hat{C}^{(g,1)}\bar{u}_1 + |BC|\hat{C}^{(g,1)}\bar{u}_3 + s_3\hat{C}^{(g,3)}\bar{u}_2 - |D'D|\hat{C}^{(g,4)}\bar{u}_3 \\
 + |A'D'|\hat{C}^{(g,5)}\bar{u}_1 - |AA'|\hat{C}^{(g,5)}\bar{u}_2 = \bar{0}
 \end{aligned} \tag{4-1}$$

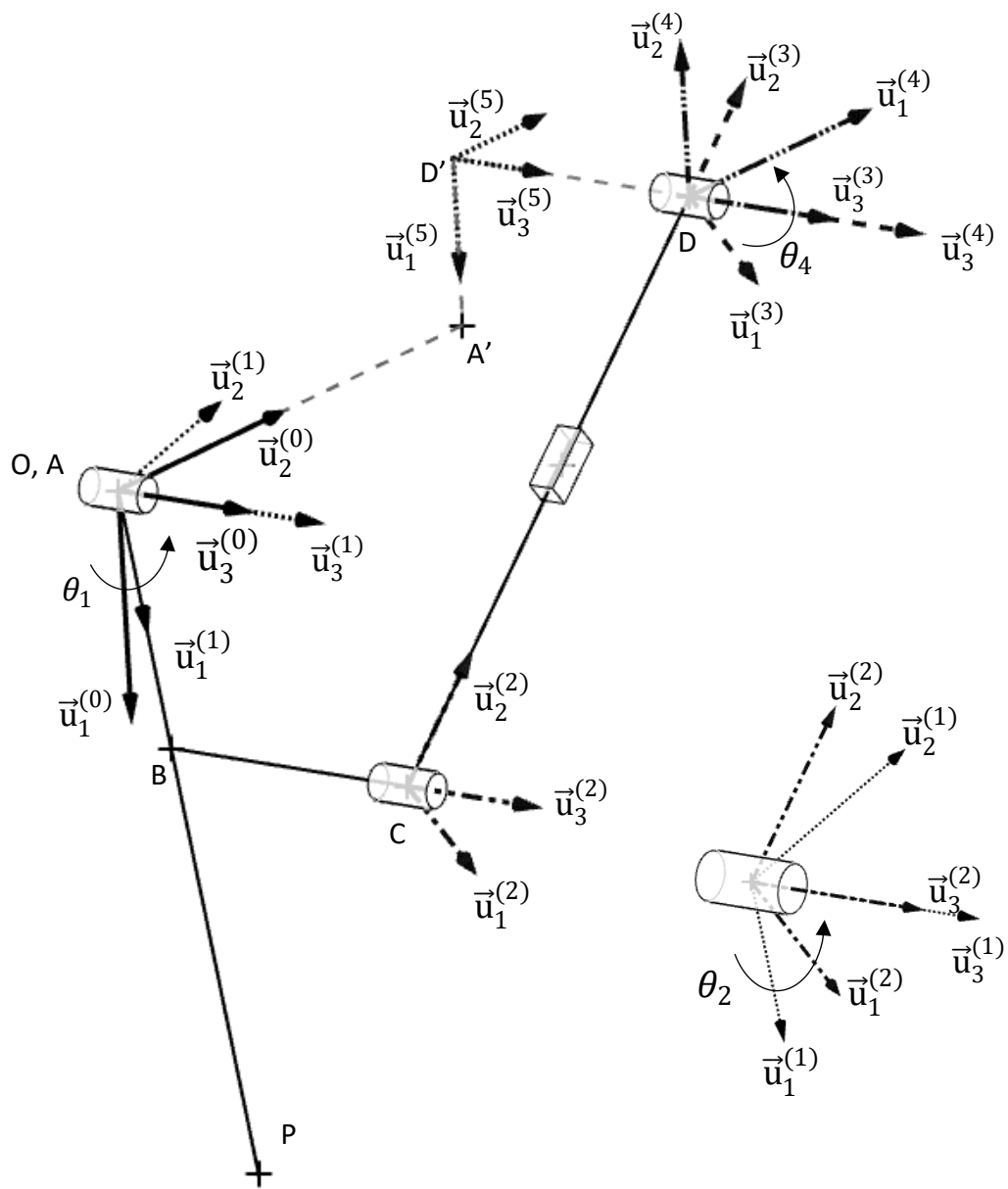


Figure 4.2. Isometric View of RRPR Mechanism

The rotation matrices, starting from the orientation of the zeroth frame with respect to the previous reference frame are:

$$\hat{C}^{(g,0)} = e^{\tilde{u}_2\pi/2} \quad (4-2)$$

$$\hat{C}^{(0,1)} = (\hat{C}^{(1,4)})^{-1} = e^{\tilde{u}_1\beta_1} e^{\tilde{u}_3\theta_1} = e^{\tilde{u}_3\theta_1} \quad (4-3)$$

$$\hat{C}^{(1,2)} = e^{\tilde{u}_1\beta_2} e^{\tilde{u}_3\theta_2} = e^{\tilde{u}_3\theta_2} \quad (4-4)$$

$$\hat{C}^{(2,3)} = e^{\tilde{u}_1\beta_3} e^{\tilde{u}_3\theta_3} = \hat{I} \quad (4-5)$$

$$\hat{C}^{(3,4)} = e^{\tilde{u}_1\beta_4} e^{\tilde{u}_3\theta_4} = e^{\tilde{u}_3\theta_4} \quad (4-6)$$

$$\hat{C}^{(4,5)} = e^{-\tilde{u}_3\pi/2} \quad (4-7)$$

$$\hat{C}^{(5,g)} = e^{-\tilde{u}_2\pi/2} \quad (4-8)$$

$$\hat{C}^{(0,5)} = \hat{C}^{(0,g)} \hat{C}^{(g,5)} = e^{-\tilde{u}_2\pi/2} e^{\tilde{u}_2\pi/2} = \hat{I} \quad (4-9)$$

Since joint 3 is a prismatic joint, equation (4-5) is identity.

The rotation matrices, starting from the orientation of the first frame with respect to the global frame are:

$$\hat{C}^{(g,1)} = \hat{C}^{(g,0)} \hat{C}^{(0,1)} = e^{\tilde{u}_2\pi/2} e^{\tilde{u}_3\theta_1} \quad (4-10)$$

$$\hat{C}^{(g,2)} = (\hat{C}^{(2,g)})^{-1} = \hat{C}^{(g,0)} \hat{C}^{(0,1)} \hat{C}^{(1,2)} = e^{\tilde{u}_2\pi/2} e^{\tilde{u}_3\theta_1} e^{\tilde{u}_3\theta_2} \quad (4-11)$$

$$\hat{C}^{(g,3)} = (\hat{C}^{(3,g)})^{-1} = \hat{C}^{(g,0)} \hat{C}^{(0,1)} \hat{C}^{(1,2)} \hat{C}^{(2,3)} = e^{\tilde{u}_2\pi/2} e^{\tilde{u}_3\theta_1} e^{\tilde{u}_3\theta_2} \quad (4-12)$$

$$\begin{aligned} \hat{C}^{(g,4)} &= (\hat{C}^{(4,g)})^{-1} = \hat{C}^{(g,0)} \hat{C}^{(0,1)} \hat{C}^{(1,2)} \hat{C}^{(2,3)} \hat{C}^{(3,4)} \\ &= e^{\tilde{u}_2\pi/2} e^{\tilde{u}_3\theta_1} e^{\tilde{u}_3\theta_2} e^{\tilde{u}_3\theta_4} = e^{\tilde{u}_2\pi/2} e^{\tilde{u}_3\pi/2} \end{aligned} \quad (4-13)$$

$$\begin{aligned} \hat{C}^{(g,5)} &= (\hat{C}^{(5,g)})^{-1} = \hat{C}^{(g,0)} \hat{C}^{(0,1)} \hat{C}^{(1,2)} \hat{C}^{(2,3)} \hat{C}^{(3,4)} \hat{C}^{(4,5)} \\ &= e^{\tilde{u}_2\pi/2} e^{\tilde{u}_3\theta_1} e^{\tilde{u}_3\theta_2} e^{\tilde{u}_3\theta_4} e^{-\tilde{u}_3\pi/2} e^{-\tilde{u}_2\pi/2} = e^{\tilde{u}_2\pi/2} \end{aligned} \quad (4-14)$$

By equations (4-10) to (4-14), the loop closure equation (4-1) can be re-stated as:

$$\begin{aligned}
& |AB|e^{\tilde{u}_2\pi/2}e^{\tilde{u}_3\theta_1}\bar{u}_1 + |BC|e^{\tilde{u}_2\pi/2}e^{\tilde{u}_3\theta_1}\bar{u}_3 + s_3e^{\tilde{u}_2\pi/2}e^{\tilde{u}_3\theta_1}e^{\tilde{u}_3\theta_2}\bar{u}_2 \\
& \quad - |D'D|e^{\tilde{u}_2\pi/2}e^{\tilde{u}_3\pi/2}\bar{u}_3 + |A'D'|e^{\tilde{u}_2\pi/2}\bar{u}_1 \\
& \quad - |AA'|e^{\tilde{u}_2\pi/2}\bar{u}_2 = \bar{0}
\end{aligned} \tag{4-15}$$

The exponential terms in equation (4-15) are expressed in open form as:

$$e^{\tilde{u}_2\pi/2}e^{\tilde{u}_3\theta_1}\bar{u}_1 = \bar{u}_2 \sin(\theta_1) - \bar{u}_3 \cos(\theta_1) \tag{4-16}$$

$$e^{\tilde{u}_2\pi/2}e^{\tilde{u}_3\theta_1}\bar{u}_3 = e^{\tilde{u}_2\pi/2}\bar{u}_3 = \bar{u}_1 \tag{4-17}$$

$$\begin{aligned}
e^{\tilde{u}_2\pi/2}e^{\tilde{u}_3\theta_1}e^{\tilde{u}_3\theta_2}\bar{u}_2 &= e^{\tilde{u}_2\pi/2}e^{\tilde{u}_3(\theta_1+\theta_2)}\bar{u}_2 \\
&= \bar{u}_3 \sin(\theta_1 + \theta_2) + \bar{u}_2 \cos(\theta_1 + \theta_2)
\end{aligned} \tag{4-18}$$

$$e^{\tilde{u}_2\pi/2}e^{\tilde{u}_3\pi/2}\bar{u}_3 = e^{\tilde{u}_2\pi/2}\bar{u}_3 = \bar{u}_1 \tag{4-19}$$

$$e^{\tilde{u}_2\pi/2}\bar{u}_1 = -\bar{u}_3 \tag{4-20}$$

Utilizing equations from (4-16) to (4-20), equation (4-15) is re-stated as:

$$\begin{aligned}
& \bar{u}_2|AB| \sin(\theta_1) - \bar{u}_3|AB| \cos(\theta_1) + \bar{u}_1|BC| \\
& \quad + \bar{u}_3s_3 \sin(\theta_1 + \theta_2) + \bar{u}_2s_3 \cos(\theta_1 + \theta_2) \\
& \quad - \bar{u}_1|D'D| - \bar{u}_3|A'D'| - \bar{u}_2|AA'| = \bar{0}
\end{aligned} \tag{4-21}$$

By separating the equation (4-21) into its basis vectors, three separate equations are obtained as follows:

$$|BC| - |D'D| = 0 \tag{4-22}$$

$$s_3 \cos(\theta_1 + \theta_2) + |AB| \sin(\theta_1) - |AA'| = 0 \tag{4-23}$$

$$s_3 \sin(\theta_1 + \theta_2) - |AB| \cos(\theta_1) - |A'D'| = 0 \tag{4-24}$$

From equation (4-22), $|BC| = |D'D|$.

Taking the squares of equations (4-23) and (4-24):

$$|AB|^2 \sin^2(\theta_1) - 2|AB||AA'| \sin(\theta_1) + |AA'|^2 = s_3^2 \cos^2(\theta_1 + \theta_2) \quad (4-25)$$

$$|AB|^2 \cos^2(\theta_1) + 2|AB||A'D'| \cos(\theta_1) + |A'D'|^2 = s_3^2 \sin^2(\theta_1 + \theta_2) \quad (4-26)$$

The summation of the squares of equations (4-25) and (4-26) is:

$$\begin{aligned} |AB|^2 + 2|AB|(|A'D'| \cos(\theta_1) - |AA'| \sin(\theta_1)) + |AA'|^2 + |A'D'|^2 \\ = s_3^2 \end{aligned} \quad (4-27)$$

Therefore, the general displacement equation of the RRPR (constrained RRCR) mechanism is:

$$\begin{aligned} |AB|^2 + 2|AB|(|A'D'| \cos(\theta_1) - |AA'| \sin(\theta_1)) + |AA'|^2 + |A'D'|^2 \\ - s_3^2 = 0 \end{aligned} \quad (4-28)$$

4.1.2.1 Numerical Example

Point coordinate set and link lengths are given at the fully extended position of the landing gear.

Table 4.1 Point Coordinates at Extended Position

| Points | Coordinates | | | Link | Length (mm) |
|--------|-------------|--------|--------|------|-------------|
| | x (mm) | y (mm) | z (mm) | | |
| A | 6855 | 1390 | 1055 | AB | 240 |
| | | | | BC | 115 |
| | | | | CD | 754 |
| B | 6855 | 1390 | 815 | AA' | 470 |
| | | | | A'D' | 350 |
| C | 6970 | 1390 | 815 | DD' | 115 |
| | | | | | |
| D | 6970 | 550 | 1191.5 | | |

The required actuator length with respect to the change of position of a landing gear, whose dimensions are given in Table 4.1 is illustrated on Figure 4.3 as an input-output curve. In general, the region of interest for the design of the landing gear actuator is the output angle between 0 and 100 degrees (towards the helicopter body). As seen from Figure 4.3, the actuator shortens through the retraction operation.

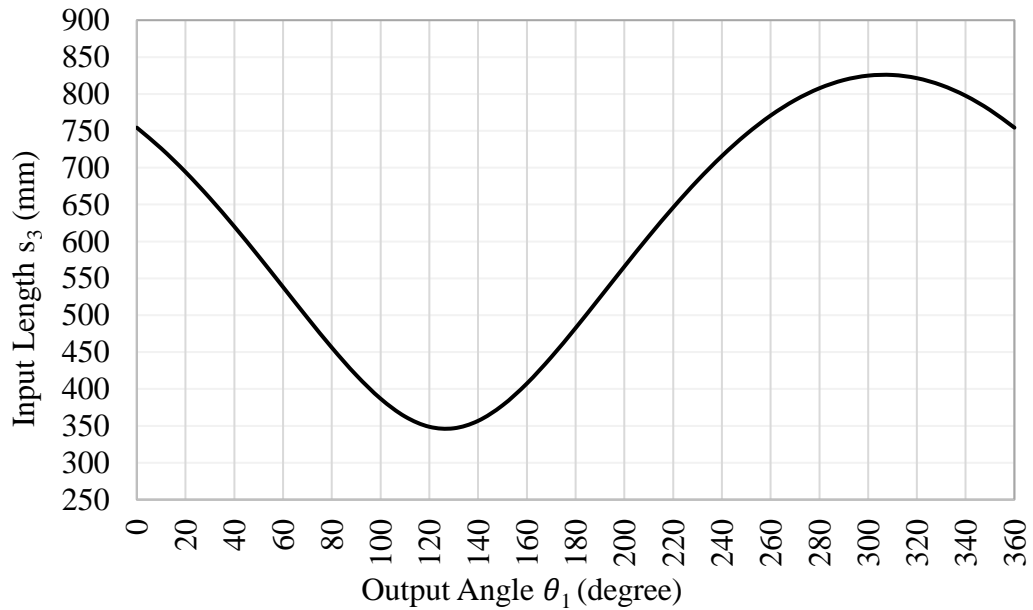


Figure 4.3. Required Actuator Length with-respect-to the Change of Landing Gear Position

From the actuator stroke change, the link length varies between 825mm and 345mm, which indicates that the stroke limit is 480mm. As a requirement from SAE International ARP1311 [27], over-travel clearance of 3/8 inches at both ends must be added to be sure that the actuator never bottoms out. It is also recommended to reserve length for structural details in the load path, preferably as 3.5 times the bore plus the stroke. Considering that the required output angle is between 0 and 100 degrees, resulting in a stroke of 367.5mm in the given output interval, minimum actuator length at extended position shall be above 995mm. The length of actuator, calculated from the positions of *C* and *D* is about 1025mm, resulting in an appropriate design for its use.

4.1.3 Path Generation Synthesis of the Constrained RRCR Mechanism

Tracer point, P, represents the wheel center (axle center) of the landing gear.

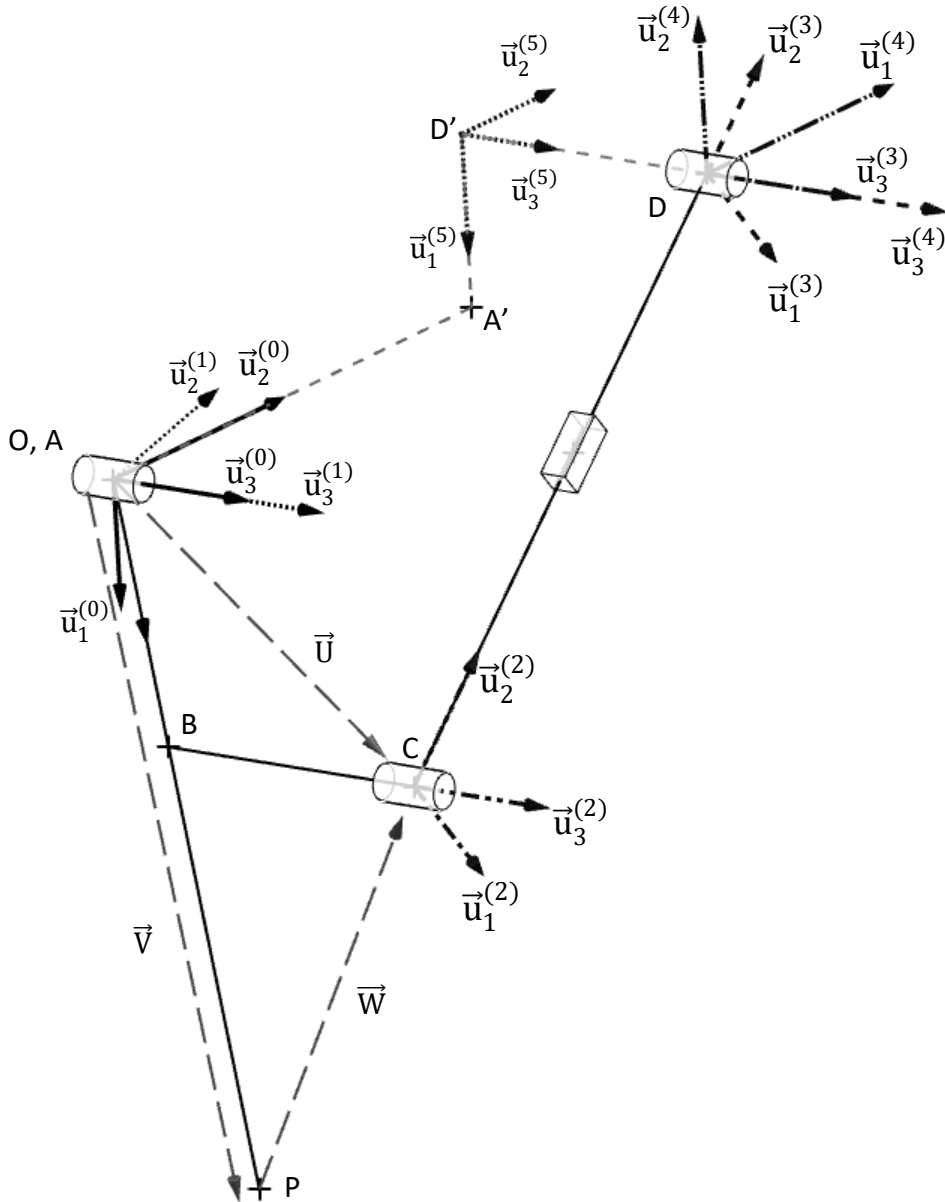


Figure 4.4. Isometric View of RRPR Mechanism for Path Generation

The link on which the precision point is located is the first link of the mechanism, which is the landing gear itself:

$$\vec{U}^{(1)} = \begin{bmatrix} U_x \\ U_y \\ U_z \end{bmatrix} = \begin{bmatrix} |AB| \\ 0 \\ |BC| \end{bmatrix} \quad (4-29)$$

$$\vec{V}^{(1)} = \begin{bmatrix} V_x \\ V_y \\ V_z \end{bmatrix} = \begin{bmatrix} |AP| \\ 0 \\ V_z \end{bmatrix} \quad (4-30)$$

$$\vec{W}^{(1)} = \begin{bmatrix} W_x \\ W_y \\ W_z \end{bmatrix} = \begin{bmatrix} |BP| \\ 0 \\ W_z \end{bmatrix} \quad (4-31)$$

Since \vec{U} , \vec{V} and \vec{W} are on the same plane ($\vec{u}_1^{(1)} x \vec{u}_3^{(1)}$) that is rotating around the axis $\vec{u}_3^{(1)} = \vec{u}_1^{(g)}$:

$$R_{0x} = R_{1x} = R_{2x} = V_y = W_y = 0 \quad (4-32)$$

for every position on its path, the point P is on the axis of $\vec{u}_1^{(1)}$. Therefore,

$$V_z = 0 \quad (4-33)$$

$$\vec{U}^{(1)} = \vec{V}^{(1)} + \vec{W}^{(1)} = |AB|\vec{u}_1 + |BC|\vec{u}_3 \quad (4-34)$$

Table 4.2 Components of Position Vectors \vec{V} and \vec{W}

| Axis | Equations | Unknowns | Eq. # |
|-------------|--------------------|--------------------------|--------|
| \vec{u}_1 | $V_x - W_x = AB $ | $V_x, W_x, AB $ | (4-35) |
| \vec{u}_2 | $V_y + W_y = 0$ | $V_y = 0, \quad W_y = 0$ | (4-36) |
| \vec{u}_3 | $V_z + W_z = BC $ | $W_z = BC $ | (4-37) |

Vectors that originate from the origin of global frame towards the precision points are defined as:

$$\hat{C}^{(g,1)}\vec{V}^{(1)} = \vec{R}_i \quad (4-38)$$

$$\begin{aligned} \hat{C}^{(g,1)}\vec{W}^{(1)} + s_3\hat{C}^{(g,3)}\vec{u}_2 - |D'D|\hat{C}^{(g,4)}\vec{u}_3 - |AA'|\hat{C}^{(g,5)}\vec{u}_2 \\ + |A'D'|\hat{C}^{(g,5)}\vec{u}_1 = -\vec{R}_i \end{aligned} \quad (4-39)$$

For any i^{th} position of the tracing point, using the rotation matrix definitions (4-10), (4-12), (4-13) and (4-14), the equations (4-38) and (4-39) can be re-written as:

$$e^{\tilde{u}_2\pi/2} e^{\tilde{u}_3\theta_1^i} \overline{V}^{(1)} = \overline{R}_i \quad (4-40)$$

$$e^{\tilde{u}_2\pi/2} e^{\tilde{u}_3\theta_1^i} \overline{W}^{(1)} + s_3^i e^{\tilde{u}_2\pi/2} e^{\tilde{u}_3\theta_1^i} e^{\tilde{u}_3\theta_2^i} \overline{u}_2 - \overline{u}_1 |D'D| - \overline{u}_2 |AA'| - \overline{u}_3 |A'D'| = -\overline{R}_i \quad (4-41)$$

Equations (4-40) and (4-41) can be separated into their components as:

$$e^{\tilde{u}_2\pi/2} e^{\tilde{u}_3\theta_1^i} (\overline{u}_1 V_x + \overline{u}_2 V_y + \overline{u}_3 V_z) = \overline{u}_1 R_{ix} + \overline{u}_2 R_{iy} + \overline{u}_3 R_{iz} \quad (4-42)$$

$$\begin{aligned} \overline{u}_1 V_z + \overline{u}_2 V_x \sin(\theta_1^i) + \overline{u}_2 V_y \cos(\theta_1^i) - \overline{u}_3 V_x \cos(\theta_1^i) + \overline{u}_3 V_y \sin(\theta_1^i) \\ = \overline{u}_1 R_{ix} + \overline{u}_2 R_{iy} + \overline{u}_3 R_{iz} \end{aligned} \quad (4-43)$$

$$e^{\tilde{u}_2\pi/2} e^{\tilde{u}_3\theta_1^i} (-\overline{u}_1 W_x + \overline{u}_2 W_y + \overline{u}_3 W_z) + s_3^i e^{\tilde{u}_2\pi/2} e^{\tilde{u}_3\theta_1^i} e^{\tilde{u}_3\theta_2^i} \overline{u}_2 - \overline{u}_1 |D'D| - \overline{u}_2 |AA'| - \overline{u}_3 |A'D'| = -\overline{R}_i \quad (4-44)$$

$$\begin{aligned} \overline{u}_1 W_z - \overline{u}_2 W_x \sin(\theta_1^i) + -\overline{u}_3 W_x \cos(\theta_1^i) + \overline{u}_2 W_y \cos(\theta_1^i) \\ + \overline{u}_3 W_y \sin(\theta_1^i) + \overline{u}_2 s_3^i \cos(\theta_1^i + \theta_2^i) \\ + \overline{u}_3 s_3^i \sin(\theta_1^i + \theta_2^i) - \overline{u}_1 |D'D| - \overline{u}_2 |AA'| - \overline{u}_3 |A'D'| \\ = -\overline{u}_1 R_{ix} - \overline{u}_2 R_{iy} - \overline{u}_3 R_{iz} \end{aligned} \quad (4-45)$$

Initial (Fully Extended) Position

For the initial position P_0 , equation (4-43) can be separated into its components as:

Table 4.3 Components of Equation (4-43) for the Initial Position P_0

| Axis | Equations | Unknowns | Eq. # |
|-------------|---|-------------------|--------|
| \bar{u}_1 | $V_z = R_{0x} = 0$ | $V_z = 0$ | (4-33) |
| \bar{u}_2 | $V_x \sin(\theta_1^0) + V_y \cos(\theta_1^0) = R_{0y}$ | V_x, θ_1^0 | (4-46) |
| \bar{u}_3 | $-V_x \cos(\theta_1^0) + V_y \sin(\theta_1^0) = R_{0z}$ | V_x, θ_1^0 | (4-47) |

For the initial position, equation (4-45) can be separated into its components as:

Table 4.4 Components of Equation (4-45) for the Initial Position P_0

| Axis | Equations | Unknowns | Eq. # |
|-------------|--|---|--------|
| \bar{u}_1 | $W_z + D'D = R_{0x}$ | $W_z, D'D $ | (4-48) |
| \bar{u}_2 | $-W_x \sin(\theta_1^0) + W_y \cos(\theta_1^0) + s_3^0 \cos(\theta_1^0 + \theta_2^0)$ $- AA' = -R_{0y}$ | $\theta_1^0, \theta_2^0, s_3^0,$ $W_x, AA' $ | (4-49) |
| \bar{u}_3 | $+W_x \cos(\theta_1^0) + W_y \sin(\theta_1^0) + s_3^0 \sin(\theta_1^0 + \theta_2^0)$ $- A'D' = -R_{0z}$ | $\theta_1^0, \theta_2^0, s_3^0,$ $W_x, A'D' $ | (4-50) |

In-between Position

Assuming that the path tracer point can pass through at most 3 points, P_0, P_1 and P_2 , for the in-between position P_1 equation (4-43) is separated into its components as:

Table 4.5 Components of Equation (4-43) for the In-Between Position P_1

| Axis | Equations | Unknowns | Eq. # |
|-------------|---|-------------------|--------|
| \bar{u}_1 | $V_z = R_{1x} = 0$ | $V_z = 0$ | (4-33) |
| \bar{u}_2 | $V_x \sin(\theta_1^1) + V_y \cos(\theta_1^1) = R_{1y}$ | V_x, θ_1^1 | (4-51) |
| \bar{u}_3 | $-V_x \cos(\theta_1^1) + V_y \sin(\theta_1^1) = R_{1z}$ | V_x, θ_1^1 | (4-52) |

For the in-between position P_1 equation (4-45) is separated into its components as:

Table 4.6 Components of Equation (4-45) for the In-Between Position P_1

| Axis | Equations | Unknowns | Eq. # |
|-------------|--|--|--------|
| \bar{u}_1 | $W_z + D'D = R_{1x}$ | $W_z, D'D $ | (4-53) |
| \bar{u}_2 | $-W_x \sin(\theta_1^1) + W_y \cos(\theta_1^1) + s_3^1 \cos(\theta_1^1 + \theta_2^1)$ $- AA' = -R_{1y}$ | $\theta_1^1, \theta_2^1, s_3^1$ $W_x, AA' $ | (4-54) |
| \bar{u}_3 | $+W_x \cos(\theta_1^1) + W_y \sin(\theta_1^1) + s_3^1 \sin(\theta_1^1 + \theta_2^1)$ $- A'D' = -\bar{R}_{1z}$ | $\theta_1^1, \theta_2^1, s_3^1$ $W_x, A'D' $ | (4-55) |

Final (Fully Retracted) Position

For the fully retracted position P_2 equation (4-43) is separated into its components as:

Table 4.7 Components of Equation (4-43) for the Final Position P_2

| Axis | Equations | Unknowns | Eq. # |
|-------------|---|-------------------|--------|
| \bar{u}_1 | $V_z = R_{2x} = 0$ | $V_z = 0$ | (4-33) |
| \bar{u}_2 | $V_x \sin(\theta_1^2) + V_y \cos(\theta_1^2) = R_{2y}$ | V_x, θ_1^2 | (4-56) |
| \bar{u}_3 | $-V_x \cos(\theta_1^2) + V_y \sin(\theta_1^2) = R_{2z}$ | V_x, θ_1^2 | (4-57) |

For fully retracted position P_2 equation (4-45) is separated into its components as:

Table 4.8 Components of Equation (4-45) for the Final Position P_2

| Axis | Equations | Unknowns | Eq. # |
|-------------|--|--|--------|
| \bar{u}_1 | $W_z + D'D = R_{2x}$ | $W_z, D'D $ | (4-58) |
| \bar{u}_2 | $-W_x \sin(\theta_1^2) + W_y \cos(\theta_1^2) + s_3^2 \cos(\theta_1^2 + \theta_2^2)$ $- AA' = -R_{2y}$ | $\theta_1^2, \theta_2^2, s_3^2$ $W_x, AA' $ | (4-59) |
| \bar{u}_3 | $+W_x \cos(\theta_1^2) + W_y \sin(\theta_1^2) + s_3^2 \sin(\theta_1^2 + \theta_2^2)$ $- A'D' = -R_{2z}$ | $\theta_1^2, \theta_2^2, s_3^2$ $W_x, A'D' $ | (4-60) |

4.1.3.1 Prescribed Orientations of Fixed Joints

Table 4.9 The Number of Unknown Parameters and Free Parameters for the Three Positions of RRPR (Constrained RRCR) Mechanism, for the Synthesis Task When Orientations of Fixed Joints are Prescribed

| # of Precision Points | # of Scalar Equations | # of Unknowns | Unknowns | # of Free Parameters |
|-----------------------|-----------------------|---------------|--|----------------------|
| 1 | 7 | 8 | $ AB , BC , W_x, W_z, V_x, s_3^0, \theta_1^0, \theta_2^0$ | 1 |
| 2 | 12 | 11 | $ AB , BC , W_x, W_z, V_x, s_3^0, \theta_1^0, \theta_2^0, s_3^1, \theta_1^1, \theta_2^1$ | 1 |
| 3 | 13 | 14 | $ AB , BC , W_x, W_z, V_x, s_3^0, \theta_1^0, \theta_2^0, s_3^1, \theta_1^1, \theta_2^1, s_3^2, \theta_1^2, \theta_2^2$ | 1 |

Table 4.10 Equation Set to be Used for the RRPR (Constrained RRCR) Mechanism Synthesis Task When Orientations of Fixed Joints are Prescribed

| Equations | Unknowns | Eq. # |
|---|---------------------------------|--------|
| $W_z + D'D = R_{0x}$ | W_z | (4-48) |
| $W_z = BC $ | $W_z, BC $ | (4-37) |
| $V_x \sin(\theta_1^0) = R_{0y}$ | V_x, θ_1^0 | (4-46) |
| $-V_x \cos(\theta_1^0) = R_{0z}$ | V_x, θ_1^0 | (4-47) |
| $\theta_1^1 = -atan2(R_{1y}, R_{1z})$ | θ_1^1 | (4-61) |
| $\theta_1^2 = -atan2(R_{2y}, R_{2z})$ | θ_1^2 | (4-62) |
| $V_x - W_x = AB $ | $V_x, W_x, AB $ | (4-35) |
| $-W_x \sin(\theta_1^0) + s_3^0 \cos(\theta_1^0 + \theta_2^0) - AA' = -R_{0y}$ | $\theta_1^0, \theta_2^0, s_3^0$ | (4-49) |

Table 4.10 Continued

| Equations | Unknowns | Eq. # |
|--|---------------------------------|--------|
| $+W_x \cos(\theta_1^0) + s_3^0 \sin(\theta_1^0 + \theta_2^0) - A'D' = -R_{0z}$ | $\theta_1^0, \theta_2^0, s_3^0$ | (4-50) |
| $-W_x \sin(\theta_1^1) + s_3^1 \cos(\theta_1^1 + \theta_2^1) - AA' = -R_{1y}$ | $\theta_1^1, \theta_2^1, s_3^1$ | (4-54) |
| $+W_x \cos(\theta_1^1) + s_3^1 \sin(\theta_1^1 + \theta_2^1) - A'D' = -R_{1z}$ | $\theta_1^1, \theta_2^1, s_3^1$ | (4-55) |
| $-W_x \sin(\theta_1^2) + s_3^2 \cos(\theta_1^2 + \theta_2^2) - AA' = -R_{2y}$ | $\theta_1^2, \theta_2^2, s_3^2$ | (4-59) |
| $+W_x \cos(\theta_1^2) + s_3^2 \sin(\theta_1^2 + \theta_2^2) - A'D' = -R_{2z}$ | $\theta_1^2, \theta_2^2, s_3^2$ | (4-60) |

Utilizing equation (4-32), synthesis equations are given in their simplified versions at Table 4.10. If the free parameter is chosen to be the crank length $|AB|$, the axial position of actuator connection on trunnion:

- From equations (4-48) and (4-37), $|BC|$ and W_z can be found.
- From equations (4-46) and (4-47), V_x and θ_1^0 can be found.
- θ_1^1 and θ_1^2 can be found from equation (4-61) and (4-62) respectively.
- W_x can be found from equation (4-35).
- By summing squares of equation (4-49) and (4-50), s_3^0 can be found.
- Using equations (4-54) and (4-55), θ_2^0 can be found.
- Using the same approach used for finding s_3^0 and θ_2^0 , $\theta_2^1, s_3^1, \theta_2^2$ and s_3^2 can be found from equations (4-54) with (4-55) and (4-59) with (4-60).

4.1.3.2 Unprescribed Positions of the Ground Pivots

The position of the origin of the reference frame attached to the fourth link \bar{r}_4 is:

$$\bar{r}_4 = \bar{u}_1|D'D| + \bar{u}_2|AA'| + \bar{u}_3|A'D'| \quad (4-63)$$

\bar{r}_4 can be re-written from the loop closure equation based on the initial position of precision point as:

$$\begin{aligned} \bar{r}_4 = & \bar{u}_1W_z + \bar{u}_2W_x \sin(\theta_1^0) - \bar{u}_3W_x \cos(\theta_1^0) + \bar{u}_2W_y \cos(\theta_1^0) \\ & + \bar{u}_3W_y \sin(\theta_1^0) + \bar{u}_2s_3^0 \cos(\theta_1^0 + \theta_2^0) \\ & + \bar{u}_3s_3^0 \sin(\theta_1^0 + \theta_2^0) + \bar{u}_1R_{0x} + \bar{u}_2R_{0y} + \bar{u}_3R_{0z} \end{aligned} \quad (4-64)$$

The loop closure equation based on the i^{th} position of precision point is:

$$\begin{aligned} & \bar{u}_1W_z + \bar{u}_2W_x \sin(\theta_1^i) - \bar{u}_3W_x \cos(\theta_1^i) + \bar{u}_2W_y \cos(\theta_1^i) \\ & + \bar{u}_3W_y \sin(\theta_1^i) + \bar{u}_2s_3^i \cos(\theta_1^i + \theta_2^i) \\ & + \bar{u}_3s_3^i \sin(\theta_1^i + \theta_2^i) - \bar{r}_4 = -\bar{u}_1R_{ix} - \bar{u}_2R_{iy} - \bar{u}_3R_{iz} \end{aligned} \quad (4-65)$$

Inserting \bar{r}_4 found from the initial position, P_0 into above equation (4-65):

$$\begin{aligned} & \bar{u}_2W_x \sin(\theta_1^i) - \bar{u}_2W_x \sin(\theta_1^0) + \bar{u}_3W_x \cos(\theta_1^0) - \bar{u}_3W_x \cos(\theta_1^i) \\ & + \bar{u}_2W_y \cos(\theta_1^i) - \bar{u}_2W_y \cos(\theta_1^0) + \bar{u}_3W_y \sin(\theta_1^i) \\ & - \bar{u}_3W_y \sin(\theta_1^0) + \bar{u}_2s_3^i \cos(\theta_1^i + \theta_2^i) \\ & - \bar{u}_2s_3^0 \cos(\theta_1^0 + \theta_2^0) + \bar{u}_3s_3^i \sin(\theta_1^i + \theta_2^i) \\ & - \bar{u}_3s_3^0 \sin(\theta_1^0 + \theta_2^0) \\ & = \bar{u}_1R_{0x} - \bar{u}_1R_{ix} + \bar{u}_2R_{0y} - \bar{u}_2R_{iy} + \bar{u}_3R_{0z} - \bar{u}_3R_{iz} \end{aligned} \quad (4-66)$$

Using equations (4-32) and (4-33), R_{0x} , R_{1x} , R_{2x} , V_y , W_y and V_z are known.

Equation (4-66) can be separated into its components as:

Table 4.11 Components of Equation (4-66)

| Axis | Equations | Unknowns | Eq. # |
|-------------|---|---|--------|
| \bar{u}_1 | $R_{0x} - R_{ix} = 0$ | N/A | (4-67) |
| \bar{u}_2 | $W_x \sin(\theta_1^i) - W_x \sin(\theta_1^0) + W_y \cos(\theta_1^i)$ $- W_y \cos(\theta_1^0) + s_3^i \cos(\theta_1^i + \theta_2^i)$ $- s_3^0 \cos(\theta_1^0 + \theta_2^0) = R_{0y} - R_{iy}$ | $\theta_1^0, \theta_1^i,$ $\theta_2^0, \theta_2^i,$ s_3^0, s_3^i, W_x | (4-68) |
| \bar{u}_3 | $W_x \cos(\theta_1^0) - W_x \cos(\theta_1^i) + W_y \sin(\theta_1^i)$ $- W_y \sin(\theta_1^0) + s_3^i \sin(\theta_1^i + \theta_2^i)$ $- s_3^0 \sin(\theta_1^0 + \theta_2^0) = R_{0z} - R_{iz}$ | $\theta_1^0, \theta_1^i,$ $\theta_2^0, \theta_2^i,$ s_3^0, s_3^i, W_x | (4-69) |

Table 4.12 The Number of Unknown Parameters and Free Parameters for The Three Positions of RRPR (Constrained RRCR) Mechanism, for the Synthesis Task When Orientations of Fixed Joints are Unprescribed

| # of Precision Points | # of Scalar Equations | # of Unknowns | Unknowns | # of Free Parameters |
|-----------------------|-----------------------|---------------|--|----------------------|
| 1 | 7 | 11 | $ AB , BC , AA' , A'D' ,$ $ D'D , W_x, W_z, V_x, s_3^0, \theta_1^0,$ θ_2^0 | 4 |
| 2 | 10 | 14 | $ AB , BC , AA' , A'D' ,$ $ D'D , W_x, W_z, V_x, s_3^0, \theta_1^0,$ $\theta_2^0, s_3^1, \theta_1^1, \theta_2^1$ | 4 |
| 3 | 13 | 17 | $ AB , BC , AA' , A'D' ,$ $ D'D , W_x, W_z, V_x, s_3^0, \theta_1^0,$ $\theta_2^0, s_3^1, \theta_1^1, \theta_2^1, s_3^2, \theta_1^2, \theta_2^2$ | 4 |

Table 4.13 Equation Set to be Used for The RRPR (Constrained RRCR) Mechanism Synthesis Task When Orientations of Fixed Joints are Unprescribed

| Equations | Unknowns | Eq. # |
|---|---|--------|
| $W_z + D'D = R_{0x}$ | $W_z, D'D $ | (4-48) |
| $W_z = BC $ | $W_z, BC $ | (4-37) |
| $V_x \sin(\theta_1^0) = R_{0y}$ | V_x, θ_1^0 | (4-46) |
| $-V_x \cos(\theta_1^0) = R_{0z}$ | V_x, θ_1^0 | (4-47) |
| $\theta_1^1 = -atan2(R_{1y}, R_{1z})$ | θ_1^1 | (4-61) |
| $\theta_1^2 = -atan2(R_{2y}, R_{2z})$ | θ_1^2 | (4-62) |
| $V_x + W_x = AB $ | $V_x, W_x, AB $ | (4-35) |
| $W_x \sin(\theta_1^1) - W_x \sin(\theta_1^0) + W_y \cos(\theta_1^1) - W_y \cos(\theta_1^0)$ $+ s_3^1 \cos(\theta_1^1 + \theta_2^1) - s_3^0 \cos(\theta_1^0 + \theta_2^0)$ $= R_{0y} - R_{1y}$ | $\theta_1^0, \theta_1^1,$ $\theta_2^0, \theta_2^1,$ s_3^0, s_3^1, W_x | (4-70) |
| $W_x \cos(\theta_1^0) - W_x \cos(\theta_1^1) + W_y \sin(\theta_1^1) - W_y \sin(\theta_1^0)$ $+ s_3^1 \sin(\theta_1^1 + \theta_2^1) - s_3^0 \sin(\theta_1^0 + \theta_2^0)$ $= R_{0z} - R_{1z}$ | $\theta_1^0, \theta_1^1,$ $\theta_2^0, \theta_2^1,$ s_3^0, s_3^1, W_x | (4-71) |
| $W_x \sin(\theta_1^2) - W_x \sin(\theta_1^0) + W_y \cos(\theta_1^2) - W_y \cos(\theta_1^0)$ $+ s_3^2 \cos(\theta_1^2 + \theta_2^2) - s_3^0 \cos(\theta_1^0 + \theta_2^0)$ $= R_{0y} - R_{2y}$ | $\theta_1^0, \theta_1^1,$ $\theta_2^0, \theta_2^1,$ s_3^0, s_3^2, W_x | (4-72) |
| $W_x \cos(\theta_1^0) - W_x \cos(\theta_1^2) + W_y \sin(\theta_1^2) - W_y \sin(\theta_1^0)$ $+ s_3^2 \sin(\theta_1^2 + \theta_2^2) - s_3^0 \sin(\theta_1^0 + \theta_2^0)$ $= R_{0z} - R_{2z}$ | $\theta_1^0, \theta_1^2,$ $\theta_2^0, \theta_2^2,$ s_3^0, s_3^2, W_x | (4-73) |
| $W_x \sin(\theta_1^0) + W_y \cos(\theta_1^0) + s_3^0 \cos(\theta_1^0 + \theta_2^0) + R_{0y}$ $= AA' $ | $\theta_1^0, \theta_2^0, s_3^0,$ $W_x, AA' $ | (4-49) |
| $-W_x \cos(\theta_1^0) + W_y \sin(\theta_1^0) + s_3^0 \sin(\theta_1^0 + \theta_2^0) + R_{0z}$ $= A'D' $ | $\theta_1^0, \theta_2^0, s_3^0,$ $W_x, A'D' $ | (4-50) |

Utilizing equation (4-32), synthesis equations are given in their simplified versions at Table 4.13. If the free parameter is chosen to be the crank length $|AB|$, $|BC|$, s_3^0 and s_3^2 which are the axial and lateral position of actuator connection on trunnion, and the stroke values at the extended and retracted positions respectively:

- From equations (4-48) and (4-37), W_z and $|D'D|$ can be found.
- From equations (4-46) and (4-47), V_x and θ_1^0 can be found. θ_1^1 and θ_1^2 can be found from equation (4-61) and (4-62) respectively.
- W_x can be found from equation (4-35).
- By leaving θ_2^0 and θ_2^2 terms at one side of the equations (4-72) and (4-73) $\cos(\theta_1^2 + \theta_2^2)$ and $\cos(\theta_1^0 + \theta_2^0)$ can be written.
- Similarly, by leaving θ_2^0 and θ_2^2 terms at one side of the equations (4-72) and (4-73) and $\sin(\theta_1^2 + \theta_2^2)$ and $\sin(\theta_1^0 + \theta_2^0)$ can be written.
- From $\sin^2(\theta_1^0 + \theta_2^0) + \cos^2(\theta_1^0 + \theta_2^0) = 1$ and $\sin^2(\theta_1^2 + \theta_2^2) + \cos^2(\theta_1^2 + \theta_2^2) = 1$ and half angle transformation of sine and cosine functions in terms of tangent function, values of $\tan\left(\frac{\theta_1^0 + \theta_2^0}{2}\right)$ and $\tan\left(\frac{\theta_1^2 + \theta_2^2}{2}\right)$, thus θ_2^0 and θ_2^2 can be found.
- By summing squares of equations (4-70) and (4-71), s_3^1 can be found.
- Using equations (4-70) and (4-71), θ_2^1 can be found.
- The ground pivot position parameters $|AA'|$ and $|A'D'|$ can be determined using equations (4-49) and (4-50) respectively.

4.2 The RRRR Mechanism with Shock Absorber as the Output Link

4.2.1 Degree of Freedom

For the RRRR mechanism, $\lambda_s = 3$, $n = j = 4$ and $f_1 = f_2 = f_3 = f_4 = 1$, degree of freedom $DOF = 1$.

The only freedom of motion is the rotation of the links. Link 2 and link 3 are the drag beams. It is desired to keep the drag beams at dead-center position to provide down-locking. The actuator is either attached to the first link, or the fourth link.

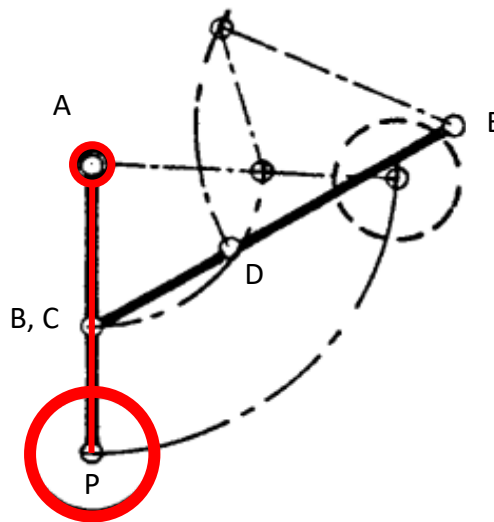


Figure 4.5. Landing Gear Hardpoint Definitions for RRRR Linkage with Shock Absorber as the Output Link [26]

4.2.2 General Displacement Equation

Utilizing D-H convention, the reference frames are placed on the mechanism. Frames 0, 4 and 5 are located on the fixed link, which is the structural frame of helicopter for the given case study. 5th reference frame is defined to facilitate transformation from the 0th reference frame to the 4th one.

In Figure 4.6, the mechanism is given at an intermediate position to define the angular parameters clearly.

The Loop Closure Equation starting from and ending at the zeroth link is:

$$|AB|\hat{C}^{(g,1)}\bar{u}_1 + |BC|\hat{C}^{(g,1)}\bar{u}_3 + |CD|\hat{C}^{(g,2)}\bar{u}_1 + |DE|\hat{C}^{(g,3)}\bar{u}_1 - |EE'|\hat{C}^{(g,4)}\bar{u}_3 + |E'A'|\hat{C}^{(g,5)}\bar{u}_1 - |A'A|\hat{C}^{(g,5)}\bar{u}_2 = \bar{0} \quad (4-74)$$

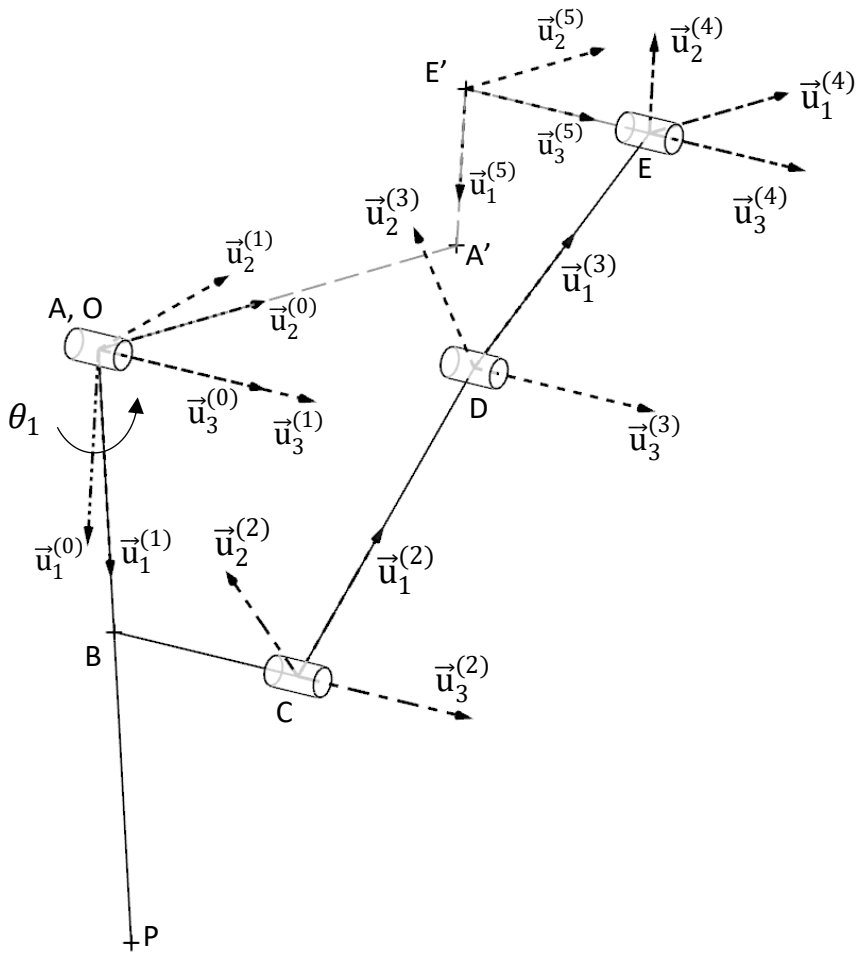


Figure 4.6. Isometric View of RRRR Mechanism with Shock Absorber as the Output Link

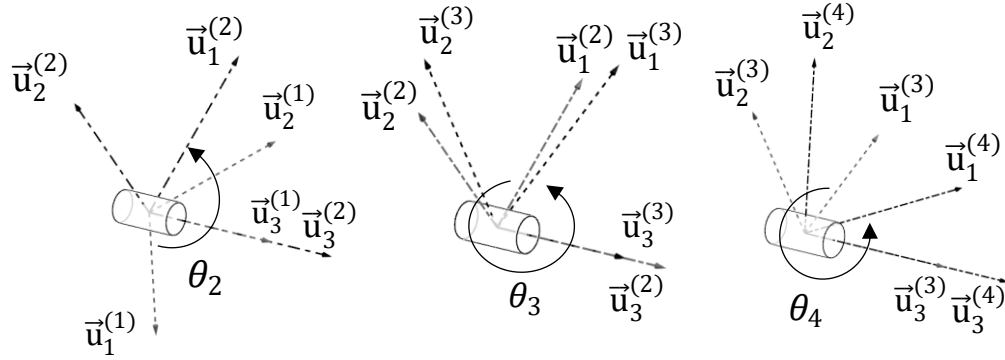


Figure 4.7. Angle Definitions of the RRRR Linkage with Shock Absorber as the Output Link

The rotation matrices, starting from the orientation of the zeroth frame with respect to the previous reference frame.

$$\hat{C}^{(g,0)} = e^{\tilde{u}_2\pi/2} \quad (4-2)$$

$$\hat{C}^{(0,1)} = (\hat{C}^{(1,4)})^{-1} = e^{\tilde{u}_1\beta_1} e^{\tilde{u}_3\theta_1} = e^{\tilde{u}_3\theta_1} \quad (4-3)$$

$$\hat{C}^{(1,2)} = e^{\tilde{u}_1\beta_2} e^{\tilde{u}_3\theta_2} = e^{\tilde{u}_3\theta_2} \quad (4-4)$$

$$\hat{C}^{(2,3)} = e^{\tilde{u}_1\beta_3} e^{\tilde{u}_3\theta_3} = e^{\tilde{u}_3\theta_3} \quad (4-75)$$

$$\hat{C}^{(3,4)} = e^{\tilde{u}_1\beta_4} e^{\tilde{u}_3\theta_4} = e^{\tilde{u}_3\theta_4} \quad (4-76)$$

$$\hat{C}^{(4,5)} = e^{-\tilde{u}_3\pi/2} \quad (4-7)$$

$$\hat{C}^{(5,g)} = e^{-\tilde{u}_2\pi/2} \quad (4-8)$$

$$\hat{C}^{(0,5)} = \hat{C}^{(0,g)} \hat{C}^{(g,5)} = e^{-\tilde{u}_2\pi/2} e^{\tilde{u}_2\pi/2} = \hat{I} \quad (4-9)$$

The rotation matrices, starting from the orientation of the first frame with respect to the global frame:

$$\hat{C}^{(g,1)} = \hat{C}^{(g,0)} \hat{C}^{(0,1)} = e^{\tilde{u}_2\pi/2} e^{\tilde{u}_3\theta_1} \quad (4-10)$$

$$\begin{aligned} \hat{C}^{(g,2)} &= (\hat{C}^{(2,g)})^{-1} = \hat{C}^{(g,0)} \hat{C}^{(0,1)} \hat{C}^{(1,2)} = e^{\tilde{u}_2\pi/2} e^{\tilde{u}_3\theta_1} e^{\tilde{u}_3\theta_2} \\ &= e^{\tilde{u}_2\pi/2} e^{\tilde{u}_3(\theta_1+\theta_2)} \end{aligned} \quad (4-11)$$

$$\begin{aligned}
\hat{C}^{(g,3)} &= (\hat{C}^{(3,g)})^{-1} = \hat{C}^{(g,0)} \hat{C}^{(0,1)} \hat{C}^{(1,2)} \hat{C}^{(2,3)} \\
&= e^{\tilde{u}_2\pi/2} e^{\tilde{u}_3\theta_1} e^{\tilde{u}_3\theta_2} e^{\tilde{u}_3\theta_3} = e^{\tilde{u}_2\pi/2} e^{\tilde{u}_3(\theta_1+\theta_2+\theta_3)} \\
&= e^{\tilde{u}_2\pi/2} e^{\tilde{u}_3\pi/2} e^{-\tilde{u}_3\theta_4}
\end{aligned} \tag{4-77}$$

$$\begin{aligned}
\hat{C}^{(g,4)} &= (\hat{C}^{(4,g)})^{-1} = \hat{C}^{(g,0)} \hat{C}^{(0,1)} \hat{C}^{(1,2)} \hat{C}^{(2,3)} \hat{C}^{(3,4)} \\
&= e^{\tilde{u}_2\pi/2} e^{\tilde{u}_3\theta_1} e^{\tilde{u}_3\theta_2} e^{\tilde{u}_3\theta_3} e^{\tilde{u}_3\theta_4} \\
&= e^{\tilde{u}_2\pi/2} e^{\tilde{u}_3(\theta_1+\theta_2+\theta_3+\theta_4)} = e^{\tilde{u}_2\pi/2} e^{\tilde{u}_3\pi/2}
\end{aligned} \tag{4-78}$$

$$\begin{aligned}
\hat{C}^{(g,5)} &= (\hat{C}^{(5,g)})^{-1} = \hat{C}^{(g,0)} \hat{C}^{(0,1)} \hat{C}^{(1,2)} \hat{C}^{(2,3)} \hat{C}^{(3,4)} \hat{C}^{(4,5)} \\
&= e^{\tilde{u}_2\pi/2} e^{\tilde{u}_3\theta_1} e^{\tilde{u}_3\theta_2} e^{\tilde{u}_3\theta_3} e^{\tilde{u}_3\theta_4} e^{-\tilde{u}_3\pi/2} \\
&= e^{\tilde{u}_2\pi/2} e^{\tilde{u}_3(\theta_1+\theta_2+\theta_3+\theta_4-\pi/2)} = e^{\tilde{u}_2\pi/2}
\end{aligned} \tag{4-79}$$

The loop closure equation is:

$$\begin{aligned}
&|AB|e^{\tilde{u}_2\pi/2} e^{\tilde{u}_3\theta_1} \bar{u}_1 + |BC|e^{\tilde{u}_2\pi/2} e^{\tilde{u}_3\theta_1} \bar{u}_3 + |CD|e^{\tilde{u}_2\pi/2} e^{\tilde{u}_3(\theta_1+\theta_2)} \bar{u}_1 \\
&\quad + |DE|e^{\tilde{u}_2\pi/2} e^{\tilde{u}_3\pi/2} e^{-\tilde{u}_3\theta_4} \bar{u}_1 - |EE'|e^{\tilde{u}_2\pi/2} e^{\tilde{u}_3\pi/2} \bar{u}_3 \\
&\quad + |E'A'|e^{\tilde{u}_2\pi/2} \bar{u}_1 - |A'A|e^{\tilde{u}_2\pi/2} \bar{u}_2 = \bar{0}
\end{aligned} \tag{4-80}$$

The exponential terms in equation (4-80) are expressed in the open form as:

$$e^{\tilde{u}_2\pi/2} e^{\tilde{u}_3\theta_1} \bar{u}_1 = \bar{u}_2 \sin(\theta_1) - \bar{u}_3 \cos(\theta_1) \tag{4-16}$$

$$e^{\tilde{u}_2\pi/2} e^{\tilde{u}_3\theta_1} \bar{u}_3 = e^{\tilde{u}_2\pi/2} \bar{u}_3 = \bar{u}_1$$

$$e^{\tilde{u}_2\pi/2} e^{\tilde{u}_3(\theta_1+\theta_2)} \bar{u}_1 = \bar{u}_2 \sin(\theta_1 + \theta_2) - \bar{u}_3 \cos(\theta_1 + \theta_2) \tag{4-81}$$

$$e^{\tilde{u}_2\pi/2} e^{\tilde{u}_3(\pi/2-\theta_4)} \bar{u}_1 = \bar{u}_2 \cos(\theta_4) - \bar{u}_3 \sin(\theta_4) \tag{4-82}$$

$$e^{\tilde{u}_2\pi/2} e^{\tilde{u}_3\pi/2} \bar{u}_3 = \bar{u}_1 \tag{4-17}$$

$$e^{\tilde{u}_2\pi/2} \bar{u}_2 = \bar{u}_2 \tag{4-83}$$

$$e^{\tilde{u}_2\pi/2} \bar{u}_1 = -\bar{u}_3 \tag{4-20}$$

Utilizing above equations, equation (4-80) is re-stated as:

$$\begin{aligned}
& \bar{u}_2|AB| \sin(\theta_1) - \bar{u}_3|AB| \cos(\theta_1) + \bar{u}_1|BC| + \bar{u}_2|CD| \sin(\theta_1 + \theta_2) \\
& \quad - \bar{u}_3|CD| \cos(\theta_1 + \theta_2) + \bar{u}_2|DE| \cos(\theta_4) \\
& \quad - \bar{u}_3|DE| \sin(\theta_4) - \bar{u}_1|EE'| - \bar{u}_3|E'A'| - \bar{u}_2|A'A| = \bar{0}
\end{aligned} \tag{4-84}$$

By separating the equations based on the basis vectors, three separate equations can be obtained as follows:

$$|BC| - |EE'| = 0 \tag{4-85}$$

$$|AB| \sin(\theta_1) + |CD| \sin(\theta_1 + \theta_2) + |DE| \cos(\theta_4) - |A'A| = 0 \tag{4-86}$$

$$|AB| \cos(\theta_1) + |CD| \cos(\theta_1 + \theta_2) + |DE| \sin(\theta_4) + |E'A'| = 0 \tag{4-87}$$

From equation (4-85), $|BC| = |EE'|$.

Taking the squares of equations (4-86) and (4-87):

$$\begin{aligned}
& |CD|^2 \sin^2(\theta_1 + \theta_2) \\
& \quad = |A'A|^2 + |AB|^2 \sin^2(\theta_1) + |DE|^2 \cos^2(\theta_4) \\
& \quad \quad - 2|A'A||AB| \sin(\theta_1) - 2|A'A||DE| \cos(\theta_4) \\
& \quad \quad + 2|AB||DE| \sin(\theta_1) \cos(\theta_4)
\end{aligned} \tag{4-88}$$

$$\begin{aligned}
& |CD|^2 \cos^2(\theta_1 + \theta_2) \\
& \quad = |E'A'|^2 + |AB|^2 \cos^2(\theta_1) + |DE|^2 \sin^2(\theta_4) \\
& \quad \quad + 2|E'A'||DE| \sin(\theta_4) + 2|E'A'||AB| \cos(\theta_1) \\
& \quad \quad + 2|AB||DE| \sin(\theta_4) \cos(\theta_1)
\end{aligned} \tag{4-89}$$

The summation of the squares of equations (4-86) and (4-87) is:

$$\begin{aligned}
|CD|^2 &= |A'A|^2 + |E'A'|^2 + |AB|^2 + |DE|^2 - 2|A'A||AB| \sin(\theta_1) \\
& \quad - 2|A'A||DE| \cos(\theta_4) + 2|E'A'||DE| \sin(\theta_4) \\
& \quad + 2|E'A'||AB| \cos(\theta_1) \\
& \quad + 2|AB||DE|(\sin(\theta_4) \cos(\theta_1) + \sin(\theta_1) \cos(\theta_4))
\end{aligned} \tag{4-90}$$

To define an implicit relation between the position variables θ_2 and θ_4 , equation (4-90) can be stated in the form of Freudenstein's Equation [21] as:

$$K_5 = K_1 \sin(\theta_1) + K_2 \cos(\theta_4) + K_3 \sin(\theta_4) + K_4 \cos(\theta_1) + \sin(\theta_4 - \theta_1) \quad (4-91)$$

Where the coefficients K_1, K_2, K_3, K_4 and K_5 of equation (4-91) are:

$$K_1 = -\frac{|A'A|}{|DE|} \quad (4-92)$$

$$K_2 = -\frac{|A'A|}{|AB|} \quad (4-93)$$

$$K_3 = \frac{|E'A'|}{|AB|} \quad (4-94)$$

$$K_4 = \frac{|E'A'|}{|DE|} \quad (4-95)$$

$$K_5 = \frac{|CD|^2 - |A'A|^2 - |E'A'|^2 - |AB|^2 - |DE|^2}{2|AB||DE|} \quad (4-96)$$

Defining the half-tangent of θ_4 as X :

$$\tan\left(\frac{\theta_4}{2}\right) = X \quad (4-97)$$

Using the tangent half-angle formula form of sine and cosine terms, Freudenstein's Equation (4-91) becomes:

$$\begin{aligned} K_5 - K_1 \sin(\theta_1) - K_2 \frac{1 - X^2}{1 + X^2} - K_3 \frac{2X}{1 + X^2} - K_4 \cos(\theta_1) \\ = \frac{2X}{1 + X^2} \cos(\theta_1) + \sin(\theta_1) \frac{1 - X^2}{1 + X^2} \end{aligned} \quad (4-98)$$

Grouping the X^2 , X and other terms of equation (4-98):

$$\begin{aligned}
& K_5 X^2 - K_1 \sin(\theta_1) X^2 + K_2 X^2 - K_4 \cos(\theta_1) X^2 + \sin(\theta_1) X^2 - 2K_3 X \\
& \quad - 2 \cos(\theta_1) X + K_5 - K_1 \sin(\theta_1) - K_2 - K_4 \cos(\theta_1) \quad (4-99) \\
& \quad - \sin(\theta_1) = 0
\end{aligned}$$

Equation (4-99) can be simplified to:

$$AX^2 + BX + C = 0 \quad (4-100)$$

Where terms A , B and C , which are functions of θ_4 are:

$$A = K_5 - K_1 \sin(\theta_1) + K_2 - K_4 \cos(\theta_1) + \sin(\theta_1) \quad (4-101)$$

$$B = -2K_3 - 2 \cos(\theta_1) \quad (4-102)$$

$$C = K_5 - K_1 \sin(\theta_1) - K_2 - K_4 \cos(\theta_1) - \sin(\theta_1) \quad (4-103)$$

Therefore θ_4 , for each value of θ_1 is:

$$\theta_4 = 2 \tan^{-1} \left(\frac{-B \pm \sqrt{B^2 - 4AC}}{2A} \right) \quad (4-104)$$

The plus or minus sign in equation (4-104) refers to two different closures of the four-bar mechanism.

4.2.2.1 Numerical Example

Point coordinate set and link lengths are given at the fully extended position of the landing gear.

Table 4.14 Point Coordinates at Extended Position

| Points | Coordinates | | | Link | Length (mm) |
|--------|-------------|--------|--------|------|-------------|
| | x (mm) | y (mm) | z (mm) | | |
| A | 6855 | 1390 | 1055 | AB | 145 |
| | | | | BC | 115 |
| | | | | CD | 260.1 |
| B | 6855 | 1390 | 910 | DE | 220 |
| | | | | A'A | 320 |
| C | 6970 | 1390 | 910 | E'A' | 75 |
| D | 6970 | 1130 | 918.3 | AE' | 328.7 |
| E | 6970 | 1070 | 1130 | | |
| E' | 6855 | 1070 | 1130 | | |

For the given system, θ_4 is the rotation of drag beam for the given input rotation θ_1 of landing gear strut is given in Figure 4.8 below.

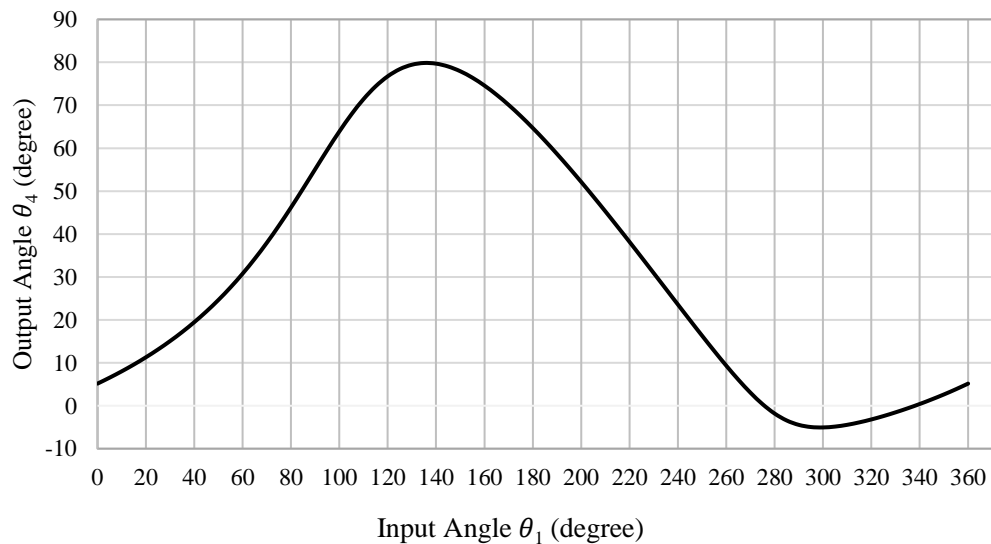


Figure 4.8. The Correlation of Input angle θ_1 with Output Angle θ_4

4.2.3 Path Generation Synthesis of the RRRR Mechanism with Shock Absorber as the Output Link

Similar to the RRPR mechanism, tracer point P represents the wheel center (axle center) of the landing gear.

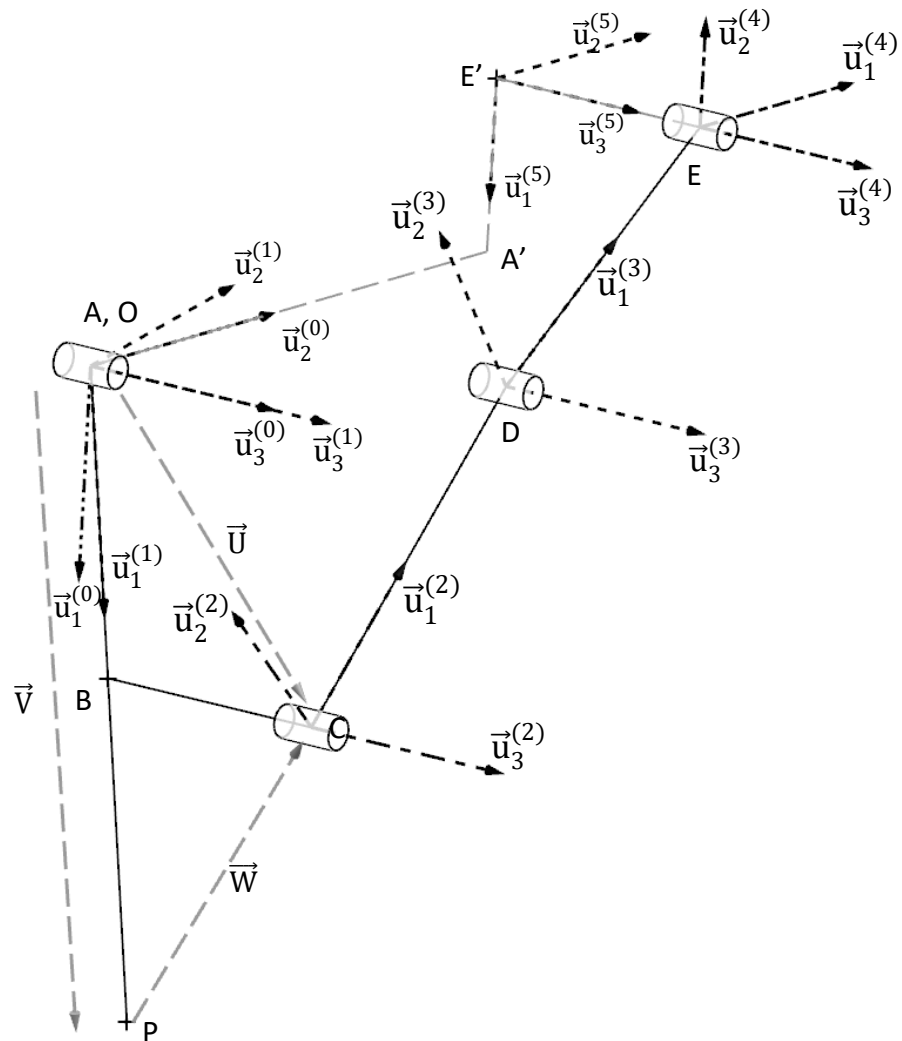


Figure 4.9. Isometric View of RRRR Mechanism with S/A as the Output Link for Path Generation

The link on which the precision point is located is the first link of the mechanism, which is the landing gear itself.

Equations (4-29) to (4-37) defined for RRPR mechanism are also applicable for the RRRR mechanism.

Vectors that originate from the origin of global frame towards the precision points are defined as:

$$\hat{C}^{(g,1)}\bar{V}^{(1)} = \bar{R}_i \quad (4-38)$$

$$\begin{aligned} \hat{C}^{(g,1)}\bar{W}^{(1)} + |CD|\hat{C}^{(g,2)}\bar{u}_1 + |DE|\hat{C}^{(g,3)}\bar{u}_1 - |E'E|\hat{C}^{(g,4)}\bar{u}_3 \\ - |A'A|\hat{C}^{(g,5)}\bar{u}_2 + |E'A'|\hat{C}^{(g,5)}\bar{u}_1 = -\bar{R}_i \end{aligned} \quad (4-105)$$

For any i^{th} position of the tracing point, using the rotation matrix definitions from equations (4-2) to (4-11) and (4-77) to (4-79), equations (4-38) and (4-105) can be re-written as:

$$V_z e^{\tilde{u}_2\pi/2} e^{\tilde{u}_3\theta_1^i} (\bar{u}_1 V_x + \bar{u}_2 V_y + \bar{u}_3 V_z) = \bar{u}_1 R_{ix} + \bar{u}_2 R_{iy} + \bar{u}_3 R_{iz} \quad (4-40)$$

$$\begin{aligned} e^{\tilde{u}_2\pi/2} e^{\tilde{u}_3\theta_1^i} (\bar{u}_1 W_x + \bar{u}_2 W_y + \bar{u}_3 W_z) + |CD| e^{\tilde{u}_2\pi/2} e^{\tilde{u}_3(\theta_1^i + \theta_2^i)} \bar{u}_1 \\ + |DE| e^{\tilde{u}_2\pi/2} e^{\tilde{u}_3\pi/2} e^{-\tilde{u}_3\theta_4^i} \bar{u}_1 - |EE'| e^{\tilde{u}_2\pi/2} e^{\tilde{u}_3\pi/2} \bar{u}_3 \\ - |A'A| e^{\tilde{u}_2\pi/2} \bar{u}_2 + |E'A'| e^{\tilde{u}_2\pi/2} \bar{u}_1 \\ = -\bar{u}_1 R_{ix} - \bar{u}_2 R_{iy} - \bar{u}_3 R_{iz} \end{aligned} \quad (4-106)$$

Equations (4-40) and (4-106) can be separated into their components as:

$$\begin{aligned} \bar{u}_1 V_z + \bar{u}_2 V_x \sin(\theta_1^i) + \bar{u}_2 V_y \cos(\theta_1^i) - \bar{u}_3 V_x \cos(\theta_1^i) + \bar{u}_3 V_y \sin(\theta_1^i) \\ = \bar{u}_1 R_{ix} + \bar{u}_2 R_{iy} + \bar{u}_3 R_{iz} \end{aligned} \quad (4-43)$$

$$\begin{aligned} \bar{u}_1 W_z + \bar{u}_2 W_x \sin(\theta_1^i) - \bar{u}_3 W_x \cos(\theta_1^i) + \bar{u}_2 W_y \cos(\theta_1^i) \\ + \bar{u}_3 W_y \sin(\theta_1^i) + \bar{u}_2 |CD| \sin(\theta_1^i + \theta_2^i) \\ - \bar{u}_3 |CD| \cos(\theta_1^i + \theta_2^i) + \bar{u}_2 |DE| \cos(\theta_4^i) \\ - \bar{u}_3 |DE| \sin(\theta_4^i) - \bar{u}_1 |E'E| - \bar{u}_3 |E'A'| - \bar{u}_2 |A'A| \\ = -\bar{u}_1 R_{ix} - \bar{u}_2 R_{iy} - \bar{u}_3 R_{iz} \end{aligned} \quad (4-107)$$

Initial (Fully Extended) Position

For the initial position P_0 , equation (4-43) can be separated into its components as equations (4-33), (4-46) and (4-47). For the initial position, equation (4-107) can be separated into its components as:

Table 4.15 Components of Equation (4-107) for the Initial Position P_0

| Axis | Equations | Unknowns | Eq. # |
|-------------|---|---|---------|
| \bar{u}_1 | $W_z - EE' = -R_{0x}$ | $W_z, EE' $ | (4-108) |
| \bar{u}_2 | $W_x \sin(\theta_1^0) + W_y \cos(\theta_1^0) + CD \sin(\theta_1^0 + \theta_2^0) + DE \cos(\theta_4^0) - A'A = -R_{0y}$ | $\theta_1^0, \theta_2^0, \theta_4^0, CD , DE , W_x, A'A $ | (4-109) |
| \bar{u}_3 | $W_y \sin(\theta_1^0) - W_x \cos(\theta_1^0) - CD \cos(\theta_1^0 + \theta_2^0) - DE \sin(\theta_4^0) - E'A' = -R_{0z}$ | $\theta_1^0, \theta_2^0, \theta_4^0, CD , DE , W_x, E'A' $ | (4-110) |

As a certification requirement, a locking mechanism shall be provided to keep the gear extended. Therefore, the initial position is chosen to be at dead center, thus θ_2^0 and θ_4^0 can be found as:

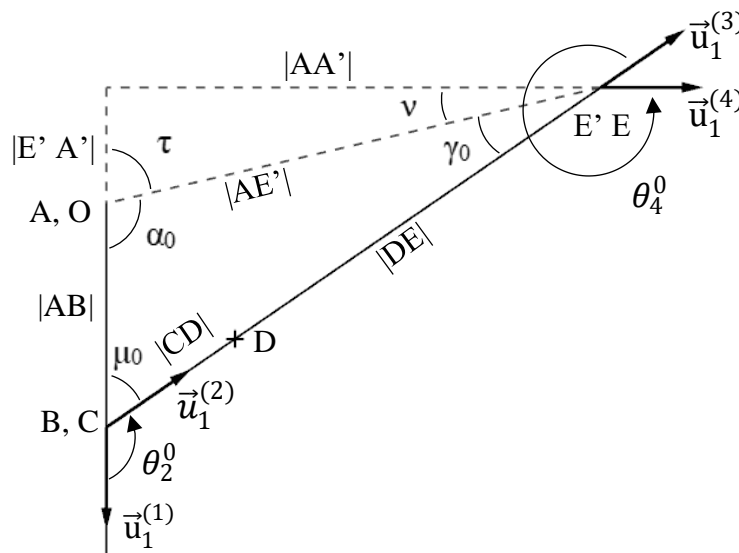


Figure 4.10. Side View of The Mechanism at Extended Dead Center Position

$$\theta_2^0 = 180^\circ - \text{atan2}(|AA'|, |E'A'| + |AB|) \quad (4-111)$$

$$\theta_4^0 = 450^\circ - \theta_2^0 \quad (4-112)$$

$$|CD| + |DE| = ((|E'A'| + |AB|)^2 + |AA'|^2)^{0.5} \quad (4-113)$$

From law of sines, the relation between link lengths and angles at the initial position of the mechanism is:

$$\frac{|AB|}{\sin(\gamma_0)} = \frac{(|E'A'|^2 + |AA'|^2)^{0.5}}{\sin(\mu_0)} = \frac{|CD| + |DE|}{\sin(\alpha_0)} \quad (4-114)$$

Where γ and μ being the initial crank rotation and the transmission angle. α is the angle between the projected line connecting the two ends of the stationary link and the output link.

In-between Position

Assuming that the path tracer point can pass through at most 3 points, P_0 , P_1 and P_2 , for the in-between position P_1 , equation (4-43) can be separated into its components as equations (4-33), (4-51) and (4-52). For the in-between position P_1 equation (4-107) can be separated into its components as:

Table 4.16 Components of Equation (4-107) for the In-Between Position P_1

| Axis | Equations | Unknowns | Eq. # |
|-------------|---|---|---------|
| \bar{u}_1 | $W_z - EE' = -R_{1x}$ | $W_z, EE' $ | (4-115) |
| \bar{u}_2 | $W_x \sin(\theta_1^1) + W_y \cos(\theta_1^1) + CD \sin(\theta_1^1 + \theta_2^1) + DE \cos(\theta_4^1) - A'A = -R_{1y}$ | $\theta_1^1, \theta_2^1, \theta_4^1, CD , DE , W_x, A'A $ | (4-116) |
| \bar{u}_3 | $W_y \sin(\theta_1^1) - W_x \cos(\theta_1^1) - CD \cos(\theta_1^1 + \theta_2^1) - DE \sin(\theta_4^1) - E'A' = -R_{1z}$ | $\theta_1^1, \theta_2^1, \theta_4^1, CD , DE , W_x, E'A' $ | (4-117) |

Final (Fully Retracted) Position

For the fully retracted position P_2 equation (4-43) can be separated into its components as equations (4-33), (4-56) and (4-57). For fully retracted position P_2 equation (4-107) can be separated into its components as:

Table 4.17 Components of Equation (4-107) for the Final Position P_2

| Axis | Equations | Unknowns | Eq. # |
|-------------|---|---|---------|
| \bar{u}_1 | $W_z - EE' = -R_{2x}$ | $W_z, EE' $ | (4-118) |
| \bar{u}_2 | $W_x \sin(\theta_1^2) + W_y \cos(\theta_1^2) + CD \sin(\theta_1^2 + \theta_2^2) + DE \cos(\theta_4^2) - A'A = -R_{2y}$ | $\theta_1^2, \theta_2^2, \theta_4^2, CD , DE , W_x, A'A $ | (4-119) |
| \bar{u}_3 | $W_y \sin(\theta_1^2) - W_x \cos(\theta_1^2) - CD \cos(\theta_1^2 + \theta_2^2) - DE \sin(\theta_4^2) - E'A' = -R_{2z}$ | $\theta_1^2, \theta_2^2, \theta_4^2, CD , DE , W_x, E'A' $ | (4-120) |

As a certification requirement, a locking mechanism shall be provided to keep the gear retracted. Therefore, the final position is chosen to be at the folded dead center, thus θ_2^0 and θ_4^0 can be found as:

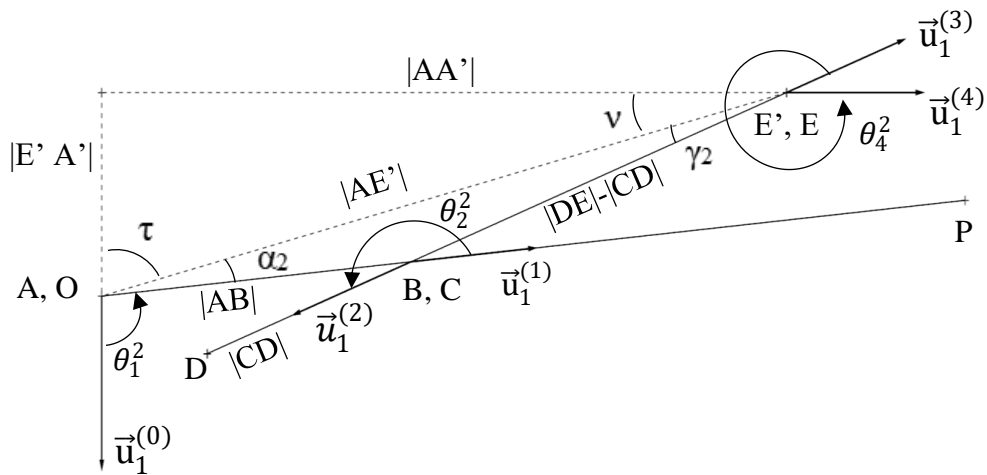


Figure 4.11. Side View of The Mechanism at Folded Dead Center Position

$$\alpha_2 = 180^\circ - \theta_1^2 - \tan^{-1} \left(\frac{|AA'|}{|E'A'|} \right) \quad (4-121)$$

From law of sines, the relation between link lengths and angles at the final position of the mechanism is:

$$\frac{|AB|}{\sin(\gamma_2)} = \frac{(|E'A'|^2 + |AA'|^2)^{0.5}}{\sin(\theta_2^2)} = \frac{|DE| - |CD|}{\sin(\alpha_2)} \quad (4-122)$$

From law of cosines, the relation between link lengths and the angle α_2 at the final position of the mechanism is:

$$\cos(\alpha_2) = \frac{|AB|^2 + |E'A'|^2 + |AA'|^2 - (|DE| - |CD|)^2}{2 |AB| (|E'A'|^2 + |AA'|^2)^{0.5}} \quad (4-123)$$

4.2.3.1 Prescribed Orientations of Fixed Joints

Table 4.18 The Number of Unknown Parameters and Free Parameters for the Three Positions of RRRR Mechanism with Shock Absorber as the Output Link, for the Synthesis Task When Orientations of Fixed Joints are Prescribed

| # of Precision Points | # of Scalar Equations | # of Unknowns | Unknowns | # of Free Parameters |
|-----------------------|-----------------------|---------------|---|----------------------|
| 1 | 7 | 8 | $ AB , BC , CD , DE , W_x, W_z, V_x, \theta_1^0$ | 1 |
| 2 | 9 | 11 | $ AB , BC , CD , DE , W_x, W_z, V_x, \theta_1^0, \theta_1^1, \theta_2^1, \theta_4^1$ | 1 |
| 3 | 13 | 14 | $ AB , BC , CD , DE , W_x, W_z, V_x, \theta_1^0, \theta_1^1, \theta_2^1, \theta_4^1, \theta_1^2, \theta_2^2, \theta_4^2$ | 1 |

Table 4.19 Equation Set to be Used for the RRRR Mechanism (with Shock Absorber as the Output Link) Synthesis Task When Orientations of Fixed Joints are Prescribed

| Equations | Unknowns | Eq. # |
|--|---|---------|
| $W_z - EE' = -R_{0x}$ | W_z | (4-108) |
| $W_z = BC $ | $W_z, BC $ | (4-37) |
| $V_x \sin(\theta_1^0) = R_{0y}$ | V_x, θ_1^0 | (4-46) |
| $-V_x \cos(\theta_1^0) = R_{0z}$ | V_x, θ_1^0 | (4-47) |
| $\theta_1^1 = -atan2(R_{1y}, R_{1z})$ | θ_1^1 | (4-61) |
| $\theta_1^2 = -atan2(R_{2y}, R_{2z})$ | θ_1^2 | (4-62) |
| $V_x + W_x = AB $ | $V_x, W_x, AB $ | (4-35) |
| $\alpha_2 = 180^\circ - \theta_1^2 - atan2(AA' , E'A')$ | α_2 | (4-121) |
| $(DE - CD)^2 = AB ^2 + E'A' ^2 + AA' ^2 - 2 \cos(\alpha_2) AB (E'A' ^2 + AA' ^2)^{0.5}$ | $ CD , DE , \alpha_2$ | (4-123) |
| $ CD + DE = ((E'A' + AB)^2 + AA' ^2)^{0.5}$ | $ CD , DE $ | (4-124) |
| $W_x \sin(\theta_1^1) + CD \sin(\theta_1^1 + \theta_2^1) + DE \cos(\theta_4^1) - A'A = -R_{1y}$ | $\theta_1^1, \theta_2^1, \theta_4^1, CD , DE , W_x$ | (4-116) |
| $-W_x \cos(\theta_1^1) - CD \cos(\theta_1^1 + \theta_2^1) - DE \sin(\theta_4^1) - E'A' = -R_{1z}$ | $\theta_1^1, \theta_2^1, \theta_4^1, CD , DE , W_x$ | (4-117) |
| $\cos(\gamma_2) = \frac{(DE - CD)^2 + E'A' ^2 + AA' ^2 - AB ^2}{2(DE - CD) (E'A' ^2 + AA' ^2)^{0.5}}$ | $\gamma_2, CD , DE , AB $ | (4-125) |
| $\cos(\theta_2^2) = \frac{ AB ^2 + (DE - CD)^2}{2(DE - CD) AB } - \frac{ E'A' ^2 + AA' ^2}{2(DE - CD) AB }$ | $\theta_2^2, CD , DE , AB $ | (4-126) |

Utilizing equation (4-32), synthesis equations are given in their simplified versions in Table 4.19. If the free parameter is chosen to be the crank length $|AB|$, the axial position of actuator connection on trunnion:

- Based on the initial position of the mechanism, θ_2^0 and θ_4^0 are found from equations (4-111) and (4-112) respectively.
- From equations (4-108) and (4-37), $|BC|$ and W_z can be found.
- From equations (4-46) and (4-47), V_x and θ_1^0 can be found. θ_1^1 and θ_1^2 can be found from equation (4-61) and (4-62) respectively.
- W_x can be found from equation (4-35).
- From equations (4-123) and (4-124)(4-110), $|CD|$ and $|DE|$ can be found.
- θ_2^1 and θ_4^1 can be found by the equation set of (4-116) and (4-117).
- θ_2^2 and θ_4^2 can be found by the equation set of (4-125), (4-126) and (4-122).

4.2.3.2 Unprescribed Positions of the Ground Pivots

Using equations (4-32) and (4-33) R_{0x} , R_{1x} , R_{2x} , V_y , W_y and V_z are known. Utilizing the classical transmission angle problem to determine the crank-rocker proportions of a four-bar mechanism with a given swing angle ϕ and corresponding crank rotation ψ such that the maximum deviation of the transmission angle from 90° is a minimized. There exists a particular four-bar mechanism amongst infinite options that provides deviation of the transmission angle from 90° is a minimum.

Considering λ as the ratio of coupler link length to the crank length, and γ as the initial crank angle, one can obtain optimum four-bar mechanism proportions a_1 , a_2 , a_3 and a_4 as follows obeying the limits for swing angle and crank rotation of $0 < \psi < 180^\circ$ and $90^\circ + \frac{1}{2}\psi < \phi < 270^\circ + \frac{1}{2}\psi$.

$$\psi = \theta_1^2 - \theta_1^0 \quad (4-127)$$

$$\phi = \theta_4^2 - \theta_4^0 \quad (4-128)$$

$$\lambda = \frac{a_3}{a_2} = \frac{|CD|}{|DE|} \quad (4-129)$$

$$t = \tan\left(\frac{1}{2}\phi\right) \quad (4-130)$$

$$u = \tan\left(\frac{1}{2}(\phi - \psi)\right) \quad (4-131)$$

$$v = \tan\left(\frac{1}{2}\psi\right) \quad (4-132)$$

$$a_1^2 = \frac{u^2 + \lambda^2}{1 + u} \quad (4-133)$$

$$a_2^2 = \frac{v^2}{1 + v^2} \quad (4-134)$$

$$a_3^2 = \frac{\lambda^2 v^2}{1 + v^2} \quad (4-135)$$

$$a_4^2 = \frac{t^2 + \lambda^2}{1 + t^2} \quad (4-136)$$

$$\frac{(|E'A'|^2 + |AA'|^2)^{0.5}}{a_1} = \frac{|DE|}{a_2} = \frac{|CD|}{a_3} = \frac{|AB|}{a_4} \quad (4-137)$$

For a selected crank rotation, ϕ , t and u can be found from equations (4-130) and (4-131); therefore λ_{opt} can be found by the root of the equation (4-139) where:

$$Q = t^2 / \lambda_{opt}^2 \quad (4-138)$$

$$Q^3 + 2Q^2 - t^2Q - \frac{t^2(1 + t^2)}{u^2} \quad (4-139)$$

Solving equation (4-139) for the root that is between $\frac{1}{u^2} < Q < t^2$ yields λ_{opt} .

From the link lengths, initial crank rotation can be found as:

$$\beta = \text{atan2}(|E'A'| + |AB|, |AA'|) \quad (4-140)$$

Table 4.20 The Number of Unknown Parameters and Free Parameters for the Three Positions of RRRR Mechanism with Shock Absorber as the Output Link, for the Synthesis Task When Orientations of Fixed Joints are Unprescribed

| # of Precision Points | # of Scalar Equations | # of Unknowns | Unknowns | # of Free Parameters |
|-----------------------|-----------------------|---------------|---|----------------------|
| 1 | 10 | 11 | $ AB , BC , CD , DE , AA' , E'A' , W_x, W_z, V_x, \beta, \theta_1^0$ | 1 |
| 2 | 13 | 14 | $ AB , BC , CD , DE , AA' , E'A' , W_x, W_z, V_x, \beta, \theta_1^0, \theta_1^1, \theta_2^1, \theta_4^1$ | 1 |
| 3 | 16 | 17 | $ AB , BC , CD , DE , AA' , E'A' , W_x, W_z, V_x, \beta, \theta_1^0, \theta_1^1, \theta_2^1, \theta_4^1, \theta_2^2, \theta_4^2$ | 1 |

Table 4.21 Equation Set to be Used for the RRRR Mechanism (with Shock Absorber as the Output Link) Synthesis Task When Orientations of Fixed Joints are Unprescribed

| Equations | Unknowns | Eq. # |
|---------------------------------------|-------------------|---------|
| $W_z - EE' = -R_{0x}$ | W_z | (4-108) |
| $W_z = BC $ | $W_z, BC $ | (4-37) |
| $V_x \sin(\theta_1^0) = R_{0y}$ | V_x, θ_1^0 | (4-46) |
| $-V_x \cos(\theta_1^0) = R_{0z}$ | V_x, θ_1^0 | (4-47) |
| $\theta_1^1 = -atan2(R_{1y}, R_{1z})$ | θ_1^1 | (4-61) |
| $\theta_1^2 = -atan2(R_{2y}, R_{2z})$ | θ_1^2 | (4-62) |
| $V_x + W_x = AB $ | $V_x, W_x, AB $ | (4-35) |

Table 4.21 Continued

| Equations | Unknowns | Eq. # |
|--|---|---------|
| $\theta_4^0 = 450^\circ - \theta_2^0$ | θ_2^0, θ_4^0 | (4-112) |
| $\frac{(E'A' ^2 + AA' ^2)^{0.5}}{a_1} = \frac{ DE }{a_2} = \frac{ CD }{a_3} = \frac{ AB }{a_4}$ | $ AA' , E'A' , AB ,$ $ CD , DE $ | (4-137) |
| $\cos(\mu_0)$ $= \frac{(CD + DE)^2 + AB ^2 - 2\left(AB \frac{a_1}{a_4}\right)^2}{2 AB (CD + DE)}$ | $ AB ,$ $ CD , DE $ | (4-141) |
| $W_x \sin(\theta_1^0) + CD \sin(\theta_1^0 + \theta_2^0)$ $+ DE \cos(\theta_4^0) - A'A = -R_{0y}$ | $\theta_1^0, \theta_2^0, \theta_4^0,$ $ CD , DE , AA' , W_x$ | (4-109) |
| $-W_x \cos(\theta_1^0) - CD \cos(\theta_1^0 + \theta_2^0)$ $- DE \sin(\theta_4^0) - E'A' = -R_{0z}$ | $\theta_1^0, \theta_2^0, \theta_4^0, E'A' $ $ CD , DE , W_x$ | (4-110) |
| $W_x \sin(\theta_1^1) + CD \sin(\theta_1^1 + \theta_2^1)$ $+ DE \cos(\theta_4^1) - A'A = -R_{1y}$ | $\theta_1^1, \theta_2^1, \theta_4^1,$ $ CD , DE , W_x$ | (4-116) |
| $-W_x \cos(\theta_1^1) - CD \cos(\theta_1^1 + \theta_2^1)$ $- DE \sin(\theta_4^1) - E'A' = -R_{1z}$ | $\theta_1^1, \theta_2^1, \theta_4^1,$ $ CD , DE , W_x$ | (4-117) |
| $W_x \sin(\theta_1^2) + CD \sin(\theta_1^2 + \theta_2^2)$ $+ DE \cos(\theta_4^2) - A'A = -R_{2y}$ | $\theta_1^2, \theta_2^2, \theta_4^2,$ $ CD , DE , W_x$ | (4-119) |
| $-W_x \cos(\theta_1^2) - CD \cos(\theta_1^2 + \theta_2^2)$ $- DE \sin(\theta_4^2) - E'A' = -R_{2z}$ | $\theta_1^2, \theta_2^2, \theta_4^2,$ $ CD , DE , W_x$ | (4-120) |

Utilizing equation (4-32), synthesis equations are given in their simplified versions at Table 4.21. If the free parameter is chosen to be the crank length $|AB|$, the axial position of actuator connection on trunnion:

- From equations (4-108) and (4-37), $|BC|$ and W_z can be found.
- From equations (4-46) and (4-47), V_x and θ_1^0 can be found. θ_1^1 and θ_1^2 can be found from equation (4-61) and (4-62) respectively. Therefore ψ and v are known by equations (4-127) and (4-132) respectively.
- W_x can be found from equation (4-35).
- Keeping ϕ as a free parameter, for any ϕ value t and u can be found from equations (4-130) and (4-131). λ_{opt} can be found by the root of the following equations (4-139) and (4-138). Inserting λ_{opt} value into equations (4-133), (4-135) and (4-136) link length proportions a_1 , a_3 and a_4 can be found respectively.
- From equation (4-137), $(|E'A'|^2 + |AA'|^2)^{0.5}$, $|DE|$ and $|CD|$ can be found.
- Considering that the angle μ_0 is an acute angle for the initial position of the mechanism, from the equations (4-141), (4-133) and (4-136):

$$\theta_2^0 = 180^\circ - \mu_0 \quad (4-142)$$

- From equation (4-112) and (4-142), θ_4^0 can be defined alternatively as:

$$\theta_4^0 = 270^\circ - \mu_0 \quad (4-143)$$

- Equations (4-109) and (4-110) can be used to find $|AA'|$ and $|E'A'|$.
- θ_2^1 and θ_4^1 can be found by equation set of (4-112) and (4-117).
- θ_2^2 and θ_4^2 can be found by equation set of (4-119), (4-120) and (4-122).

The transmission angle variation and link lengths shall be evaluated for a variety of ϕ selection.

CHAPTER 5

LANDING GEAR MECHANISMS INVOLVING SPATIAL MOTION

Secondary motion as an additional translation or rotation is introduced into the system for configurations where retracting landing gear around a single axis is insufficient to fit in the available bay volume.

5.1 The SSRR Mechanism

5.1.1 Degree of Freedom of the Constrained SSRR Mechanism

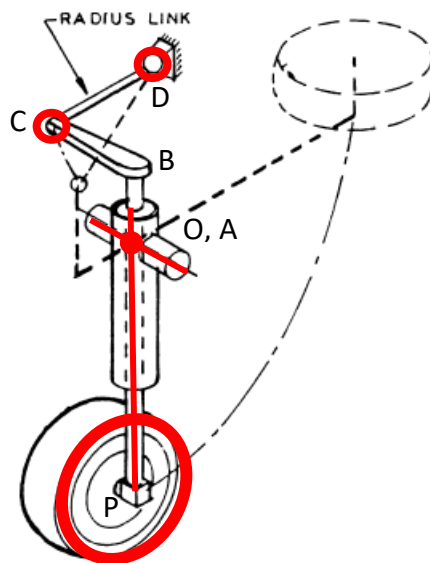


Figure 5.1. SSRR Linkage Landing Gear Hardpoint Definitions [3]

For SSRR mechanism, $\lambda_s = 6$, $n = j = 4$, $f_1 = f_2 = 3$ and, $f_3 = f_4 = 1$. Therefore $DOF = 2$.

The SSRR mechanism possesses two DOF, yet it operates as a single DOF mechanism with an extra passive degree of freedom (insignificant mobility), which involves the rotation of the radius link around its own axis.

5.1.2 General Displacement Equation

Utilizing D-H convention, the reference frames are placed on the mechanism. Frames 0 and 8 are located on the fixed link, which is the structural frame of helicopter for the given case study.

The spherical joints are represented as three consecutive revolute joints that are connected by virtual links. The joint axis sequences for the spherical joints are selected as rotated frame based 3-2-1 and 1-2-3 sequences to simplify the rotation matrices of the equation by eliminating the arbitrary rotation of S-S link.

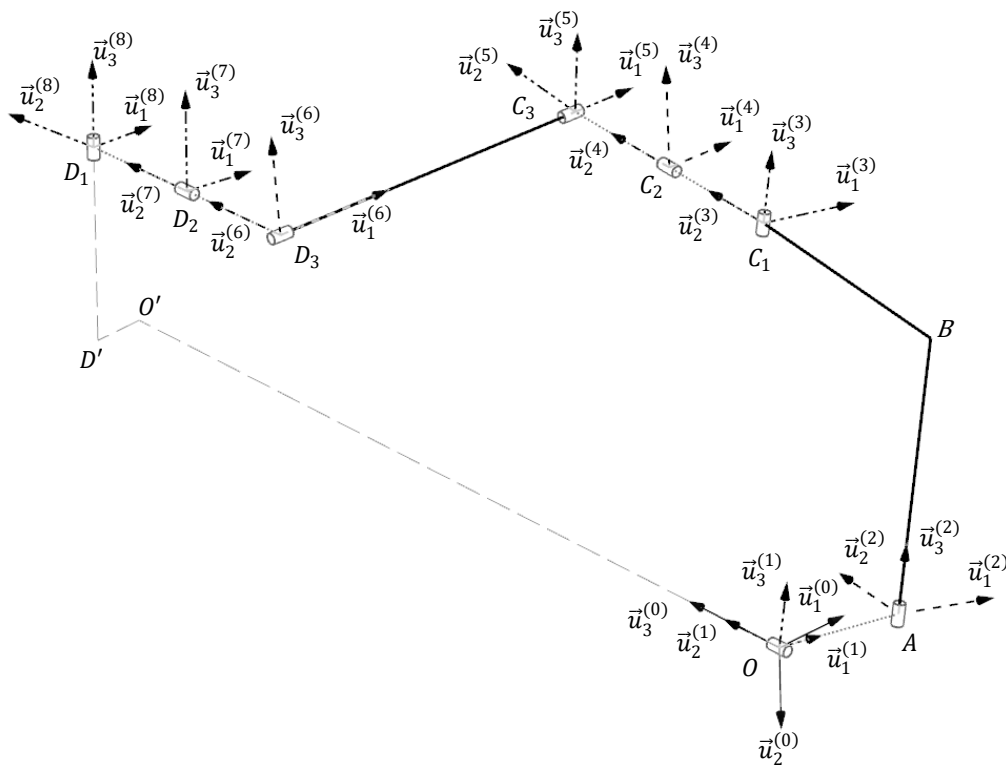


Figure 5.2. Isometric View of SSRR Mechanism with the Shock Absorber as the Output Link

The loop closure equation starting from and ending at the zeroth link is:

$$\begin{aligned}
 & |OA|\hat{C}^{(g,1)}\bar{u}_1 + |AB|\hat{C}^{(g,2)}\bar{u}_3 + |BC_1|\hat{C}^{(g,2)}\bar{u}_2 - |C_1C_2|\hat{C}^{(g,3)}\bar{u}_2 \\
 & \quad - |C_2C_3|\hat{C}^{(g,4)}\bar{u}_2 + |C_3D_3|\hat{C}^{(g,5)}\bar{u}_1 + |D_2D_3|\hat{C}^{(g,6)}\bar{u}_2 \\
 & \quad + |D_1D_2|\hat{C}^{(g,7)}\bar{u}_2 - |OO'|\hat{C}^{(g,0)}\bar{u}_3 + |O'D'|\hat{C}^{(g,0)}\bar{u}_1 \\
 & \quad - |D_1D'|\hat{C}^{(g,8)}\bar{u}_3 = \bar{0}
 \end{aligned} \tag{5-1}$$

where links OA , C_1C_2 , C_2C_3 , D_1D_2 and D_2D_3 are virtual links with lengths of zero.

$$\begin{aligned}
 & |AB|\hat{C}^{(g,2)}\bar{u}_3 + |BC_1|\hat{C}^{(g,2)}\bar{u}_2 + |C_3D_3|\hat{C}^{(g,5)}\bar{u}_1 - |OO'|\hat{C}^{(g,0)}\bar{u}_3 \\
 & \quad + |O'D'|\hat{C}^{(g,0)}\bar{u}_1 - |D_1D'|\hat{C}^{(g,8)}\bar{u}_3 = \bar{0}
 \end{aligned} \tag{5-2}$$

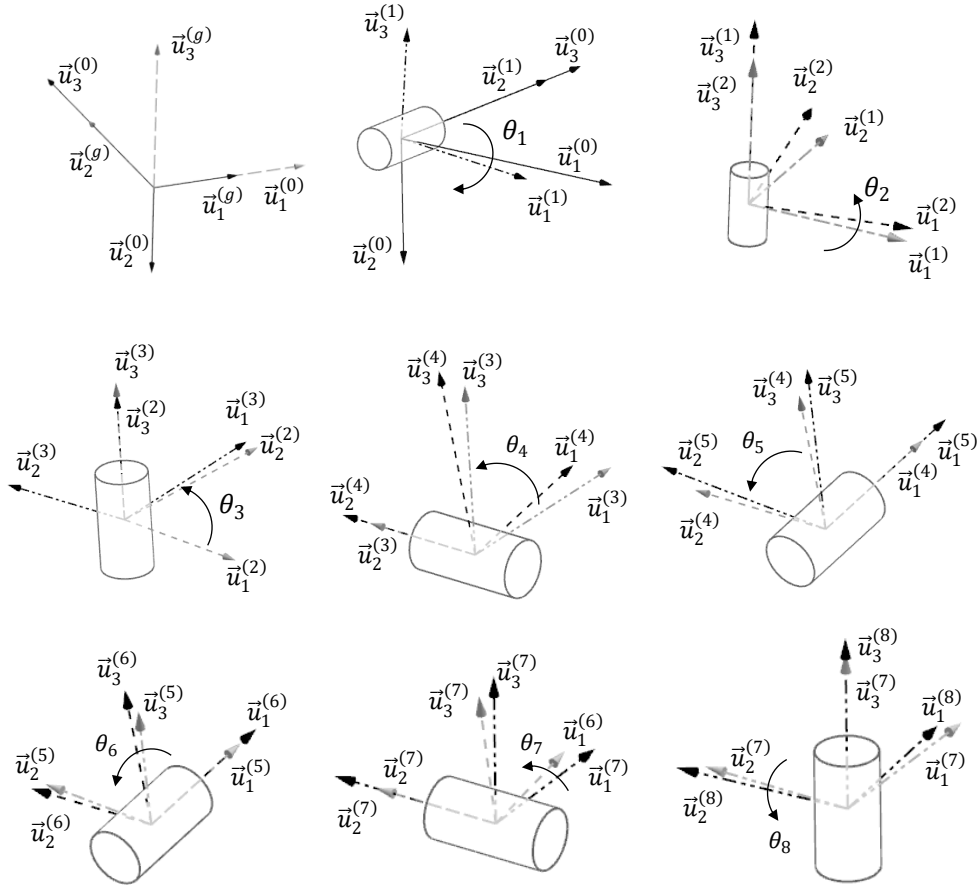


Figure 5.3. Joint Angle and Axis Definitions for the SSRR Mechanism

Based on the angle definitions of each joint given in Figure 5.2, the rotation matrices, starting from the orientation of the zeroth frame with respect to the previous reference frame are:

$$\hat{C}^{(g,0)} = e^{-\tilde{u}_1\pi/2} \quad (5-3)$$

$$\hat{C}^{(0,1)} = e^{\tilde{u}_1\beta_1} e^{\tilde{u}_3\theta_1} = e^{\tilde{u}_3\theta_1} \quad (5-4)$$

$$\hat{C}^{(1,2)} = e^{\tilde{u}_1\beta_2} e^{\tilde{u}_3\theta_2} = e^{\tilde{u}_1\pi/2} e^{\tilde{u}_3\theta_2} \quad (5-5)$$

$$\hat{C}^{(2,3)} = e^{\tilde{u}_1\beta_3} e^{\tilde{u}_3\theta_3} = e^{\tilde{u}_3\theta_3} \quad (5-6)$$

$$\hat{C}^{(3,4)} = e^{\tilde{u}_1\beta_4} e^{\tilde{u}_3\theta_4} = e^{\tilde{u}_2\theta_4} \quad (5-7)$$

$$\hat{C}^{(4,5)} = e^{\tilde{u}_1\beta_5} e^{\tilde{u}_3\theta_5} = e^{\tilde{u}_1\theta_5} \quad (5-8)$$

$$\hat{C}^{(5,6)} = e^{\tilde{u}_1\beta_6} e^{\tilde{u}_3\theta_6} = e^{\tilde{u}_1\theta_6} \quad (5-9)$$

$$\hat{C}^{(6,7)} = e^{\tilde{u}_1\beta_7} e^{\tilde{u}_3\theta_7} = e^{\tilde{u}_2\theta_7} \quad (5-10)$$

$$\hat{C}^{(7,8)} = e^{\tilde{u}_1\beta_8} e^{\tilde{u}_3\theta_8} = e^{\tilde{u}_3\theta_8} \quad (5-11)$$

$$\hat{C}^{(8,g)} = (\hat{C}^{(g,8)})^{-1} = \hat{I} \quad (5-12)$$

$$\hat{C}^{(0,8)} = \hat{C}^{(0,g)} \hat{C}^{(g,8)} = e^{\tilde{u}_1\pi/2} \hat{I} = e^{\tilde{u}_1\pi/2} \quad (5-13)$$

The closure joint is selected to be the spherical joint between radius link and the shock absorber. The necessary rotation matrices, starting from the orientation of the first frame with respect to the global frame:

$$\hat{C}^{(g,1)} = e^{-\tilde{u}_1\pi/2} e^{\tilde{u}_3\theta_1} \quad (5-14)$$

$$\hat{C}^{(g,2)} = e^{-\tilde{u}_1\pi/2} e^{\tilde{u}_3\theta_1} e^{\tilde{u}_1\pi/2} e^{\tilde{u}_3\theta_2} \quad (5-15)$$

$$\begin{aligned} \hat{C}^{(g,5)} &= \hat{C}^{(5,g)^{-1}} = e^{-\tilde{u}_1\pi/2} e^{\tilde{u}_3\theta_1} e^{\tilde{u}_1\pi/2} e^{\tilde{u}_3\theta_2} e^{\tilde{u}_3\theta_3} e^{\tilde{u}_2\theta_4} e^{\tilde{u}_1\theta_5} \\ &= e^{-\tilde{u}_3\theta_8} e^{-\tilde{u}_2\theta_7} e^{-\tilde{u}_1\theta_6} \end{aligned} \quad (5-16)$$

Since the radius link is connected to the fuselage by a spherical joint, the trajectory of point C_3 represents a point traveling on a sphere about the fixed joint located at D_1 . The position of point D_1 relative to point O , represented in the global frame is:

$$\overline{OD_1} = |OO'|e^{-\tilde{u}_1\pi/2}\bar{u}_3 - |O'D'|e^{-\tilde{u}_1\pi/2}\bar{u}_1 - |D_1D'|e^{-\tilde{u}_1\pi/2}\bar{u}_2 \quad (5-17)$$

Which can be written in matrix form as:

$$\overline{OD_1} = \begin{bmatrix} -|O'D'| \\ |OO'| \\ |D_1D'| \end{bmatrix} \quad (5-18)$$

Position of point C_3 relative to point O , represented in the global frame is:

$$\begin{aligned} \overline{OC_3} = & -|AB|e^{-\tilde{u}_1\pi/2}e^{\tilde{u}_3\theta_1}e^{\tilde{u}_1\pi/2}e^{\tilde{u}_3\theta_2}\bar{u}_3 \\ & - |BC_1|e^{-\tilde{u}_1\pi/2}e^{\tilde{u}_3\theta_1}e^{\tilde{u}_1\pi/2}e^{\tilde{u}_3\theta_2}\bar{u}_2 \end{aligned} \quad (5-19)$$

Which can be written in matrix form as:

$$\overline{OC_3} = \begin{bmatrix} |AB|\sin(\theta_1) - |BC_1|\cos(\theta_1)\sin(\theta_2) \\ |BC_1|\cos(\theta_2) \\ |AB|\cos(\theta_1) + |BC_1|\sin(\theta_1)\sin(\theta_2) \end{bmatrix} \quad (5-20)$$

The length of S-S link can be stated as follows:

$$(\overline{OD_1} - \overline{OC_3})^T (\overline{OD_1} - \overline{OC_3}) = |C_3D_3|^2 \quad (5-21)$$

The following equation of motion for SSRR linkage can be written:

$$\begin{aligned} & (|O'D'| + |AB|\sin(\theta_1) - |BC_1|\cos(\theta_1)\sin(\theta_2))^2 \\ & + (|OO'| - |BC_1|\cos(\theta_2))^2 \\ & + (|AB|\cos(\theta_1) + |BC_1|\sin(\theta_1)\sin(\theta_2) - |D_1D'|)^2 \\ & = |C_3D_3|^2 \end{aligned} \quad (5-22)$$

Expanding and reordering the terms of equation (5-22):

$$\begin{aligned}
& |OO'|^2 + |AB|^2 + |BC_1|^2 + |D_1D'|^2 + |O'D'|^2 - |C_3D_3|^2 \\
& \quad - 2|BC_1||OO'| \cos(\theta_2) + 2|O'D'||AB| \sin(\theta_1) \\
& \quad - 2|AB||D_1D'| \cos(\theta_1) \\
& \quad - 2|BC_1||O'D'| \cos(\theta_1) \sin(\theta_2) \\
& \quad - 2|BC_1||D_1D'| \sin(\theta_1) \sin(\theta_2) = 0
\end{aligned} \tag{5-23}$$

The terms of constraint equation (5-23) can be grouped as functions of θ_1 to obtain an equation for θ_2 as:

$$A(\theta_1) \cos(\theta_2) + B(\theta_1) \sin(\theta_2) + C(\theta_1) = 0 \tag{5-24}$$

where the functions $A(\theta_1)$, $B(\theta_1)$, and $C(\theta_1)$ are:

$$A(\theta_1) = -2|BC_1||OO'| \tag{5-25}$$

$$B(\theta_1) = -2|BC_1||O'D'| \cos(\theta_1) - 2|BC_1||D_1D'| \sin(\theta_1) \tag{5-26}$$

$$\begin{aligned}
C(\theta_1) = & |OO'|^2 + |AB|^2 + |BC_1|^2 + |D_1D'|^2 + |O'D'|^2 - |C_3D_3|^2 \\
& + 2|O'D'||AB| \sin(\theta_1) - 2|AB||D_1D'| \cos(\theta_1)
\end{aligned} \tag{5-27}$$

The roots of equation (5-24), which is the relation between the output angle and the coupler angle is [28]:

$$\theta_2(\theta_1) = \tan^{-1} \frac{B(\theta_1)}{A(\theta_1)} \pm \cos^{-1} \frac{C(\theta_1)}{\sqrt{A(\theta_1)^2 + B(\theta_1)^2}} \tag{5-28}$$

It should be noted that real values for coupler angle exists only if the following condition is satisfied:

$$\left| \frac{C(\theta_1)}{\sqrt{A(\theta_1)^2 + B(\theta_1)^2}} \right| \leq 1 \tag{5-29}$$

Therefore, the range of movement for the output link is within the roots of the following equation:

$$A(\theta_1)^2 + B(\theta_1)^2 - C(\theta_1)^2 = 0 \tag{5-30}$$

5.1.2.1 Numerical Example

Point coordinate set and link lengths are given at the fully extended position of the landing gear.

Table 5.1 Point Coordinates at Extended Position

| Points | Coordinates | | | Link | Length (mm) |
|--------|-------------|--------|--------|-------------------------------|-------------|
| | x (mm) | y (mm) | z (mm) | | |
| A | 6855 | -1390 | 815 | AB | 176 |
| | | | | BC ₁ | 210 |
| | | | | C ₃ D ₃ | 204 |
| B | 6855 | -1390 | 991 | D ₁ D' | 196 |
| | | | | O'D' | 203 |
| C | 6970 | -1180 | 991 | OO' | 210 |
| D | 6652 | -1180 | 1011 | | |

For the given system, θ_2 , the rotation of the shock strut around its own axis for the output retraction angle θ_1 of landing gear strut is given in Figure 5.4.

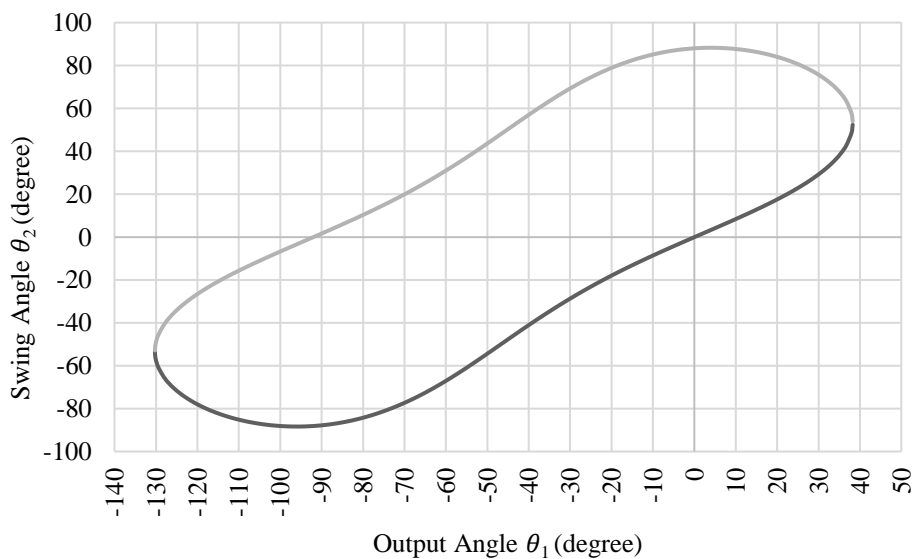


Figure 5.4. The Correlation Between Output Angle θ_1 and Swing Angle θ_2

Based on the classification performed by H. Su et al. [28], and given in Figure 5.5, the correlation plot of Output Angle θ_1 and Swing Angle θ_2 corresponds to a non-Grashof double rocker RRSS linkage.

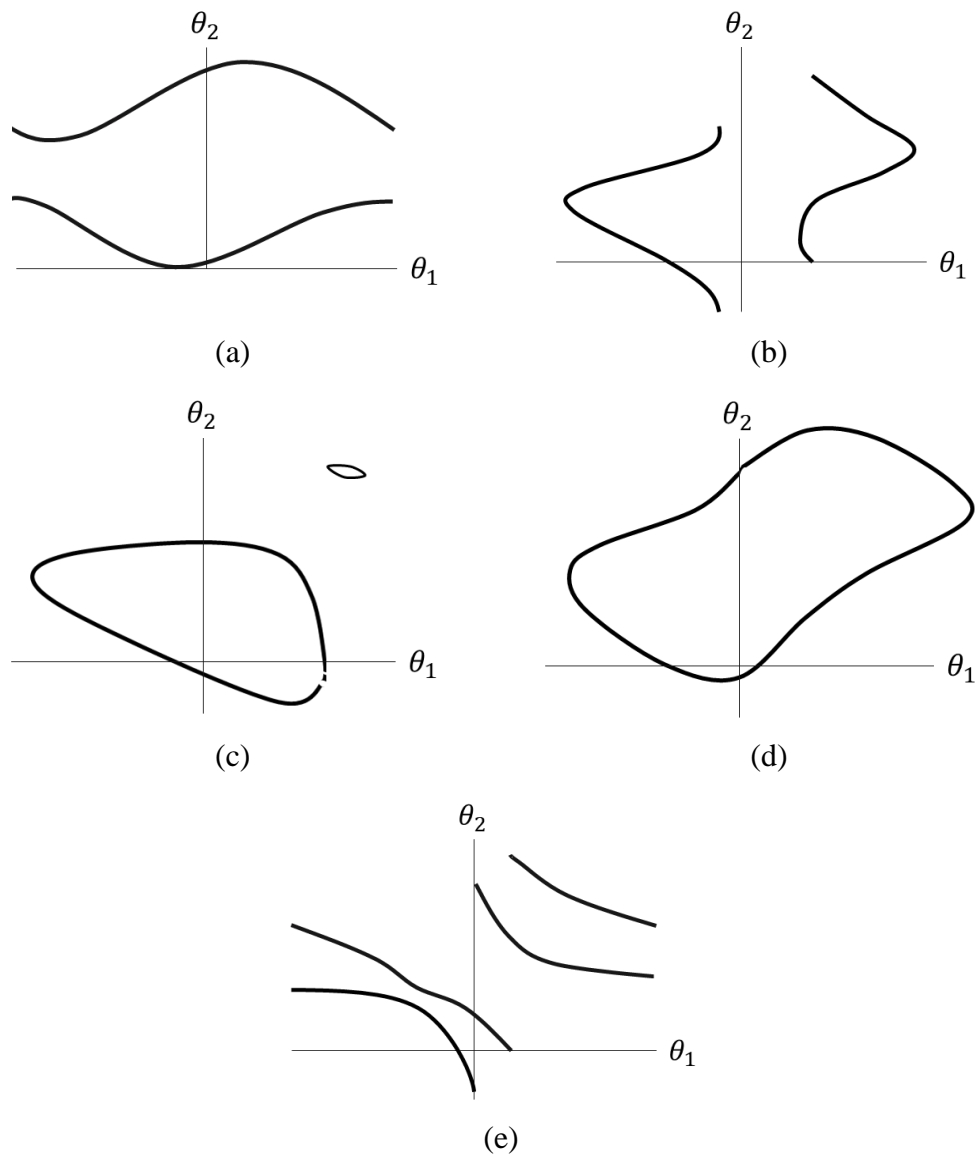


Figure 5.5. Mobility Classification for five types of RRSS Linkages [28] (a) Crank-Rocker, (b) Rocker-Crank, (c) Grashof Double Rocker, (d) Non-Grashof Double Rocker, (e) Double Crank

5.1.3 Path Generation Synthesis of the SSRR Mechanism

Likewise the two other planar mechanisms, tracer point P represents the wheel center (axle center) of the landing gear.

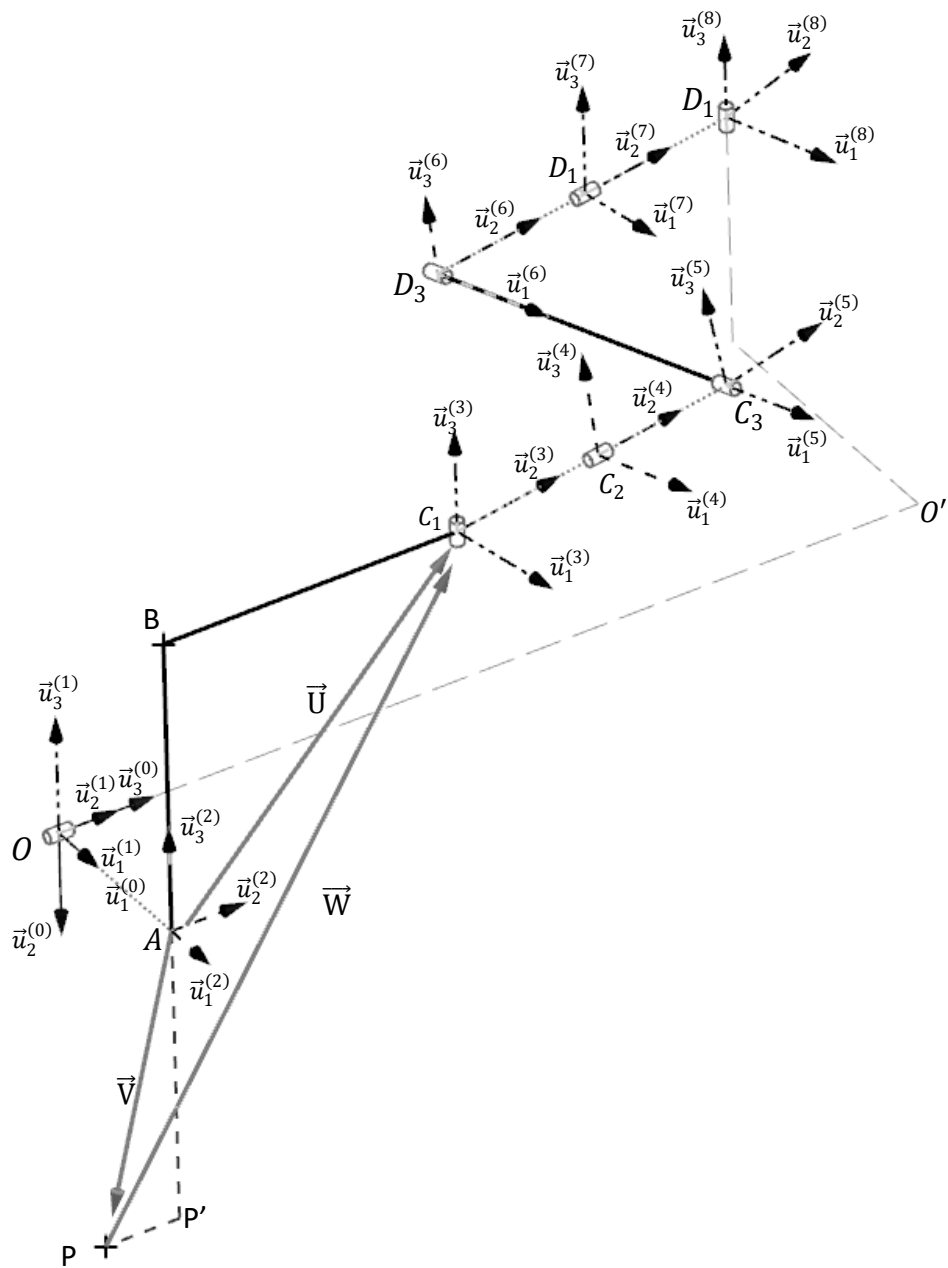


Figure 5.6. Isometric View of SSRR Mechanism with S/A as the Output Link for Path Generation

The link on which the precision point is located is the second link of the mechanism, which is the landing gear itself.

$$\bar{U}^{(2)} = \begin{bmatrix} U_x \\ U_y \\ U_z \end{bmatrix} = \begin{bmatrix} 0 \\ |BC_1| \\ |AB| \end{bmatrix} \quad (5-31)$$

$$\bar{V}^{(2)} = \begin{bmatrix} V_x \\ V_y \\ V_z \end{bmatrix} = \begin{bmatrix} 0 \\ -|PP'| \\ -|AP'| \end{bmatrix} \quad (5-32)$$

$$\bar{W}^{(2)} = \begin{bmatrix} W_x \\ W_y \\ W_z \end{bmatrix} = \begin{bmatrix} 0 \\ |PP'| + |BC_1| \\ |AP'| + |AB| \end{bmatrix} \quad (5-33)$$

for every position on its path, the point P is on the axis of $\vec{u}_3^{(2)}$. Since \vec{U} , \vec{V} and \vec{W} are on the same plane ($\vec{u}_2^{(2)} \times \vec{u}_3^{(2)}$) that is rotating around the axis $\vec{u}_3^{(1)}$, components of the position vectors \vec{V} and \vec{W} are zero. Therefore:

Table 5.2 Components of Position Vectors \vec{V} and \vec{W}

| Axis | Equations | Unknowns | Eq. # |
|-------------|----------------------|-------------------------|--------|
| \bar{u}_1 | $V_x + W_x = 0$ | $U_x = V_x = W_x = 0$ | (5-34) |
| \bar{u}_2 | $V_y + W_y = BC_1 $ | $W_y = - PP' + BC_1 $ | (5-35) |
| \bar{u}_3 | $V_z + W_z = AB $ | $W_z = AP' + AB $ | (5-36) |

Vectors that originate from the origin of global frame towards the precision points are defined as:

$$\hat{C}^{(g,2)} \bar{V}^{(2)} = \bar{R}_i \quad (5-37)$$

$$\hat{C}^{(g,2)} \bar{W}^{(2)} + |C_3 D_3| \hat{C}^{(g,5)} \bar{u}_1 - |D_1 D'| \hat{C}^{(g,8)} \bar{u}_3 + |O' D'| \hat{C}^{(g,0)} \bar{u}_1 - |OO'| \hat{C}^{(g,0)} \bar{u}_3 = -\bar{R}_i \quad (5-38)$$

For any i^{th} position of the tracing point, using the rotation matrix definitions (5-3) to (5-16), equations (5-37) and (5-38) can be re-written as:

$$e^{-\tilde{u}_1 \pi / 2} e^{\tilde{u}_3 \theta_1^i} e^{\tilde{u}_1 \pi / 2} e^{\tilde{u}_3 \theta_2^i} \bar{V}^{(2)} = \bar{R}_i \quad (5-39)$$

$$\begin{aligned}
& e^{-\tilde{u}_1\pi/2} e^{\tilde{u}_3\theta_1^i} e^{\tilde{u}_1\pi/2} e^{\tilde{u}_3\theta_2^i} \overline{W}^{(2)} + |C_3 D_3| e^{-\tilde{u}_3\theta_8^i} e^{-\tilde{u}_2\theta_7^i} e^{-\tilde{u}_1\theta_6^i} \overline{u}_1 \\
& \quad - |OO'| e^{-\tilde{u}_1\pi/2} \overline{u}_3 + |O'D'| e^{-\tilde{u}_1\pi/2} \overline{u}_1 - |D_1 D'| \overline{u}_3 \\
& \quad = -\overline{R}_i
\end{aligned} \tag{5-40}$$

Equations (5-39), (5-40) and (4-41) can be separated into their components as:

$$\begin{aligned}
& e^{-\tilde{u}_1\pi/2} e^{\tilde{u}_3\theta_1^i} e^{\tilde{u}_1\pi/2} e^{\tilde{u}_3\theta_2^i} (\overline{u}_1 V_x + \overline{u}_2 V_y + \overline{u}_3 V_z) \\
& \quad = \overline{u}_1 R_{ix} + \overline{u}_2 R_{iy} + \overline{u}_3 R_{iz}
\end{aligned} \tag{5-41}$$

$$\begin{aligned}
& \overline{u}_1 V_x \cos(\theta_1^i) \cos(\theta_2^i) - \overline{u}_1 V_y \cos(\theta_1^i) \sin(\theta_2^i) + \overline{u}_1 V_z \sin(\theta_1^i) \\
& \quad + \overline{u}_2 V_x \sin(\theta_2^i) + \overline{u}_2 V_y \cos(\theta_2^i) - \overline{u}_3 V_x \cos(\theta_2^i) \sin(\theta_1^i) \\
& \quad + \overline{u}_3 V_y \sin(\theta_1^i) \sin(\theta_2^i) + \overline{u}_3 V_z \cos(\theta_1^i) \\
& \quad = \overline{u}_1 R_{ix} + \overline{u}_2 R_{iy} + \overline{u}_3 R_{iz}
\end{aligned} \tag{5-42}$$

$$\begin{aligned}
& e^{-\tilde{u}_1\pi/2} e^{\tilde{u}_3\theta_1^i} e^{\tilde{u}_1\pi/2} e^{\tilde{u}_3\theta_2^i} (\overline{u}_1 W_x + \overline{u}_2 W_y + \overline{u}_3 W_z) \\
& \quad + |C_3 D_3| e^{-\tilde{u}_3\theta_8^i} e^{-\tilde{u}_2\theta_7^i} e^{-\tilde{u}_1\theta_6^i} \overline{u}_1 - |OO'| e^{-\tilde{u}_1\pi/2} \overline{u}_3 \\
& \quad + |O'D'| e^{-\tilde{u}_1\pi/2} \overline{u}_1 - |D_1 D'| \hat{I} \overline{u}_3 = -\overline{R}_i
\end{aligned} \tag{5-43}$$

$$\begin{aligned}
& \overline{u}_1 W_x \cos(\theta_1^i) \cos(\theta_2^i) - \overline{u}_1 W_y \cos(\theta_1^i) \sin(\theta_2^i) + \overline{u}_1 W_z \sin(\theta_1^i) \\
& \quad + \overline{u}_2 W_x \sin(\theta_2^i) + \overline{u}_2 W_y \cos(\theta_2^i) \\
& \quad - \overline{u}_3 W_x \cos(\theta_2^i) \sin(\theta_1^i) + \overline{u}_3 W_y \sin(\theta_1^i) \sin(\theta_2^i) \\
& \quad + \overline{u}_3 W_z \cos(\theta_1^i) + \overline{u}_1 |C_3 D_3| \cos(\theta_7^i) \cos(\theta_8^i) \\
& \quad - \overline{u}_2 |C_3 D_3| \cos(\theta_7^i) \sin(\theta_8^i) + \overline{u}_3 |C_3 D_3| \sin(\theta_7^i) \\
& \quad - \overline{u}_2 |OO'| + \overline{u}_1 |O'D'| - \overline{u}_3 |D_1 D'| \\
& \quad = -\overline{u}_1 R_{ix} - \overline{u}_2 R_{iy} - \overline{u}_3 R_{iz}
\end{aligned} \tag{5-44}$$

Initial (Fully Extended) Position

For the initial position P_0 , equation (5-42) can be separated into its components as:

Table 5.3 Components of Equation (5-42) for the Initial Position P_0

| Axis | Equations | Unknowns | Eq. # |
|-------------|--|---|--------|
| \bar{u}_1 | $V_x \cos(\theta_1^0) \cos(\theta_2^0) - V_y \cos(\theta_1^0) \sin(\theta_2^0) + V_z \sin(\theta_1^0) = R_{0x}$ | $V_x, V_y, V_z, \theta_1^0, \theta_2^0$ | (5-45) |
| \bar{u}_2 | $V_x \sin(\theta_2^0) + V_y \cos(\theta_2^0) = R_{0y}$ | $V_x, V_y, \theta_1^0, \theta_2^0$ | (5-46) |
| \bar{u}_3 | $-V_x \cos(\theta_2^0) \sin(\theta_1^0) + V_y \sin(\theta_1^0) \sin(\theta_2^0) + V_z \cos(\theta_1^0) = R_{0z}$ | $V_x, V_y, V_z, \theta_1^0, \theta_2^0$ | (5-47) |

For the initial position, equation (5-44) can be separated into its components as:

Table 5.4 Components of Equation (5-44) for the Initial Position P_0

| Axis | Equations | Unknowns | Eq. # |
|-------------|---|--|--------|
| \bar{u}_1 | $W_x \cos(\theta_1^0) \cos(\theta_2^0) - W_y \cos(\theta_1^0) \sin(\theta_2^0) + W_z \sin(\theta_1^0) + C_3 D_3 \cos(\theta_7^0) \cos(\theta_8^0) + O'D' = -R_{0x}$ | $W_x, W_y, W_z, C_3 D_3 , O'D' , \theta_1^0, \theta_2^0, \theta_7^0, \theta_8^0$ | (5-48) |
| \bar{u}_2 | $W_x \sin(\theta_2^0) + W_y \cos(\theta_2^0) - C_3 D_3 \cos(\theta_7^0) \sin(\theta_8^0) - OO' = -R_{0y}$ | $W_x, W_y, C_3 D_3 , OO' , \theta_1^0, \theta_2^0, \theta_7^0, \theta_8^0$ | (5-49) |
| \bar{u}_3 | $-W_x \cos(\theta_2^0) \sin(\theta_1^0) + W_y \sin(\theta_1^0) \sin(\theta_2^0) + W_z \cos(\theta_1^0) + C_3 D_3 \sin(\theta_7^0) - D_1 D' = -R_{0z}$ | $W_x, W_y, W_z, C_3 D_3 , D_1 D' , \theta_1^0, \theta_2^0, \theta_7^0, \theta_8^0$ | (5-50) |

In-between Position

Assuming that the point P can pass through at most 3 points, P_0 , P_1 and P_2 , for the in-between position P_1 equation (5-42) is decomposed into its components as:

Table 5.5 Components of Equation (5-42) for the In-Between Position P_1

| Axis | Equations | Unknowns | Eq. # |
|-------------|--|---|--------|
| \bar{u}_1 | $V_x \cos(\theta_1^1) \cos(\theta_2^1) - V_y \cos(\theta_1^1) \sin(\theta_2^1) + V_z \sin(\theta_1^1) = R_{1x}$ | $V_x, V_y, V_z, \theta_1^1, \theta_2^1$ | (5-51) |
| \bar{u}_2 | $V_x \sin(\theta_2^1) + V_y \cos(\theta_2^1) = R_{1y}$ | $V_x, V_y, \theta_1^1, \theta_2^1$ | (5-52) |
| \bar{u}_3 | $-V_x \cos(\theta_2^1) \sin(\theta_1^1) + V_y \sin(\theta_1^1) \sin(\theta_2^1) + V_z \cos(\theta_1^1) = R_{1z}$ | $V_x, V_y, V_z, \theta_1^1, \theta_2^1$ | (5-53) |

For the in-between position P_1 equation (5-44) is separated into its components as:

Table 5.6 Components of Equation (5-44) for the In-Between Position P_1

| Axis | Equations | Unknowns | Eq. # |
|-------------|---|--|--------|
| \bar{u}_1 | $W_x \cos(\theta_1^1) \cos(\theta_2^1) - W_y \cos(\theta_1^1) \sin(\theta_2^1) + W_z \sin(\theta_1^1) + C_3 D_3 \cos(\theta_7^1) \cos(\theta_8^1) + O'D' = -R_{1x}$ | $W_x, W_y, W_z, C_3 D_3 , O'D' , \theta_1^1, \theta_2^1, \theta_7^1, \theta_8^1$ | (5-54) |
| \bar{u}_2 | $W_x \sin(\theta_2^1) + W_y \cos(\theta_2^1) - C_3 D_3 \cos(\theta_7^1) \sin(\theta_8^1) - OO' = -R_{1y}$ | $W_x, W_y, C_3 D_3 , OO' , \theta_1^1, \theta_2^1, \theta_7^1, \theta_8^1$ | (5-55) |
| \bar{u}_3 | $-W_x \cos(\theta_2^1) \sin(\theta_1^1) + W_y \sin(\theta_1^1) \sin(\theta_2^1) + W_z \cos(\theta_1^1) + C_3 D_3 \sin(\theta_7^1) - D_1 D' = -R_{1z}$ | $W_x, W_y, W_z, C_3 D_3 , D_1 D' , \theta_1^1, \theta_2^1, \theta_7^1, \theta_8^1$ | (5-56) |

Final (Fully Retracted) Position

For the fully retracted position P_2 equation (5-42) is separated into its components as:

Table 5.7 Components of Equation (5-42) for the Final Position P_2

| Axis | Equations | Unknowns | Eq. # |
|-------------|---|---|--------|
| \bar{u}_1 | $V_x \cos(\theta_1^2) \cos(\theta_2^2) - V_y \cos(\theta_1^2) \sin(\theta_2^2)$ $+ V_z \sin(\theta_1^2) = R_{2x}$ | $V_x, V_y, V_z, \theta_1^2, \theta_2^2$ | (5-57) |
| \bar{u}_2 | $V_x \sin(\theta_2^2) + V_y \cos(\theta_2^2) = R_{2y}$ | $V_x, V_y, \theta_1^2, \theta_2^2$ | (5-58) |
| \bar{u}_3 | $-V_x \cos(\theta_2^2) \sin(\theta_1^2) + V_y \sin(\theta_1^2) \sin(\theta_2^2)$ $+ V_z \cos(\theta_1^2) = R_{2z}$ | $V_x, V_y, V_z, \theta_1^2, \theta_2^2$ | (5-59) |

For fully retracted position P_2 equation (5-44) is separated into its components as:

Table 5.8 Components of Equation (5-44) for the Final Position P_2

| Axis | Equations | Unknowns | Eq. # |
|-------------|--|--|--------|
| \bar{u}_1 | $W_x \cos(\theta_1^2) \cos(\theta_2^2) - W_y \cos(\theta_1^2) \sin(\theta_2^2)$ $+ W_z \sin(\theta_1^2)$ $+ C_3 D_3 \cos(\theta_7^2) \cos(\theta_8^2)$ $+ O'D' = -R_{2x}$ | $W_x, W_y, W_z,$ $ C_3 D_3 , O'D' ,$ $\theta_1^2, \theta_2^2, \theta_7^2, \theta_8^2$ | (5-60) |
| \bar{u}_2 | $W_x \sin(\theta_2^2) + W_y \cos(\theta_2^2)$ $- C_3 D_3 \cos(\theta_7^2) \sin(\theta_8^2)$ $- OO' = -R_{2y}$ | $W_x, W_y,$ $ C_3 D_3 , OO' ,$ $\theta_1^2, \theta_2^2, \theta_7^2, \theta_8^2$ | (5-61) |
| \bar{u}_3 | $-W_x \cos(\theta_2^2) \sin(\theta_1^2) + W_y \sin(\theta_1^2) \sin(\theta_2^2)$ $+ W_z \cos(\theta_1^2) + C_3 D_3 \sin(\theta_7^2)$ $- D_1 D' = -R_{2z}$ | $W_x, W_y, W_z,$ $ C_3 D_3 , D_1 D' ,$ $\theta_1^2, \theta_2^2, \theta_7^2, \theta_8^2$ | (5-62) |

Based on equation (5-23), The following equation of motion for SSRR linkage can be written for any i^{th} position of the tracing point:

$$\begin{aligned}
 & |OO'|^2 + |AB|^2 + |BC_1|^2 + |D_1D'|^2 + |O'D'|^2 - |C_3D_3|^2 \\
 & - 2|BC_1||OO'| \cos(\theta_2^i) + 2|O'D'||AB| \sin(\theta_1^i) \\
 & - 2|AB||D_1D'| \cos(\theta_1^i) \\
 & - 2|BC_1||O'D'| \cos(\theta_1^i) \sin(\theta_2^i) \\
 & - 2|BC_1||D_1D'| \sin(\theta_1^i) \sin(\theta_2^i) = 0
 \end{aligned} \tag{5-63}$$

5.1.3.1 Prescribed Orientations of Fixed Joints

Table 5.9 The Number of Unknown Parameters and Free Parameters for the Three Positions of SSRR Mechanism with Shock Absorber as the Output Link, for the Synthesis Task When Orientations of Fixed Joints are Prescribed

| # of Precision Points | # of Scalar Equations | # of Unknowns | Unknowns | # of Free Parameters |
|-----------------------|-----------------------|---------------|---|----------------------|
| 1 | 9 | 9 | $V_y, W_y, W_z, BC_1 , C_3D_3 ,$ $\theta_1^0, \theta_2^0, \theta_7^0, \theta_8^0$ | 0 |
| 2 | 13 | 13 | $V_y, W_y, W_z, BC_1 , C_3D_3 ,$ $\theta_1^0, \theta_2^0, \theta_7^0, \theta_8^0, \theta_1^1, \theta_2^1, \theta_7^1, \theta_8^1$ | 0 |
| 3 | 17 | 17 | $V_y, W_y, W_z, BC_1 , C_3D_3 ,$ $\theta_1^0, \theta_2^0, \theta_7^0, \theta_8^0, \theta_1^1, \theta_2^1, \theta_7^1, \theta_8^1,$ $\theta_1^2, \theta_2^2, \theta_7^2, \theta_8^2$ | 0 |

Table 5.10 Equation Set to be Used for the SSRR Mechanism (with Shock Absorber as the Output Link) Synthesis Task When Orientations of Fixed Joints are Prescribed

| Equations | Unknowns | Eq. # |
|--|---|--------|
| $W_y = PP' + BC_1 $ | $W_y, BC_1 $ | (5-35) |
| $W_z = AP' + AB $ | $W_z, AB $ | (5-36) |
| $V_y = - PP' $ | V_y | (5-32) |
| $\theta_2^0 = \text{atan2} \left(\left(\frac{(R_{0x})^2 + (R_{0z})^2 - PP' ^2}{V_y^2} \right)^{0.5}, \left(\frac{R_{0y}}{V_y} \right) \right)$ | V_y, θ_2^0 | (5-64) |
| $\theta_2^1 = \text{atan2} \left(\left(\frac{(R_{1x})^2 + (R_{1z})^2 - PP' ^2}{V_y^2} \right)^{0.5}, \left(\frac{R_{1y}}{V_y} \right) \right)$ | V_y, θ_2^1 | (5-65) |
| $\theta_2^2 = \text{atan2} \left(\left(\frac{(R_{2x})^2 + (R_{2z})^2 - PP' ^2}{V_y^2} \right)^{0.5}, \left(\frac{R_{2y}}{V_y} \right) \right)$ | V_y, θ_2^2 | (5-66) |
| $ PP' \cos(\theta_1^0) \sin(\theta_2^0) - AP' \sin(\theta_1^0) = R_{0x}$ | θ_1^0, θ_2^0 | (5-45) |
| $ PP' \cos(\theta_1^1) \sin(\theta_2^1) - AP' \sin(\theta_1^1) = R_{1x}$ | θ_1^1, θ_2^1 | (5-51) |
| $ PP' \cos(\theta_1^2) \sin(\theta_2^2) - AP' \sin(\theta_1^2) = R_{2x}$ | θ_1^2, θ_2^2 | (5-57) |
| $ OO' ^2 + AB ^2 + D_1D' ^2 + O'D' ^2$ $+ 2 O'D' AB \sin(\theta_1^0) - 2 AB D_1D' \cos(\theta_1^0)$ $= C_3D_3 ^2 - BC_1 ^2 + 2 BC_1 OO' \cos(\theta_2^0)$ $+ 2 BC_1 O'D' \cos(\theta_1^0) \sin(\theta_2^0)$ $+ 2 BC_1 D_1D' \sin(\theta_1^0) \sin(\theta_2^0)$ | $\theta_1^0, \theta_2^0, BC_1 ,$ $ C_3D_3 $ | (5-67) |
| $ OO' ^2 + AB ^2 + D_1D' ^2 + O'D' ^2$ $+ 2 O'D' AB \sin(\theta_1^1) - 2 AB D_1D' \cos(\theta_1^1)$ $= C_3D_3 ^2 - BC_1 ^2 + 2 BC_1 OO' \cos(\theta_2^1)$ $+ 2 BC_1 O'D' \cos(\theta_1^1) \sin(\theta_2^1)$ $+ 2 BC_1 D_1D' \sin(\theta_1^1) \sin(\theta_2^1)$ | $\theta_1^1, \theta_2^1, BC_1 ,$ $ C_3D_3 $ | (5-68) |

Table 5.10. Continued

| Equations | Unknowns | Eq. # |
|--|--|--------|
| $ C_3D_3 \cos(\theta_7^0) \cos(\theta_8^0) - W_y \cos(\theta_1^0) \sin(\theta_2^0) + W_z \sin(\theta_1^0) = - O'D' - R_{0x}$ | $W_y, W_z, C_3D_3 , \theta_1^0, \theta_2^0, \theta_7^0, \theta_8^0$ | (5-48) |
| $W_y \cos(\theta_2^0) - C_3D_3 \cos(\theta_7^0) \sin(\theta_8^0) = OO' - R_{0y}$ | $W_y, C_3D_3 , \theta_1^0, \theta_2^0, \theta_7^0, \theta_8^0$ | (5-49) |
| $ C_3D_3 \sin(\theta_7^0) + W_y \sin(\theta_1^0) \sin(\theta_2^0) + W_z \cos(\theta_1^0) = D_1D' - R_{0z}$ | $W_y, C_3D_3 , \theta_1^0, \theta_2^0, \theta_7^0$ | (5-50) |
| $ C_3D_3 \cos(\theta_7^1) \cos(\theta_8^1) - W_y \cos(\theta_1^1) \sin(\theta_2^1) + W_z \sin(\theta_1^1) = - O'D' - R_{1x}$ | $W_y, W_z, C_3D_3 , \theta_1^1, \theta_2^1, \theta_7^1, \theta_8^1$ | (5-54) |
| $W_y \cos(\theta_2^1) - C_3D_3 \cos(\theta_7^1) \sin(\theta_8^1) = OO' - R_{1y}$ | $W_y, C_3D_3 , \theta_1^1, \theta_2^1, \theta_7^1, \theta_8^1$ | (5-55) |
| $ C_3D_3 \sin(\theta_7^1) + W_y \sin(\theta_1^1) \sin(\theta_2^1) + W_z \cos(\theta_1^1) = D_1D' - R_{1z}$ | $W_y, W_z, C_3D_3 , \theta_1^1, \theta_2^1, \theta_7^1$ | (5-56) |
| $ C_3D_3 \cos(\theta_7^2) \cos(\theta_8^2) - W_y \cos(\theta_1^2) \sin(\theta_2^2) + W_z \sin(\theta_1^2) = - O'D' - R_{2x}$ | $W_y, W_z, C_3D_3 , \theta_1^2, \theta_2^2, \theta_7^2, \theta_8^2$ | (5-60) |
| $W_y \cos(\theta_2^2) - C_3D_3 \cos(\theta_7^2) \sin(\theta_8^2) = OO' - R_{2y}$ | $W_y, C_3D_3 , \theta_1^2, \theta_2^2, \theta_7^2, \theta_8^2$ | (5-61) |
| $ C_3D_3 \sin(\theta_7^2) + W_y \sin(\theta_1^2) \sin(\theta_2^2) + W_z \cos(\theta_1^2) = D_1D' - R_{2z}$ | $W_y, W_z, C_3D_3 , \theta_1^2, \theta_2^2, \theta_7^2$ | (5-62) |

With fixed pivot locations $|OO'|$, $|D_1D'|$, $|O'D'|$ and landing gear parameters $|PP'|$, $|AP'|$ and $|AB|$ known, the link lengths and angle values can be calculated as follows:

- W_z can be found from equation (5-36).
- By using equations (5-64), (5-65) and (5-66) angles θ_2^0 , θ_2^1 and θ_2^2 can be determined.
- θ_1^0 , θ_1^1 and θ_1^2 can be found by re-writing equations (5-45), (5-51) and (5-57) in $A\cos x + B\sin x + C = 0$ form and determining the root.
- Link lengths $|C_3D_3|$ and $|BC_1|$ can be found from equations (5-67) and (5-68).
- From equation (5-35), W_y can be determined.
- θ_7^0 is determined from equation (5-50) and θ_8^0 can be calculated from one of the two equations (5-48) and (5-49).
- θ_7^1 is determined from equation (5-56) and θ_8^1 can be calculated from one of the two equations (5-54) and (5-55).
- θ_7^2 is determined from equation (5-62) and θ_8^2 can be calculated from one of the two equations (5-60) and (5-61).

5.1.3.2 Unprescribed Positions of the Ground Pivots

The position of the origin of the reference frame attached to the fourth link \bar{r}_4 is:

$$\bar{r}_4 = -\bar{u}_1|O'D'| + \bar{u}_2|OO'| + \bar{u}_3|D_1D'| \quad (5-69)$$

The equation of motion based on the i^{th} position of the mechanism is:

$$\begin{aligned} &|OO'|^2 + |AB|^2 + |BC_1|^2 + |D_1D'|^2 + |O'D'|^2 - |C_3D_3|^2 \\ &\quad - 2|BC_1||OO'| \cos(\theta_2^i) - 2|BC_1||O'D'| \cos(\theta_1^i) \sin(\theta_2^i) \\ &\quad - 2|BC_1||D_1D'| \sin(\theta_1^i) \sin(\theta_2^i) + 2|O'D'||AB| \sin(\theta_1^i) \\ &\quad - 2|AB||D_1D'| \cos(\theta_1^i) = 0 \end{aligned} \quad (5-70)$$

Based on equation (5-70), the difference between equations of motion on the i^{th} and $i+1^{\text{th}}$ positions is written as:

$$\begin{aligned}
 & -2|BC_1||OO'|(\cos(\theta_2^{i+1}) - \cos(\theta_2^i)) \\
 & \quad -2|BC_1||O'D'|(\cos(\theta_1^{i+1}) \sin(\theta_2^{i+1}) - \cos(\theta_1^i) \sin(\theta_2^i)) \\
 & \quad -2|BC_1||D_1D'|(\sin(\theta_1^{i+1}) \sin(\theta_2^{i+1}) - \sin(\theta_1^i) \sin(\theta_2^i)) \quad (5-71) \\
 & \quad +2|O'D'||AB|(\sin(\theta_1^{i+1}) - \sin(\theta_1^i)) \\
 & \quad -2|AB||D_1D'|(\cos(\theta_1^{i+1}) - \cos(\theta_1^i)) = 0
 \end{aligned}$$

Table 5.11 The Number of Unknown Parameters and Free Parameters for the Three Positions of SSRR Mechanism with Shock Absorber as the Output Link, for the Synthesis Task When Orientations of Fixed Joints are Unprescribed

| # of Precision Points | # of Scalar Equations | # of Unknowns | Unknowns | # of Free Parameters |
|-----------------------|-----------------------|---------------|--|----------------------|
| 1 | 6 | 12 | $V_y, W_y, W_z, BC_1 , C_3D_3 ,$ $ O'D' , D_1D' , OO' ,$ $\theta_1^0, \theta_2^0, \theta_7^0, \theta_8^0$ | 6 |
| 2 | 12 | 16 | $V_y, W_y, W_z, BC_1 , C_3D_3 ,$ $ O'D' , D_1D' , OO' , \theta_1^0, \theta_2^0,$ $\theta_7^0, \theta_8^0, \theta_1^1, \theta_2^1, \theta_7^1, \theta_8^1$ | 4 |
| 3 | 18 | 20 | $V_y, W_y, W_z, BC_1 , C_3D_3 ,$ $ O'D' , D_1D' , OO' , \theta_1^0, \theta_2^0,$ $\theta_7^0, \theta_8^0, \theta_1^1, \theta_2^1, \theta_7^1, \theta_8^1,$ $\theta_1^2, \theta_2^2, \theta_7^2, \theta_8^2$ | 2 |

Table 5.12 Equation Set to be Used for the SSRR Mechanism (with Shock Absorber as the Output Link) Synthesis Task When Orientations of Fixed Joints are Unprescribed

| Equations | Unknowns | Eq. # |
|---|---|--------|
| $W_y = PP' + BC_1 $ | $W_y, BC_1 $ | (5-35) |
| $W_z = AP' + AB $ | $W_z, AB $ | (5-36) |
| $V_y = - PP' $ | V_y | (5-37) |
| $V_y \cos(\theta_2^0) = R_{0y}$ | V_y, θ_2^0 | (5-38) |
| $V_y \cos(\theta_2^1) = R_{1y}$ | V_y, θ_2^1 | (5-39) |
| $V_y \cos(\theta_2^2) = R_{2y}$ | V_y, θ_2^2 | (5-40) |
| $ PP' \cos(\theta_1^0) \sin(\theta_2^0) - AP' \sin(\theta_1^0) = R_{0x}$ | θ_1^0, θ_2^0 | (5-41) |
| $ PP' \cos(\theta_1^1) \sin(\theta_2^1) - AP' \sin(\theta_1^1) = R_{1x}$ | θ_1^1, θ_2^1 | (5-35) |
| $ PP' \cos(\theta_1^2) \sin(\theta_2^2) - AP' \sin(\theta_1^2) = R_{2x}$ | θ_1^2, θ_2^2 | (5-36) |
| $- OO' BC_1 (\cos(\theta_2^1) - \cos(\theta_2^0))$ $- O'D' BC_1 (\cos(\theta_1^1) \sin(\theta_2^1) - \cos(\theta_1^0) \sin(\theta_2^0))$ $- D_1D' BC_1 (\sin(\theta_1^1) \sin(\theta_2^1) - \sin(\theta_1^0) \sin(\theta_2^0))$ $+ O'D' AB (\sin(\theta_1^1) - \sin(\theta_1^0))$ $- D_1D' AB (\cos(\theta_1^1) - \cos(\theta_1^0)) = 0$ | $\theta_1^0, \theta_2^0, \theta_1^1, \theta_2^1,$ $ O'D' , D_1D' ,$ $ OO' ,$ $ AB , BC_1 $ | (5-72) |
| $- OO' BC_1 (\cos(\theta_2^2) - \cos(\theta_2^1))$ $- O'D' BC_1 (\cos(\theta_1^2) \sin(\theta_2^2) - \cos(\theta_1^1) \sin(\theta_2^1))$ $- D_1D' BC_1 (\sin(\theta_1^2) \sin(\theta_2^2) - \sin(\theta_1^1) \sin(\theta_2^1))$ $+ O'D' AB (\sin(\theta_1^2) - \sin(\theta_1^1))$ $- D_1D' AB (\cos(\theta_1^2) - \cos(\theta_1^1)) = 0$ | $\theta_1^1, \theta_2^1, \theta_1^2, \theta_2^2,$ $ O'D' , D_1D' ,$ $ OO' ,$ $ AB , BC_1 $ | (5-73) |

Table 5.12. Continued

| Equations | Unknowns | Eq. # |
|--|--|--------|
| $ C_3D_3 \cos(\theta_7^0) \cos(\theta_8^0) - W_y \cos(\theta_1^0) \sin(\theta_2^0) + W_z \sin(\theta_1^0) = - O'D' - R_{0x}$ | $W_y, W_z, C_3D_3 , O'D' , \theta_1^0, \theta_2^0, \theta_7^0, \theta_8^0$ | (5-48) |
| $W_y \cos(\theta_2^0) - C_3D_3 \cos(\theta_7^0) \sin(\theta_8^0) = OO' - R_{0y}$ | $W_y, C_3D_3 , OO' , \theta_1^0, \theta_2^0, \theta_7^0, \theta_8^0$ | (5-49) |
| $ C_3D_3 \sin(\theta_7^0) + W_y \sin(\theta_1^0) \sin(\theta_2^0) + W_z \cos(\theta_1^0) = D_1D' - R_{0z}$ | $W_y, C_3D_3 , D_1D' , \theta_1^0, \theta_2^0, \theta_7^0$ | (5-50) |
| $ C_3D_3 \cos(\theta_7^1) \cos(\theta_8^1) - W_y \cos(\theta_1^1) \sin(\theta_2^1) + W_z \sin(\theta_1^1) = - O'D' - R_{1x}$ | $W_y, W_z, C_3D_3 , O'D' , \theta_1^1, \theta_2^1, \theta_7^1, \theta_8^1$ | (5-54) |
| $W_y \cos(\theta_2^1) - C_3D_3 \cos(\theta_7^1) \sin(\theta_8^1) = OO' - R_{1y}$ | $W_y, C_3D_3 , OO' , \theta_1^1, \theta_2^1, \theta_7^1, \theta_8^1$ | (5-55) |
| $ C_3D_3 \sin(\theta_7^1) + W_y \sin(\theta_1^1) \sin(\theta_2^1) + W_z \cos(\theta_1^1) = D_1D' - R_{1z}$ | $W_y, W_z, C_3D_3 , D_1D' , \theta_1^1, \theta_2^1, \theta_7^1$ | (5-56) |
| $ C_3D_3 \cos(\theta_7^2) \cos(\theta_8^2) - W_y \cos(\theta_1^2) \sin(\theta_2^2) + W_z \sin(\theta_1^2) = - O'D' - R_{2x}$ | $W_y, W_z, C_3D_3 , O'D' , \theta_1^2, \theta_2^2, \theta_7^2, \theta_8^2$ | (5-60) |
| $W_y \cos(\theta_2^2) - C_3D_3 \cos(\theta_7^2) \sin(\theta_8^2) = OO' - R_{2y}$ | $W_y, C_3D_3 , OO' , \theta_1^2, \theta_2^2, \theta_7^2, \theta_8^2$ | (5-61) |
| $ C_3D_3 \sin(\theta_7^2) + W_y \sin(\theta_1^2) \sin(\theta_2^2) + W_z \cos(\theta_1^2) = D_1D' - R_{2z}$ | $W_y, W_z, C_3D_3 , D_1D' , \theta_1^2, \theta_2^2, \theta_7^2$ | (5-62) |

Since the spherical-spherical link variables are expressed in three dimensions, several spherical-spherical link unknowns must be specified when synthesizing the SSRR mechanism to equate the number on unknowns between the revolute-revolute and spherical-spherical links. Therefore, one of the position variables of ground pivots, $|O'D'|$ is taken as pre-determined. Based on the location of structural connection frame, which is most traditionally the lower deck of the fuselage, $|O'D'|$ can be easily determined.

With landing gear parameters $|PP'|$, $|AP'|$, $|AB|$ and $|BC|$ known, the link lengths and angle values can be calculated as follows:

- W_y and W_z can be found from equations (5-35) and (5-36) respectively.
- By taking the inverse cosines of (5-46), (5-52) and (5-58), angles θ_2^0 , θ_2^1 and θ_2^2 can be determined.
- θ_1^0 , θ_1^1 and θ_1^2 can be found by re-writing equations (5-45), (5-51) and (5-57) in $A\cos x + B\sin x + C = 0$ form and determining the root.
- $|OO'|$ and $|D_1D'|$ lengths can be found from equations (5-72) and (5-73).
- θ_8^0 can be calculated from the division of equations (5-48) and (5-49). θ_7^0 is determined by the ratio of equations (5-49) and (5-50).
- θ_8^1 can be calculated from the division of equations (5-54) and (5-55). θ_7^1 is determined by the ratio of equations (5-55) and (5-56).
- θ_8^2 can be calculated from the division of equations (5-60) and (5-61). θ_7^2 is determined by the ratio of equations (5-61) and (5-62).
- The link length $|C_3D_3|$ can be calculated from one of the following equations: (5-50), (5-56) or (5-62).

CHAPTER 6

LANDING GEAR RETRACTION MECHANISM DESIGN COMPUTER PROGRAM AND PARAMETRIC MASTER GEOMETRY MODELS

Landing gear retraction mechanism synthesis and design process consists of two main components: Graphical User Interface and CAD Program. The process starts with the positioning of the landing gear trunnion to structure joint. Based on the performance and efficiency requirements of landing, the trunnion length, piston length, wheel sizing and axle sizing are determined by the designer. By introducing these sizes to the stick CAD models, the designer can select distinct positions for the precision point. The flowchart of the mechanism synthesis and design software is presented in Figure 6.1.

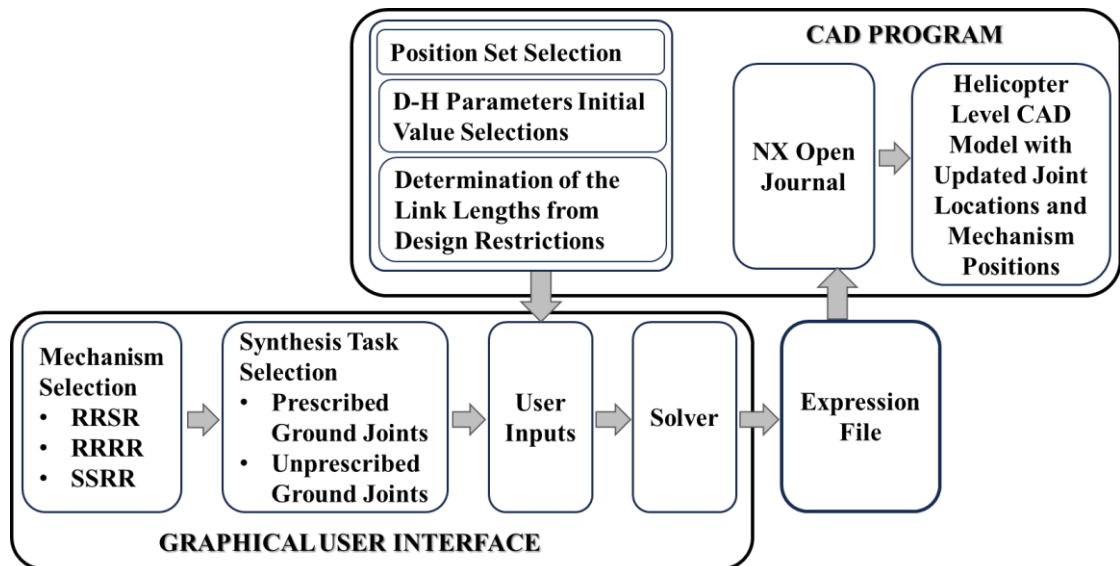


Figure 6.1. Mechanism Synthesis and Design Process

The computer program (GUI), which is written by MATLAB R2019a, has a user interface that requires several input parameters for the design, and as an output of the run, it provides an expression file that can be used by parametric master geometry models in Siemens NX. Using the NX Open developer interface, journal files for the selected mechanisms are run to automatically update the CAD models using the expression files provided by the GUI. Since the landing gear model is fully parametric, it gets updated simultaneously at each run.

6.1 Program Interface

The program interface and steps to be followed are presented in Figure 6.2. and Figure 6.3. The process starts with the selection of mechanism type (1). When the user selects the mechanism type, selection of the synthesis type is required (2).

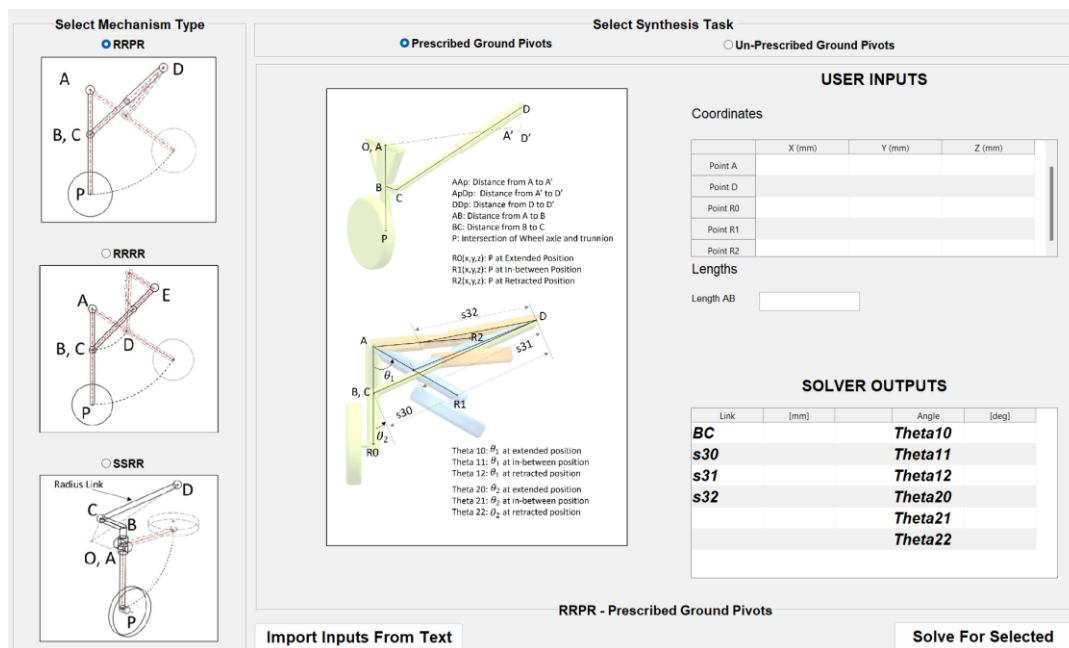


Figure 6.2. Graphical User Interface

After the synthesis type selection, the task definition given at the bottom of page (4) and the image that defines the parameters to be used are updated automatically. Input parameters are demanded from the user (3). There exist two options that can be

utilized for the input parameters: manual entry or automatic entry from a text file. When the user presses the “Solve for selected” button (5), results are presented in the solver output table (6).

1 Select Mechanism Type

RRPR

RRRR

SSRR

2 Select Synthesis Task

Prescribed Ground Pivots Un-Prescribed Ground Pivots

3 USER INPUTS

Coordinates

| | X (mm) | Y (mm) | Z (mm) |
|----------|--------|--------|--------|
| Point A | | | |
| Point D | | | |
| Point R0 | | | |
| Point R1 | | | |
| Point R2 | | | |

Lengths

Length AB

4 RRPR - Prescribed Ground Pivots

5 Solve For Selected

6 SOLVER OUTPUTS

| Link | [mm] | Angle | [deg] |
|------------|------|----------------|-------|
| BC | | Theta10 | |
| s30 | | Theta11 | |
| s31 | | Theta12 | |
| s32 | | Theta20 | |
| | | Theta21 | |
| | | Theta22 | |

3 Import Inputs From Text

Figure 6.3. Steps to be Followed on the GUI

Simultaneously with the display of solver outputs, the MATLAB interface outputs an expression file with a filetype of “.exp” that is ready to be used by NX Open Journal.

6.2 NX Models and Journal Running

For each synthesis task, there exists a separate helicopter level CAD assembly model containing the following: a simplified helicopter model, a master geometry stick diagram model for the selected distinct positions of the landing gear, fully parametric landing gear 3D models, modeled separately for all selected distinct positions, and fully parametric retraction mechanism 3D models, modeled separately for all selected distinct positions.

The NX models utilize landing gear design hardpoints, which are the joint locations of the system, as design inputs. Based on these hardpoint locations, stick diagrams of the retraction mechanism are drawn for each system. During parametric design, these stick diagrams form the master geometry of the landing gear.

As presented in Figure 6.4 and Figure 6.5, each NX model consists of a simplified helicopter model incorporating left and right main landing gears placed at all three positions of the retraction motion. For the NX model design, only the LMLGs are modeled for each system. RMLGs are generated by simply taking the mirror of LMLGs with respect to the global x-z plane.

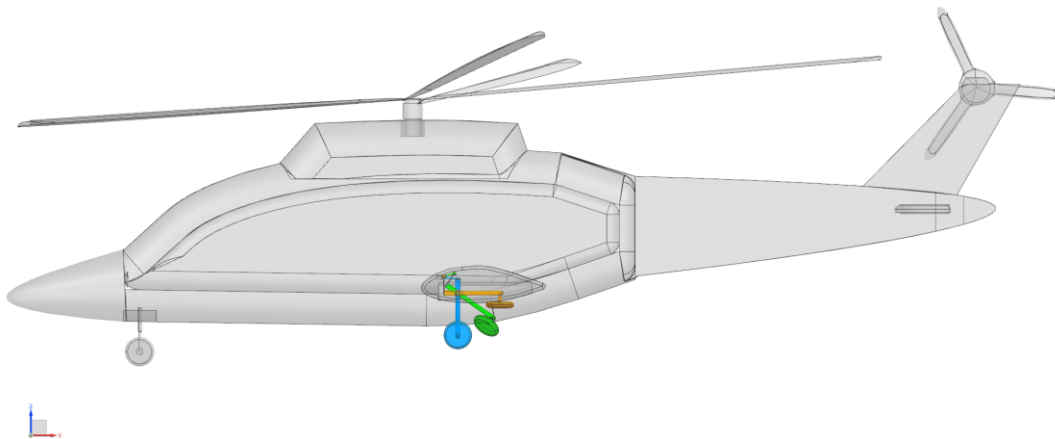


Figure 6.4. Helicopter CAD Model with SSRR Mechanism, Side View

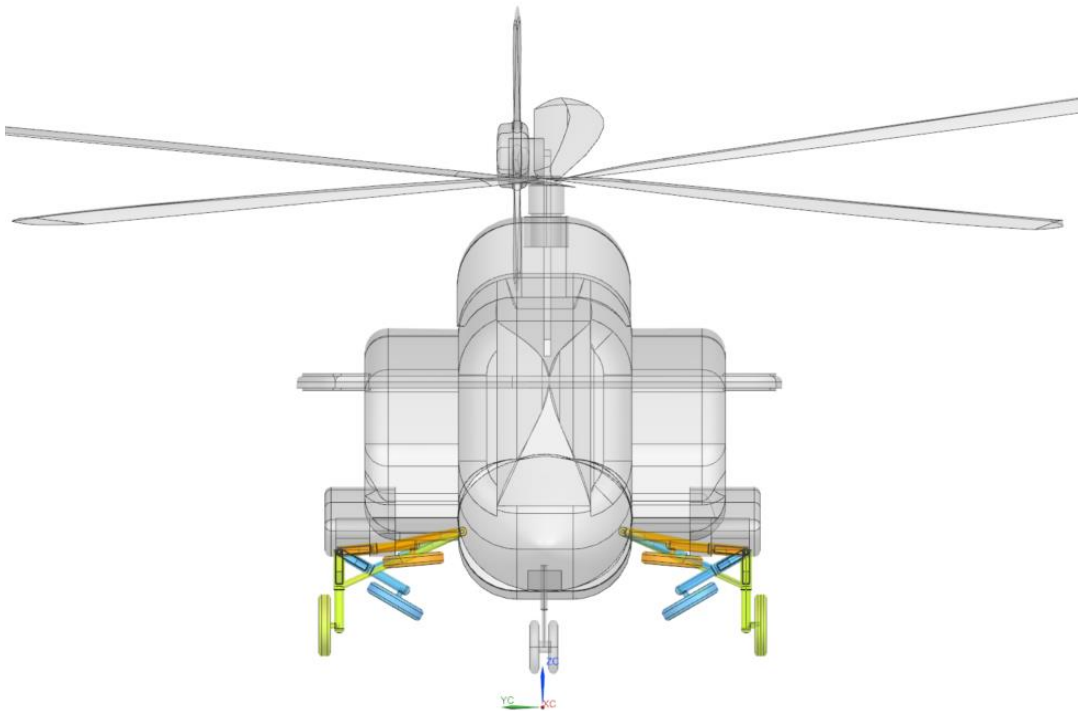


Figure 6.5. Helicopter CAD Model with RRPR Mechanism, Front View

Utilizing the NX Open developer interface shown in Figure 6.6, the journal file incorporating hardpoint coordinates obtained from the MATLAB user interface is run by opening the journal manager by clicking the “Play” button. From the Journal Manager presented in Figure 6.7, the journal file is selected or browsed appropriately.

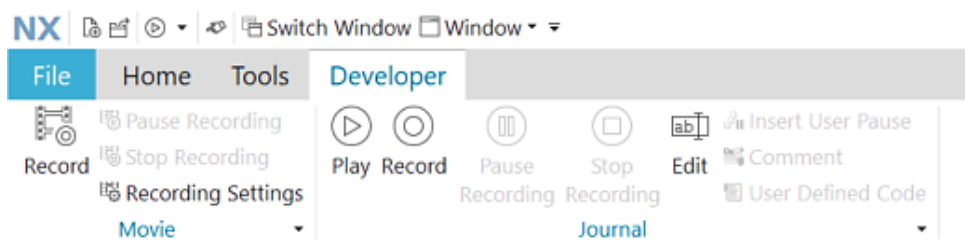


Figure 6.6. Developer Tab on NX 1855 Ribbon

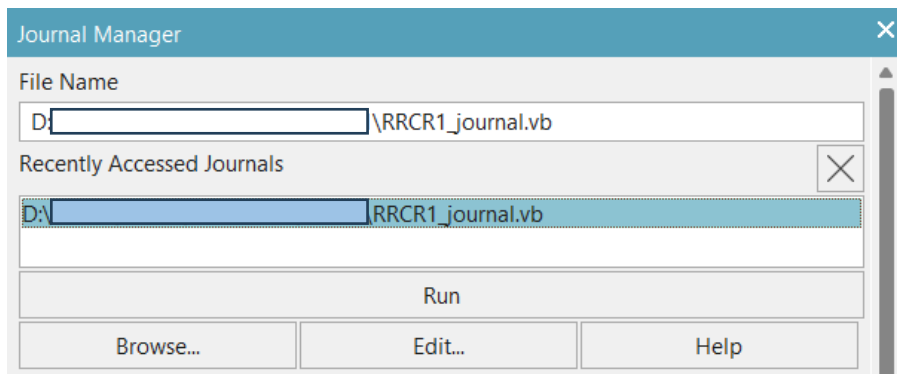


Figure 6.7. Journal Manager on NX 1855

The NX journal must be run while the program is in Gateway state (i.e., at welcome page with no open models). Once the journal code is played, it automatically opens and modifies the stick diagrams by calling the “.exp” file. Then the code opens the helicopter assembly model and updates all CAD models by consecutively activating them. The code does not automatically save the overall model to avoid unintended changes.

Separate journal codes are written for each retraction mechanism synthesis task. A sample NX journal code, written in Visual Basic is provided in Appendix 0. From the “Edit” option on the developer tab, file directory of the expression file can be modified on the Journal Editor without changing the source code of the journal. The same action can be performed by pressing “Edit...” on the Journal Manager to open the Journal Editor.

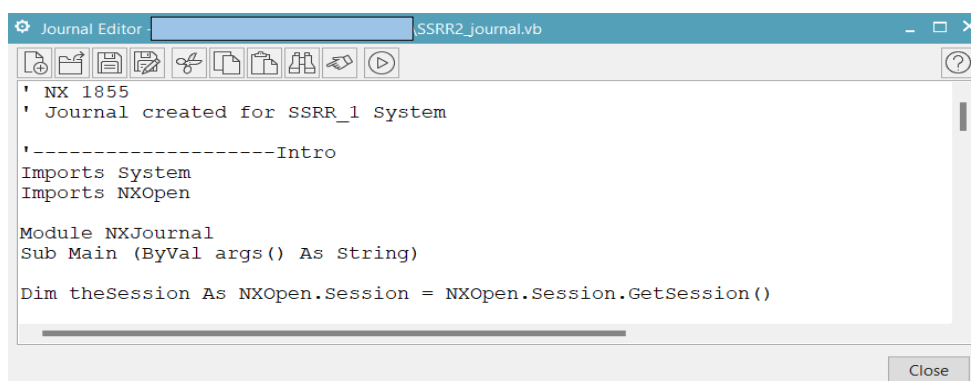


Figure 6.8. Journal Editor

CHAPTER 7

RESULTS AND DISCUSSION

Three separate retraction mechanisms with two distinct types of motion are studied: planar RRPR, planar RRRR and spatial SSRR linkage. As summarized in Table 7.1, each synthesis task is created to meet a specific need of design.

Table 7.1 Synthesis Tasks and Their Corresponding Design Conditions

| Linkage Type | Synthesis Task with | Design Needs and Conditions |
|---------------------|-------------------------------------|---|
| RRPR (planar) | Prescribed Ground Joint Positions | Retraction towards the helicopter fuselage, with specially designed actuator and restricted structural joint locations. |
| | Unprescribed Ground Joint Positions | Retraction towards the helicopter fuselage, with appropriate positioning of the on-the-shelf actuators. |
| RRRR (planar) | Prescribed Ground Joint Positions | Retraction towards the helicopter fuselage, maintaining up-lock and down-lock by dead center positions, restricted structural joint locations. |
| | Unprescribed Ground Joint Positions | Retraction towards the helicopter fuselage, with appropriate positioning for minimum transmission angle deviation between first and last positions. |
| SSRR (spatial) | Prescribed Ground Joint Positions | Retraction towards the longitudinal axis to minimize used fuselage bay while structural joint locations are restricted. |
| | Unprescribed Ground Joint Positions | Retraction towards the longitudinal axis, while the structural properties of the landing gear are prescribed. |

7.1 Numerical Examples for the Landing Gear Retraction Mechanism Synthesis Tasks

Several cases are performed consecutively for each synthesis task to test whether the solver outputs of the program can update the NX models without a modeling error. The numerical values (Solver Outputs) given on the GUI screen are compared with the measurements from the NX model to verify the results. A numerical example for each type of synthesis task is presented in the following parts of this study.

7.1.1 Constrained RRPR (RRPR) Mechanism Synthesis Tasks

For the RRPR mechanism, the stick diagram and parametric CAD model are presented in Figure 7.1 for three positions.

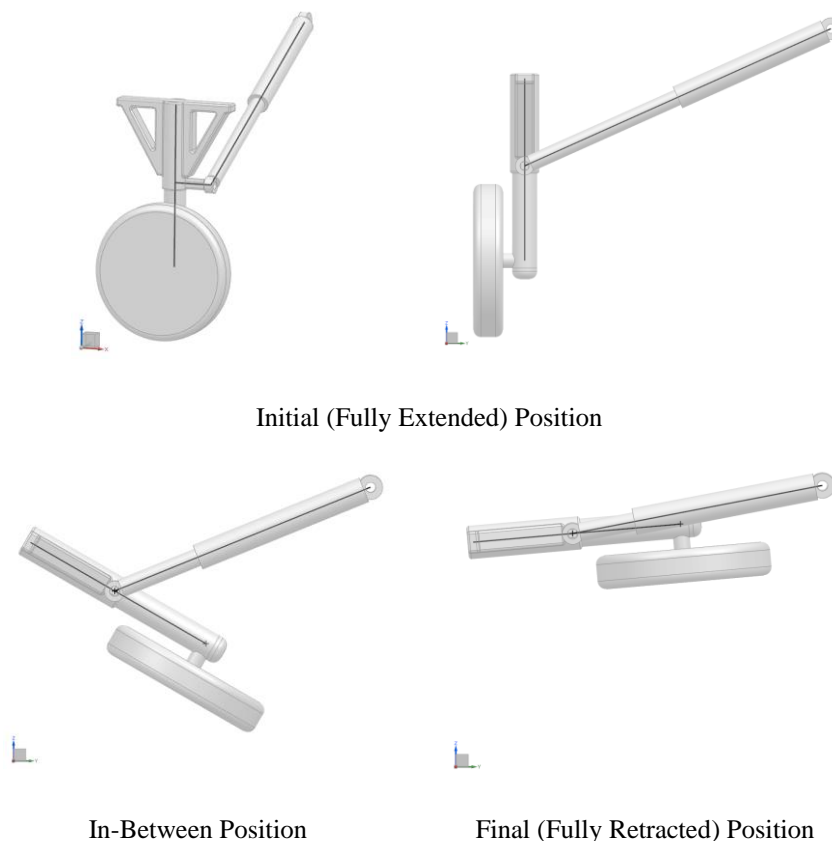


Figure 7.1. RRPR Mechanism Parametric CAD Model

7.1.1.1 RRPR Mechanism Synthesis with Prescribed Positions of the Fixed Joints

When “RRPR – Prescribed Ground Pivots” is selected on the GUI screen, the program provides Figure 7.2 for the parameter definitions.

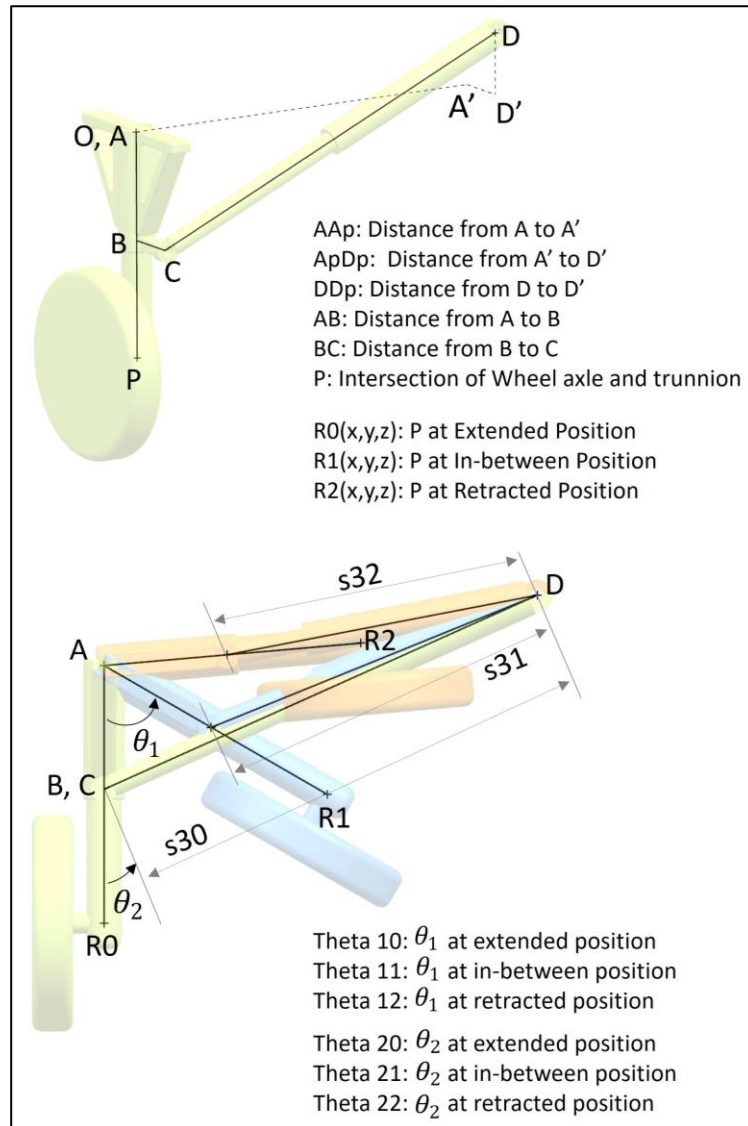


Figure 7.2. Parameter definitions for the RRPR Synthesis Tasks

Figure 7.3 contains a sample user input set for the position and link length parameters, along with the corresponding solver output.

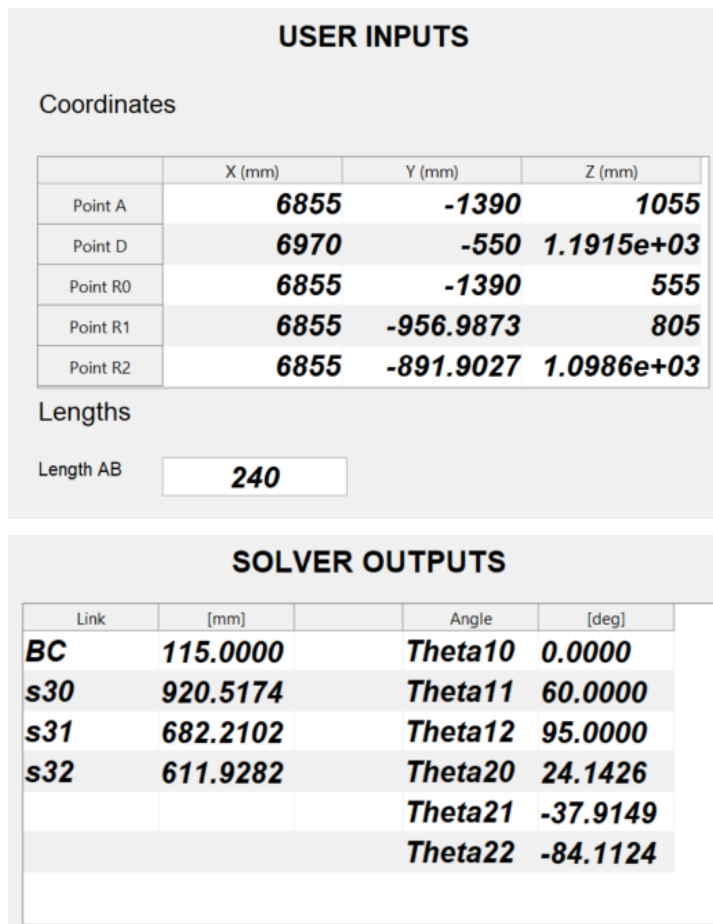


Figure 7.3. User Inputs and Solver Outputs for the RRPR Synthesis Task with Prescribed Ground Pivots

The code provides an “.exp” expression file with following parameters, as given in Figure 7.4. The expression file also stores coordinate values from user inputs. Theta11 expression is the difference between θ_1^0 and θ_1^1 whereas Theta12 expression is the difference between θ_1^0 and θ_1^2 . After the journal is run from the NX Open developer interface, the resulting model, which is updated automatically, is given in Figure 7.5.


```
RRPR1_Expressions.exp
Dosya  Düzenle  Görünüm

[mm]R0_x=6855
[mm]R0_y= -1390
[mm]R0_z= 555
[mm]A_x= 6855
[mm]A_y= -1390
[mm]A_z= 1055
[mm]D_x= 6970
[mm]D_y= -550
[mm]D_z= 1191.5
[mm]B0_x= 6855
[mm]B0_y= -1390
[mm]B0_z= 815
[mm]C0_x= 6970
[mm]C0_y= -1390
[mm]C0_z= 815
[degrees]Theta11= 60
[degrees]Theta12=95.00
```

Figure 7.4. Expression File Parameters for the RRPR Synthesis Task with Prescribed Ground Pivots

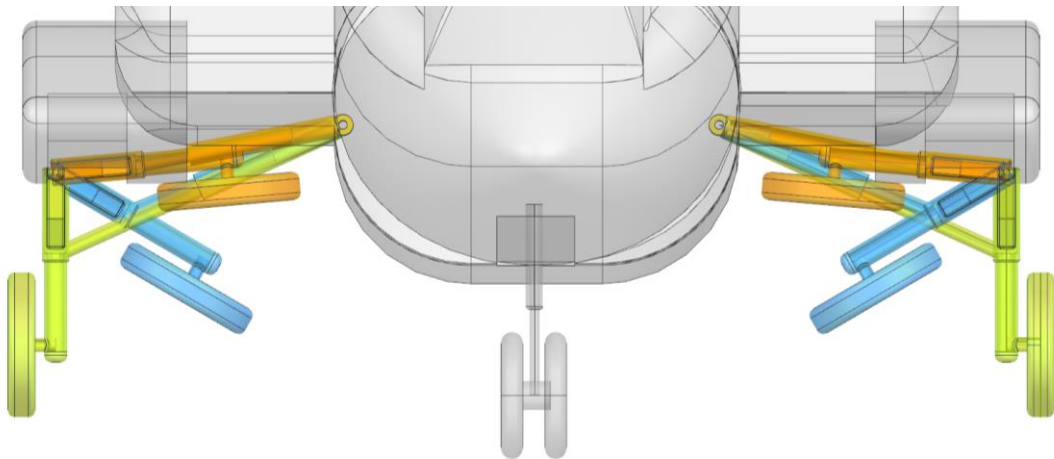


Figure 7.5. Resulting CAD Model at the Three Positions for RRPR Synthesis Task with Prescribed Ground Pivots

7.1.1.2 RRPR Mechanism Synthesis with Unprescribed Positions of the Fixed Joints

For the path generation synthesis task of the RRPR mechanism with unprescribed ground pivots, parameter definitions are as given in Figure 7.2. Sample user inputs for the position and link length parameters and relevant solver outputs that are calculated by the program are given in Figure 7.6.

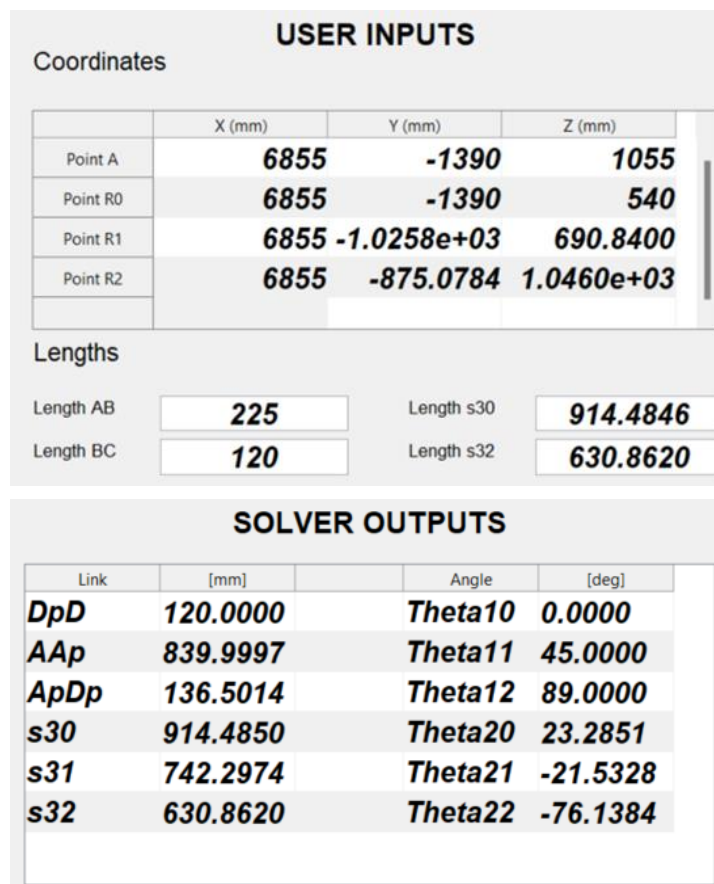


Figure 7.6. User Inputs and Solver Outputs for the RRPR Synthesis Task with Unprescribed Ground Pivots

The code provides an “.exp” expression file with the following parameters as given in Figure 7.7. The expression file also stores coordinate values and actuator lengths (s30 and s32) from user inputs.

```
RRPR2_Expressions.exp
Dosya  Düzenle  Görünüm

[mm]R0_x=6855
[mm]R0_y= -1390
[mm]R0_z= 540
[mm]A_x= 6855
[mm]A_y= -1390
[mm]A_z= 1055
[mm]AB= 225
[mm]BC= 120
[mm]ApDp= 136.49922
[mm]AAp= 840.00024
[mm]S30=914.4846
[mm]S32=630.862
[degrees]Theta11= 45.003147
[degrees]Theta12=88.999999
```

Figure 7.7. Expression File Parameters for the RRPR Synthesis Task with Unprescribed Ground Pivots

After the journal is run from the NX Open developer interface, the resulting model which is updated automatically is presented in Figure 7.8.

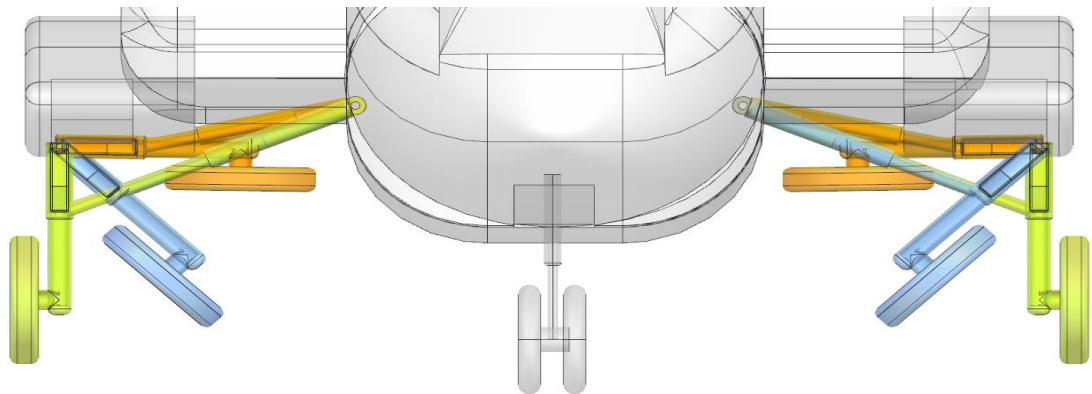


Figure 7.8. Resulting CAD Model at the Three Positions for RRPR Synthesis Task with Unprescribed Ground Pivots

7.1.2 RRRR Mechanism Synthesis Task

Regarding the RRRR mechanism, the stick diagrams for the synthesis tasks with prescribed and unprescribed ground pivots, presented at Figure 7.9 and Figure 7.10 respectively, have a difference at the landing gear to structure connection.

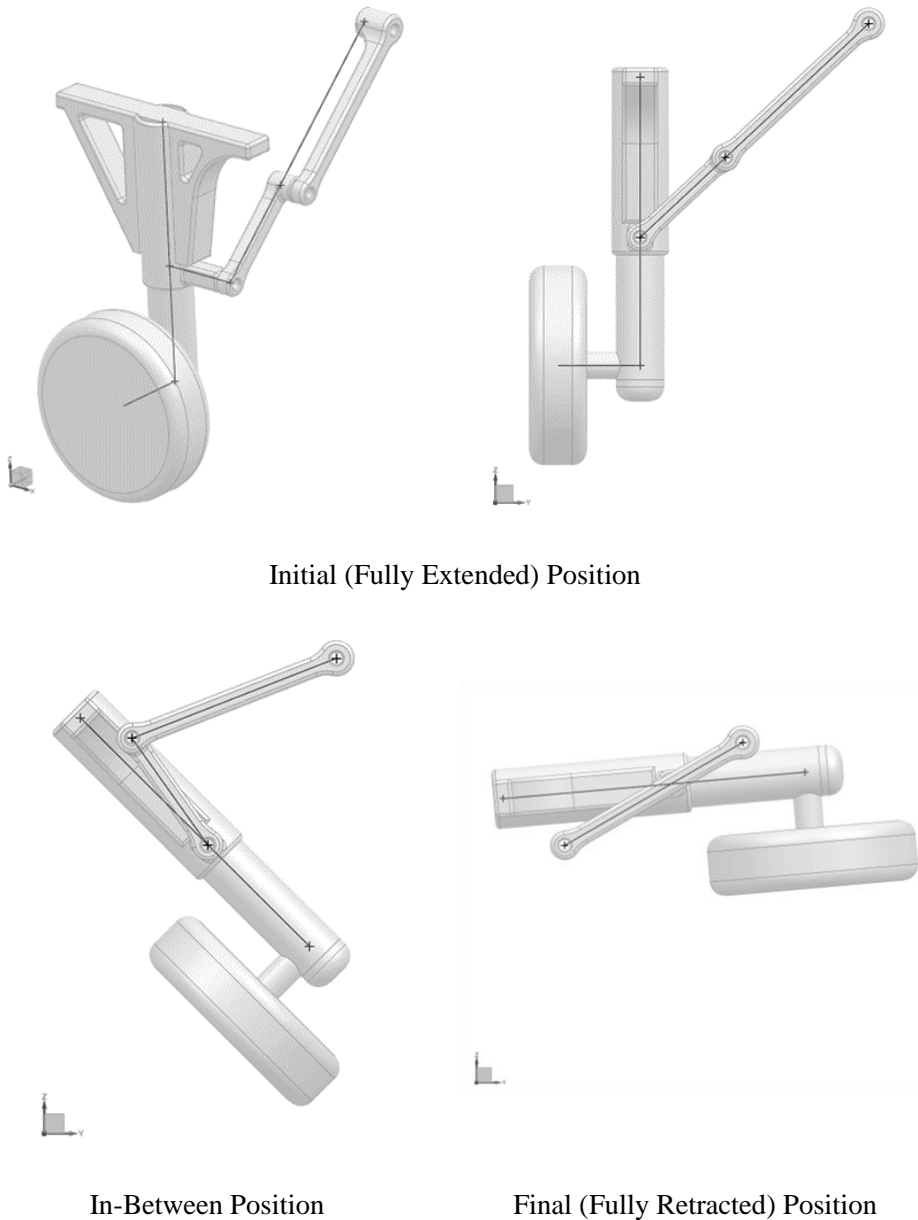


Figure 7.9. RRRR Mechanism Parametric CAD Model for the Synthesis Task with Prescribed Ground Pivots

Due to interference between the coupler link and the trunnion, the right-hand side of the trunnion to structure connection is shortened for the synthesis task with unprescribed ground pivots.

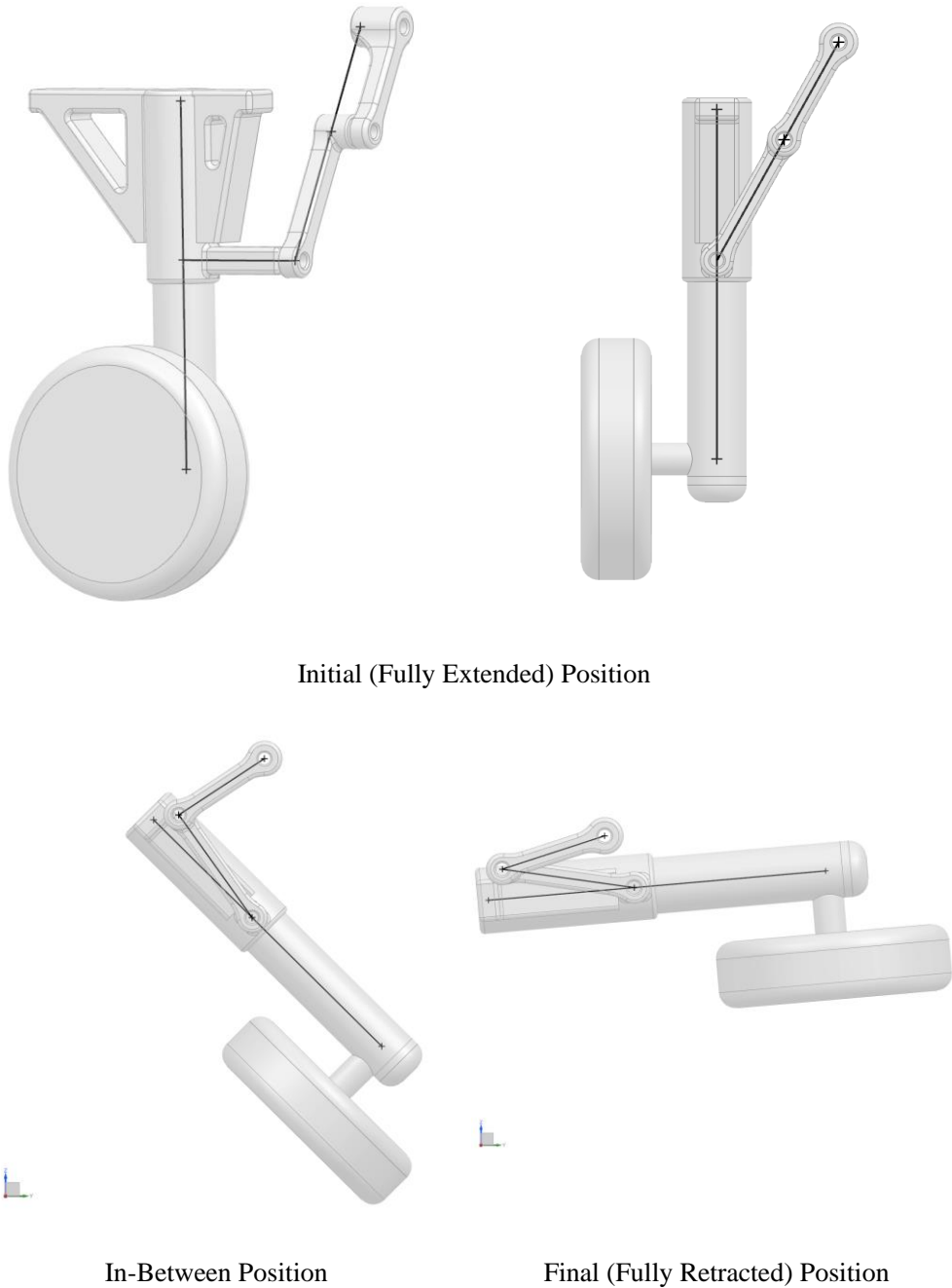


Figure 7.10. RRRR Mechanism Parametric CAD Model for the Synthesis Task with Unprescribed Ground Pivots

7.1.2.1 RRRR Mechanism Synthesis with Prescribed Positions of the Fixed Joints

User interface parameter definitions of the system for the synthesis task with the prescribed positions of the fixed joints are given in Figure 7.11.

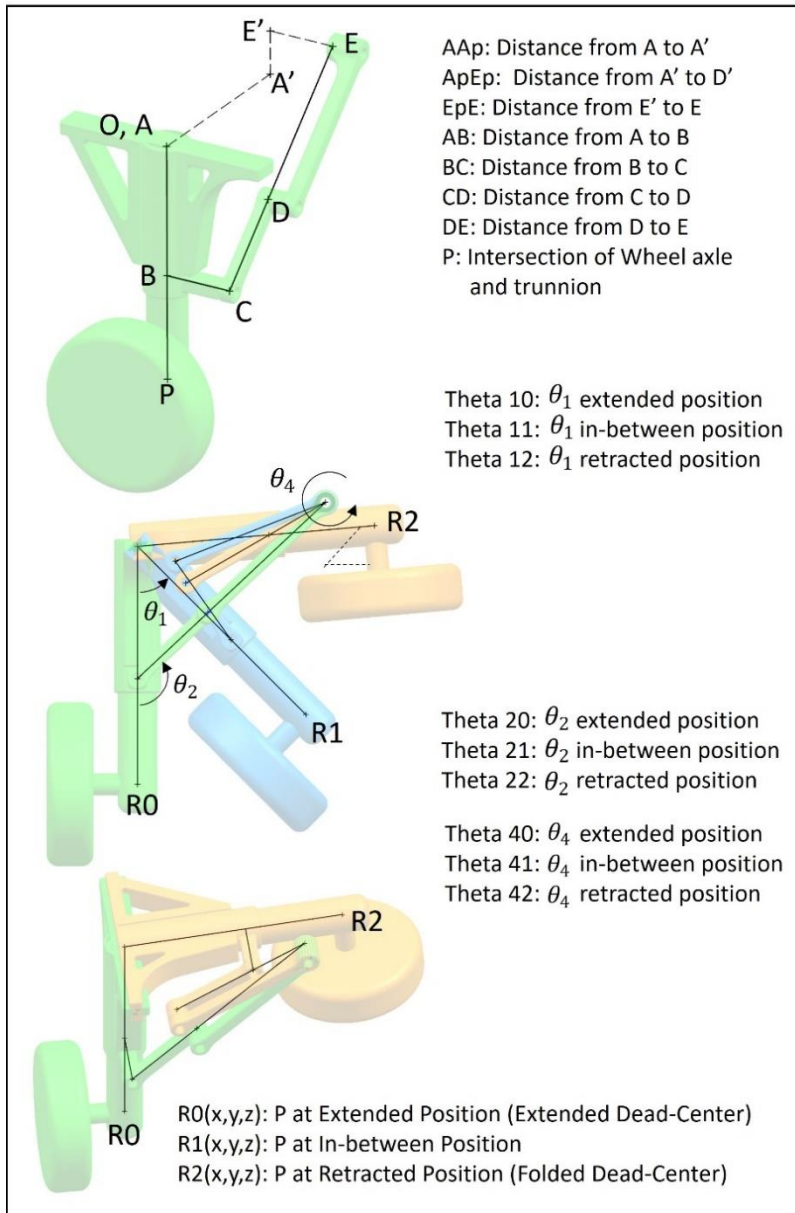


Figure 7.11. Parameter definitions for the RRRR Synthesis Task with Prescribed Ground Pivots

The synthesis task is designed to provide up-locking and down-locking of the system by defining the initial (fully extended) position at the extended dead center and the final (fully retracted) position at the folded dead center. Sample user inputs for the position and link length parameters and relevant solver outputs that are calculated by the program are given in Figure 7.12.

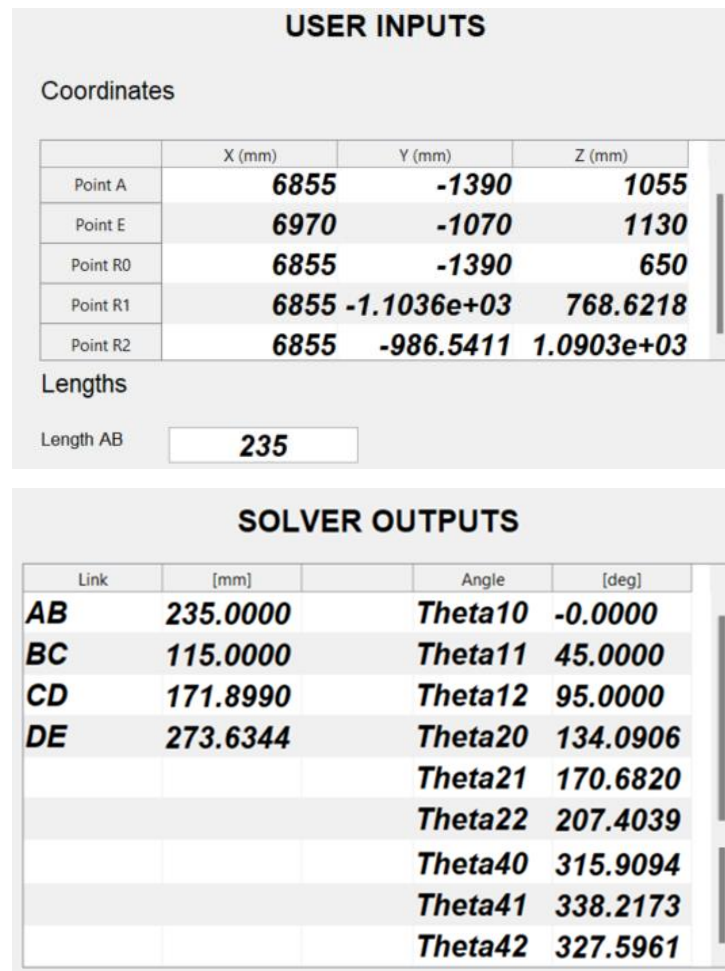


Figure 7.12. User Inputs and Solver Outputs for the RRRR Synthesis Task with Prescribed Ground Pivots

The parameter list from the “.exp” expression file output of the program is given in Figure 7.13. Since they are being used in the CAD model generation, the expression file also stores coordinate values from user inputs.

```
RRRR1_Expressions.exp
Dosya  Düzenle  Görünüm

[mm]R0_x= 6855
[mm]R0_y= -1390
[mm]R0_z= 650
[mm]A_x= 6855
[mm]A_y= -1390
[mm]A_z= 1055
[mm]E_x= 6970
[mm]E_y= -1070
[mm]E_z= 1130
[mm]B0_x= 6855
[mm]B0_y= -1390
[mm]B0_z= 820
[mm]AB= 235
[mm]BC= 115
[mm]DE= 273.63436
[degrees]theta10= 45
[degrees]theta20= 95.00
```

Figure 7.13. Expression File Parameters for the RRRR Synthesis Task with Prescribed Ground Pivots

The resulting CAD model which is simultaneously updated by the NX journal is given in Figure 7.14.

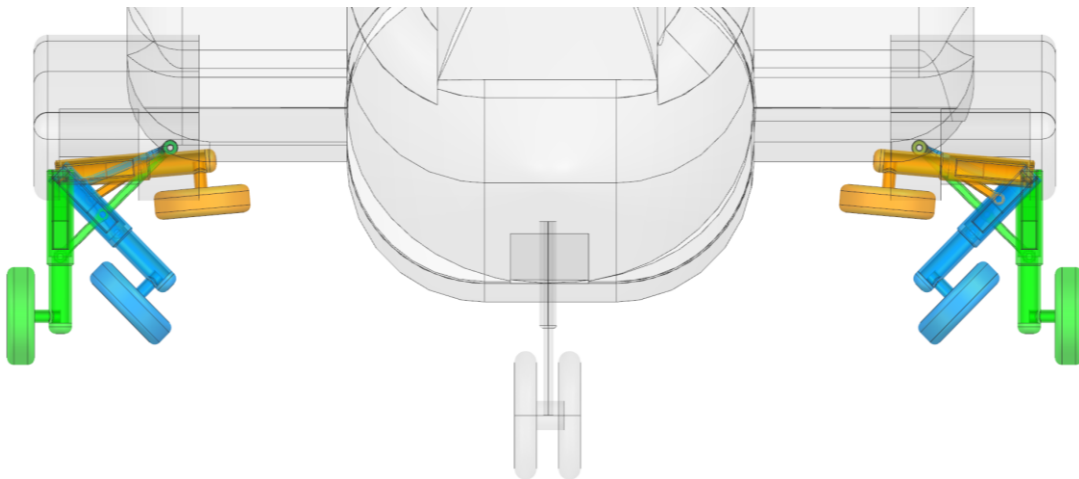


Figure 7.14. Resulting CAD Model at the Three Positions for RRRR Synthesis Task with Prescribed Ground Pivots

7.1.2.2 RRRR Mechanism Synthesis with Unprescribed Positions of the Ground Pivots

The synthesis task with unprescribed ground pivot positions is designed to provide movement between the initial (fully extended) position and the final (fully retracted) position with the minimum change in the transmission angle. Parameter definitions of the system that are provided by the program are given in

Figure 7.15. The parameter names and definitions are the same whereas the landing gear CAD model description is different.

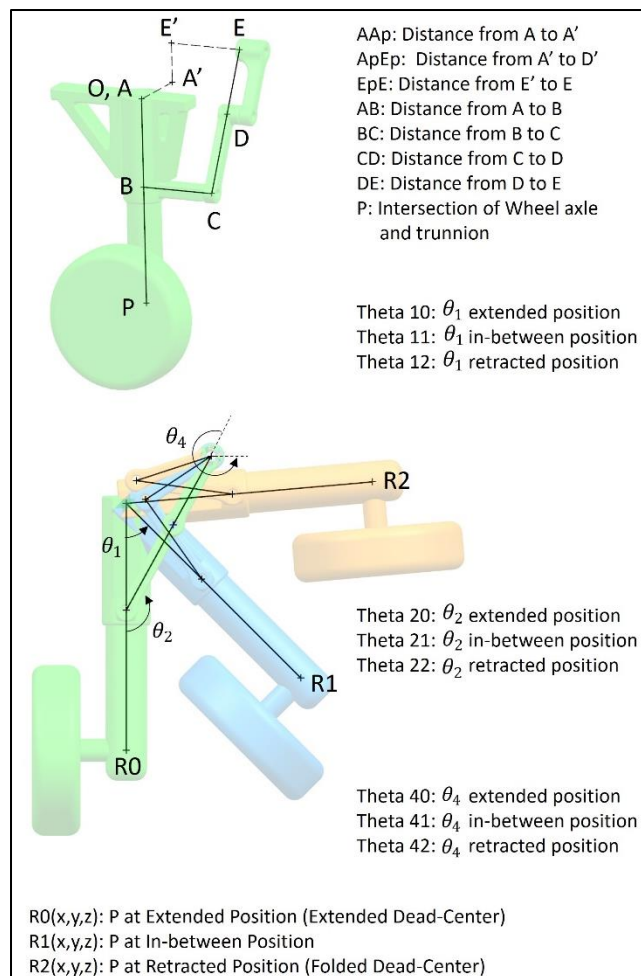


Figure 7.15. Parameter definitions for the RRRR Synthesis Task with Unprescribed Ground Pivots

Sample user inputs for the position and link length parameters and relevant solver outputs that are calculated by the program are given in Figure 7.16

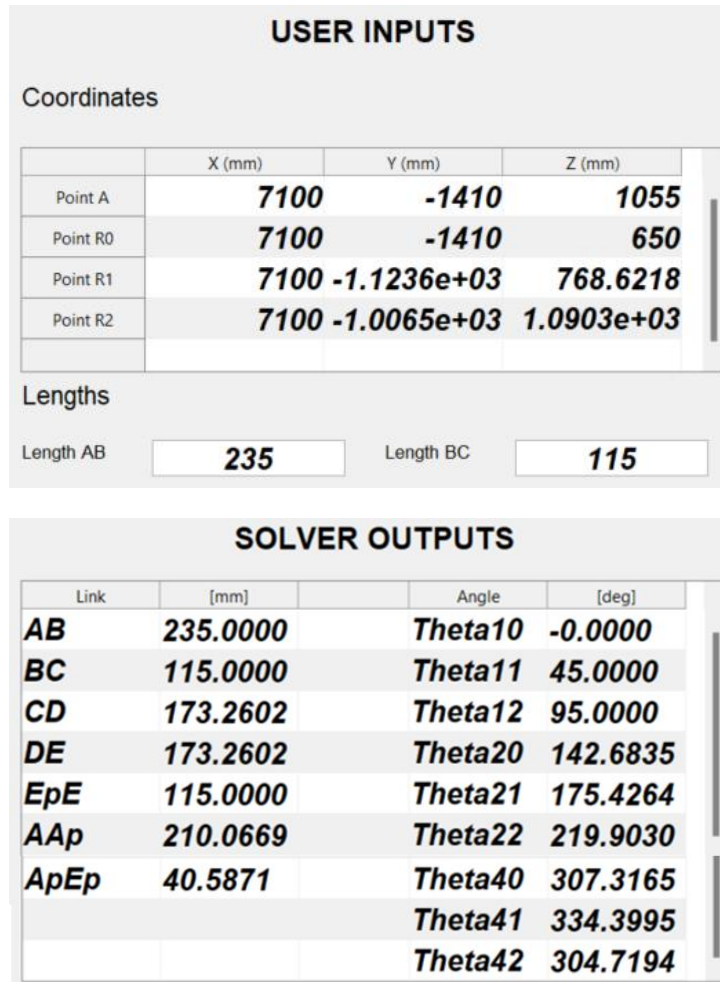


Figure 7.16. User Inputs and Solver Outputs for the RRRR Synthesis Task with Unprescribed Ground Pivots

The code provides “.exp” expression file with following parameters presented in Figure 7.17. The expression file also stores coordinate values from user inputs. Theta10 expression is the difference between θ_1^0 and θ_1^1 whereas Theta20 expression is the difference between θ_1^0 and θ_1^2 . It should be noted that the program minimizes the crank rotation to $\phi = \left(90^\circ + \frac{\theta_1^2 - \theta_1^0}{2} \right)$.

```
RRRR2_Expressions.exp
Dosya  Düzenle  Görünüm

[mm]R0_x= 7100
[mm]R0_y= -1410
[mm]R0_z= 650
[mm]A_x= 7100
[mm]A_y= -1410
[mm]A_z= 1055
[mm]E_x= 7215
[mm]E_y= -1199.9331
[mm]E_z= 1095.5871
[mm]B0_x= 7100
[mm]B0_y= -1410
[mm]B0_z= 820
[mm]AB= 235
[mm]BC= 115
[mm]DE= 173.26018
[degrees]theta10= 45
[degrees]theta20= 95.000
```

Figure 7.17. Expression File Parameters for the RRRR Synthesis Task with Unprescribed Ground Pivots

The resulting model, modified via the journal run from the NX Open developer interface, is given in Figure 7.18.

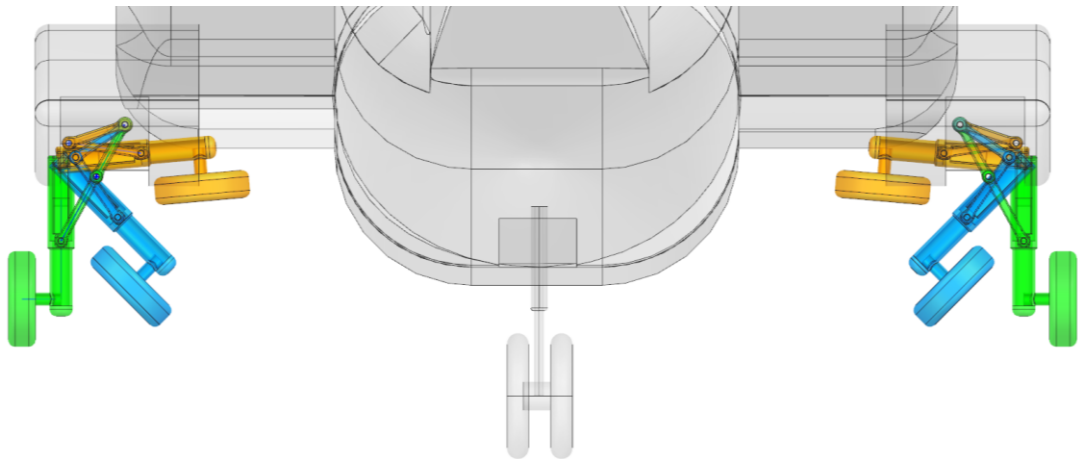


Figure 7.18. Resulting CAD Model at the Three Positions for RRRR Synthesis Task with Unprescribed Ground Pivots

7.1.3 SSRR Mechanism Synthesis Task

For the SSRR mechanism, a stick diagram and parametric CAD model illustrating three distinct configurations are given in Figure 7.19. Throughout the retraction motion, the shock absorber undergoes axial rotation along its own axis.

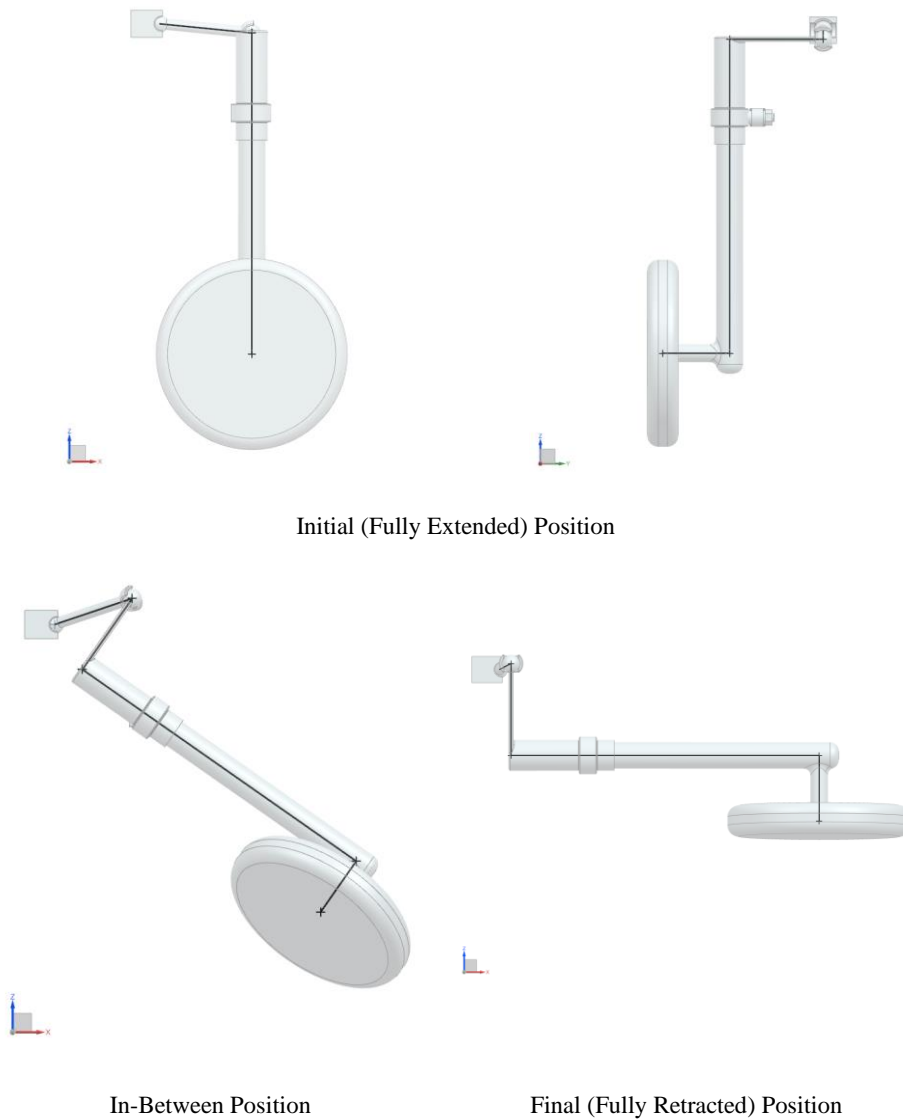


Figure 7.19. SSRR Mechanism Parametric CAD Model

7.1.3.1 SSRR Mechanism Synthesis with Prescribed Positions of the Fixed Joints

When “SSRR – Prescribed Ground Pivots” is selected on the GUI screen, parameter definitions of the system given in Figure 7.20 is provided by the program. Sample user inputs for the position and link length parameters and relevant solver outputs that are calculated by the program are given in Figure 7.21.

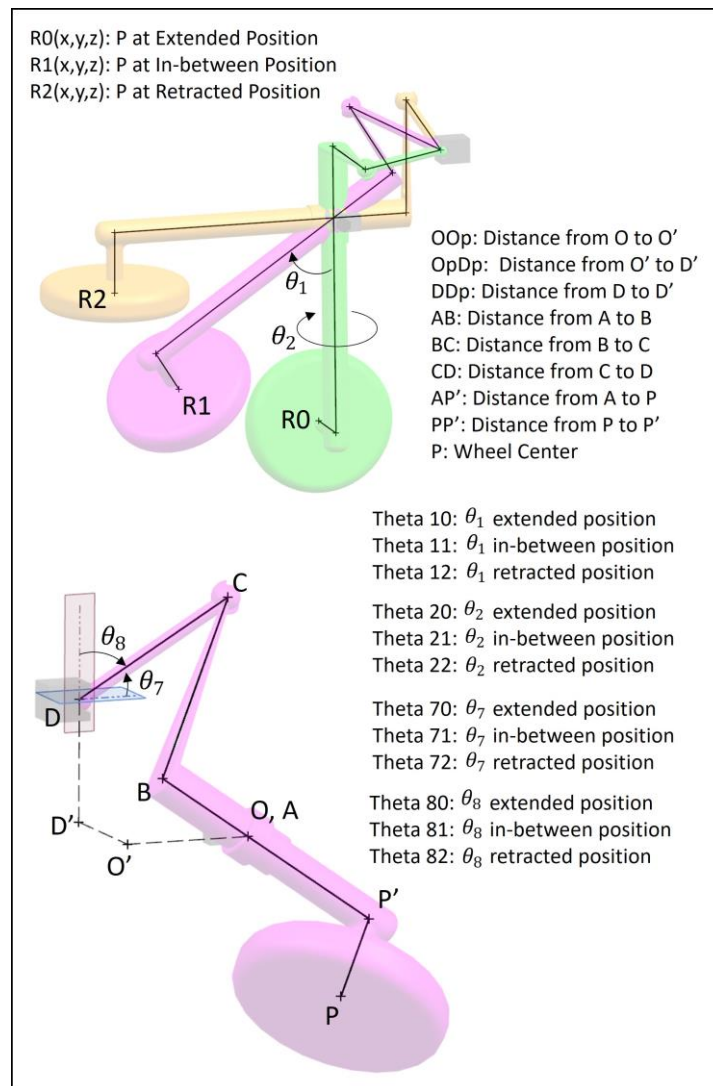


Figure 7.20. Parameter definitions for the SSRR Synthesis Tasks

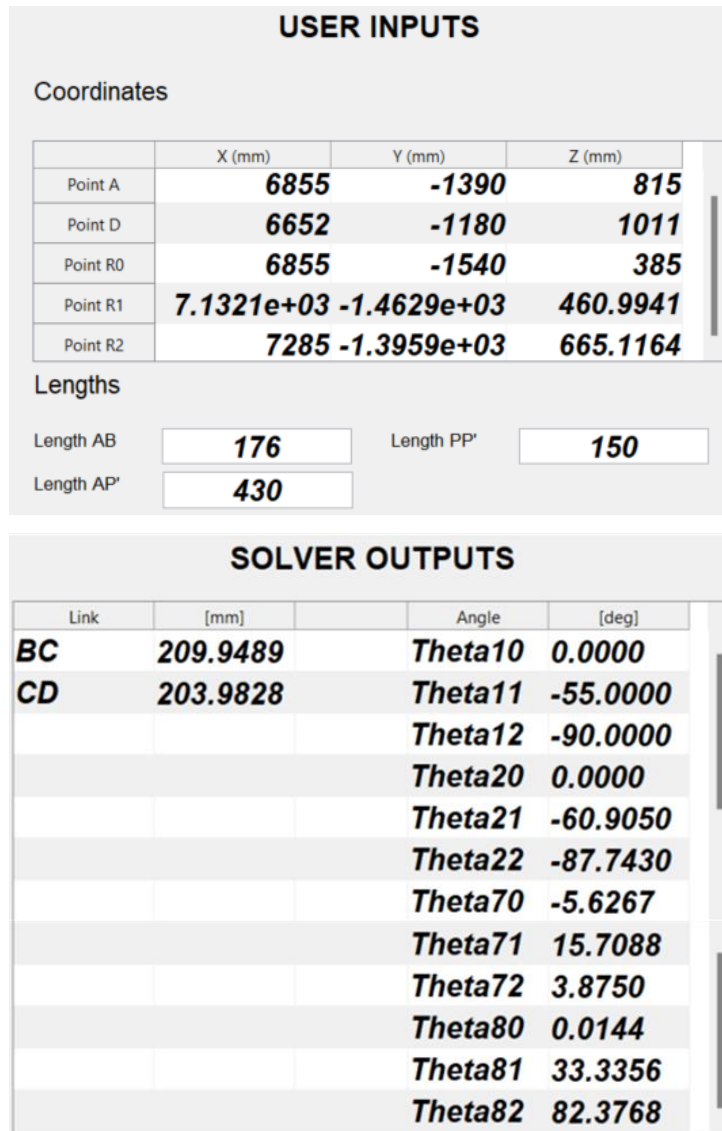


Figure 7.21. User Inputs and Solver Outputs for the SSRR Synthesis Task with Prescribed Ground Pivots

The code provides “.exp” expression file with following parameters presented in Figure 7.22. The expression file also stores coordinate values from user inputs. Parameters regarding the rotation of SS link is not utilized by the NX model. Since the model is an assembly, only the position of point D and the structural lengths of the landing gear ($|AB|$ and $|BC|$) are sufficient for the modeling of the SS link.

```
SSRR1_Expressions.exp
Dosya  Düzenle  Görünüm

[mm]R0_x=6855
[mm]R0_y= -1540
[mm]R0_z= 385
[mm]A_x= 6855
[mm]A_y= -1390
[mm]A_z= 815
[mm]D_x= 6652
[mm]D_y= -1180
[mm]D_z= 1011
[mm]AAp= 430
[mm]PPp= 150
[mm]AB= 176
[mm]BC= 209.94891
[degrees]th10= 0
[degrees]th11=-55.000006
[degrees]th12= -90
[degrees]th20=0
[degrees]th21= -60.904987
[degrees]th22=-87.742994
```

Figure 7.22. Expression File Parameters for the SSRR Synthesis Task with Prescribed Ground Pivots

After the journal run from NX Open developer interface, the resulting CAD model which is updated automatically is presented in Figure 7.23.

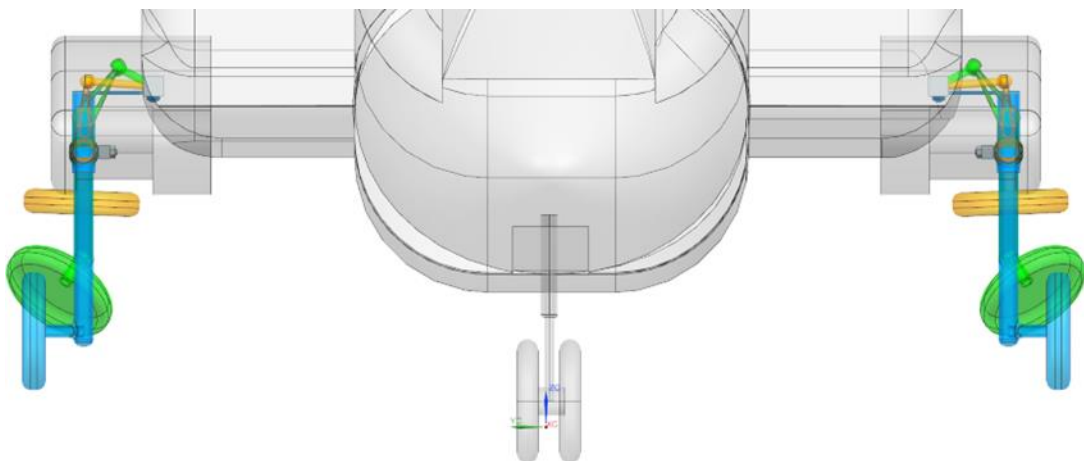


Figure 7.23. Resulting CAD Model at Three Positions for SSRR Synthesis Task with Prescribed Ground Pivots

7.1.3.2 SSRR Mechanism Synthesis with Unprescribed Positions of the Ground Pivots

For the synthesis task with the prescribed positions of the fixed joints, the program provides the same image, Figure 7.20, for the parameter definitions. Sample user inputs for the position and link length parameters and relevant solver outputs that are calculated by the program are given in Figure 7.24.

| USER INPUTS | | | |
|----------------|-------------------|--------------------|-----------------|
| Coordinates | | | |
| | X (mm) | Y (mm) | Z (mm) |
| Point A | 7000 | -1390 | 815 |
| Point R0 | 7000 | -1540 | 385 |
| Point R1 | 7.2771e+03 | -1.4629e+03 | 460.9941 |
| Point R2 | 7430 | -1.3959e+03 | 665.1164 |
| Lengths | | | |
| Length AB | 176 | Length AP' | 430 |
| Length BC | 210 | Length PP' | 150 |
| Length O'D' | 203 | | |
| SOLVER OUTPUTS | | | |
| Link | [mm] | Angle | [deg] |
| OpDp | 203.0000 | Theta10 | 0.0000 |
| OOp | 209.9896 | Theta11 | -55.0000 |
| DDp | 196.0322 | Theta12 | -90.0000 |
| CD1 | 203.9860 | Theta20 | 0.0000 |
| CD2 | 203.9860 | Theta21 | -60.9050 |
| CD3 | 203.9860 | Theta22 | -87.7430 |
| | | Theta70 | -5.6357 |
| | | Theta71 | 15.7099 |
| | | Theta72 | 3.8805 |
| | | Theta80 | -0.0029 |
| | | Theta81 | 33.3229 |
| | | Theta82 | 82.3763 |

Figure 7.24. User Inputs and Solver Outputs for the SSRR Synthesis Task with Unprescribed Ground Pivots

The code provides “.exp” expression file with following parameters given in Figure 7.25. The expression file also stores coordinate values from user inputs. It should be noted that the lateral position of point D is utilized as a free parameter. Therefore, several iterations may be performed by changing the initial value of $|O'D'|$ to obtain different link lengths.

```

[mm]R0_x=7000
[mm]R0_y= -1540
[mm]R0_z= 385
[mm]A_x= 7000
[mm]A_y= -1390
[mm]A_z= 815
[mm]D_x= 6797
[mm]D_y= -1180.0104
[mm]D_z= 1011.0322
[mm]AAP= 430

[mm]PPp= 150
[mm]AB= 176
[mm]BC= 210
[degrees]th10= 0
[degrees]th11=-55.000006
[degrees]th12= -90
[degrees]th20=0
[degrees]th21= -60.904987
[degrees]th22=-87.742994

```

Figure 7.25. Expression File Parameters for the SSRR Synthesis Task with Prescribed Ground Pivots

After the journal is run from NX Open developer interface, the resulting model which is updated automatically is given in Figure 7.26.

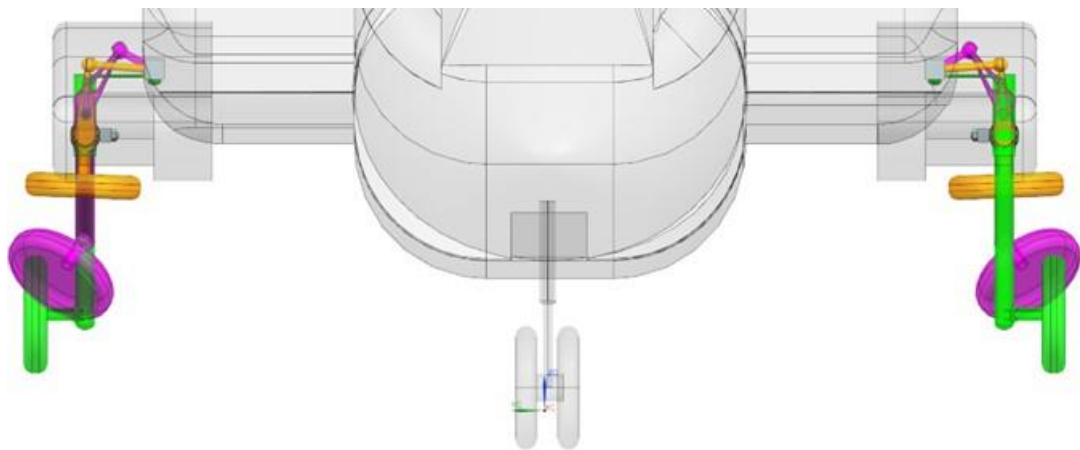


Figure 7.26. Resulting CAD Model at Three Positions for SSRR Synthesis Task with Unprescribed Ground Pivots, Front View

7.2 Model Verification Test Case: SSRR Mechanism Synthesis with Prescribed Positions of the Fixed Joints

In order to verify the GUI solver results presented in section 7.1.3.1, the resulting CAD model is opened in NX Motion, and the motion bodies are defined as highlighted in Figure 7.27.

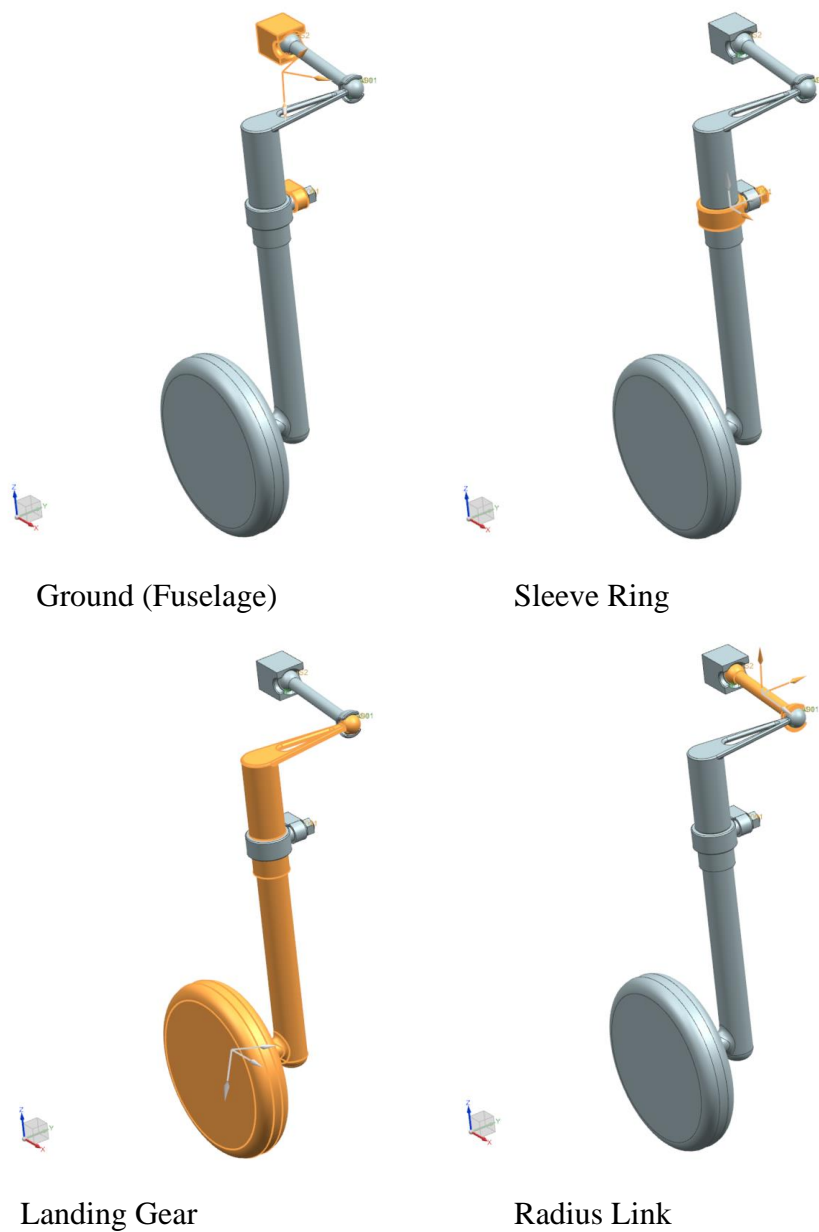


Figure 7.27. NX Motion Model, Motion Body Definitions

After the joint definitions are completed, the model is solved using the “Kinematics / Dynamics” analysis type. The mechanism is moved between the initial position of $\theta_1^0 = 0^\circ$ and the final position of $\theta_1^2 = 90^\circ$. The motion envelope model generated by NX Motion is presented in Figure 7.28.

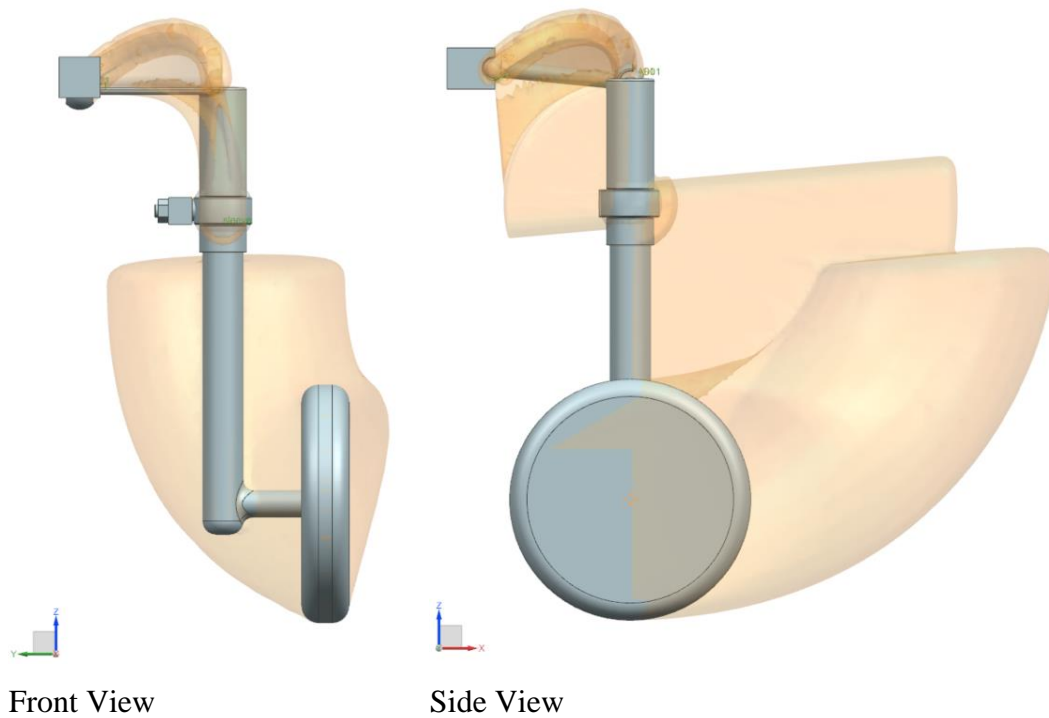


Figure 7.28. Swept Volume (Motion Envelope) Generated by NX Motion

To define the motion of the landing gear between the initial and final positions of the mechanism, the revolute joint between the ground and the sleeve ring is used as the driver. Therefore, θ_1 is taken as the input angle. The angular values of θ_2 , θ_7 and θ_8 are determined by using markers attached to each motion body, and sensors are placed between these markers to measure relative angular displacements. The sensor readings indicating change of θ_2 , θ_7 and θ_8 with respect to θ_1 for the entire motion are presented in Figure 7.29, Figure 7.30, and Figure 7.31 respectively.

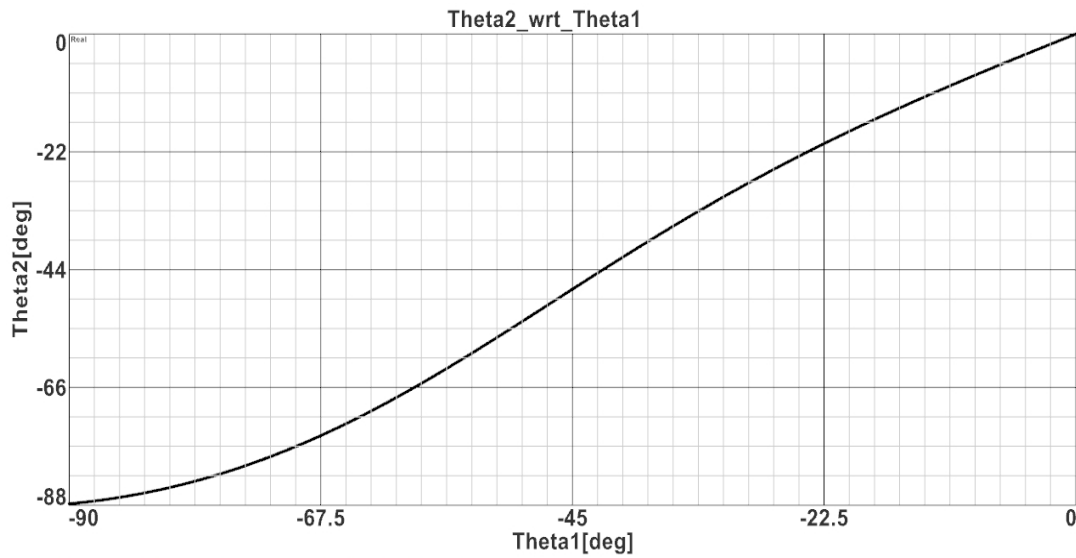


Figure 7.29. θ_2 with respect to θ_1 Graph, Plotted by NX Motion XY Result View

When compared with the values presented in Figure 7.21, the NX Motion sensor outputs of $\theta_2^0 = 0^\circ$, $\theta_2^1 = -61.0117^\circ$ and $\theta_2^2 = -87.6202^\circ$ are in accordance with the GUI solver results, with up to 0.3772° of difference.

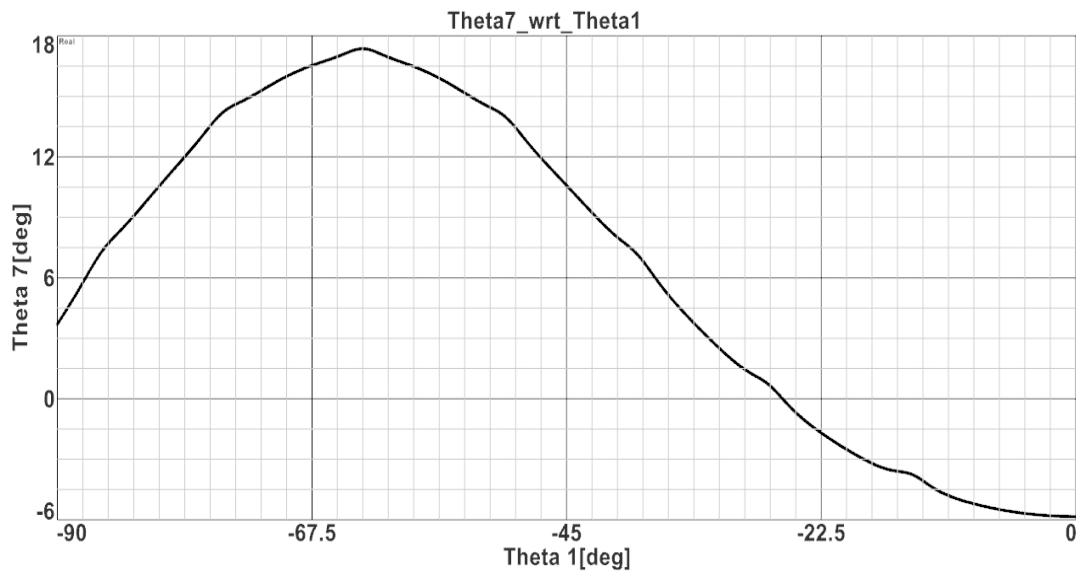


Figure 7.30. θ_7 with respect to θ_1 Graph, Plotted by NX Motion XY Result View

In comparison to the values presented in Figure 7.21, the NX Motion sensor outputs of $\theta_7^0 = -5.6452^\circ$, $\theta_7^1 = 15.6754^\circ$ and $\theta_7^2 = 3.8187^\circ$ are similar to the GUI solver results, with up to 0.0934° of difference.

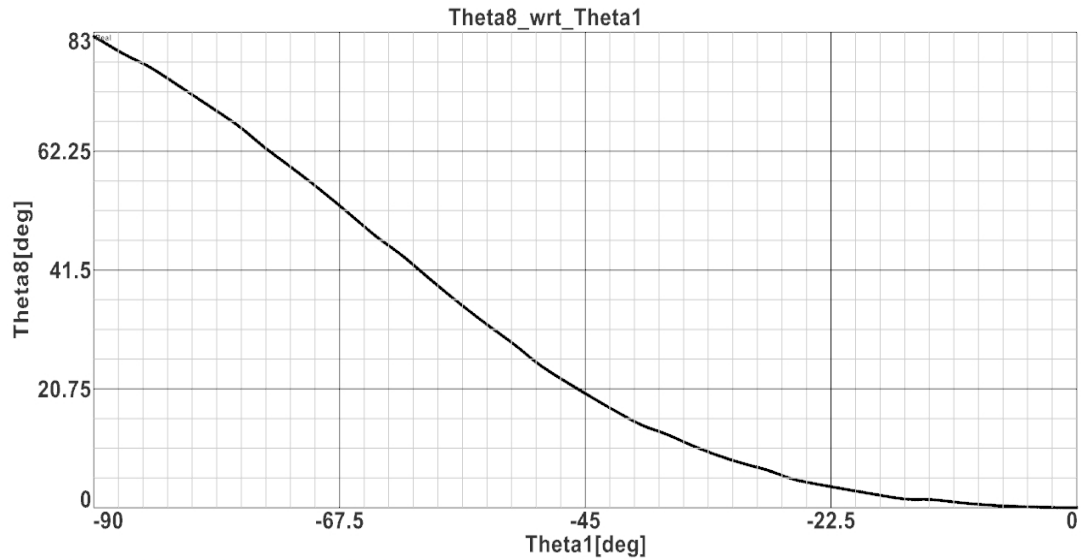


Figure 7.31. θ_8 with respect to θ_1 Graph, Plotted by NX Motion XY Result View

When compared with the values presented in Figure 7.21, the NX Motion sensor outputs of $\theta_8^0 = 0.0146^\circ$, $\theta_8^1 = 33.5243^\circ$ and $\theta_8^2 = 82.7612^\circ$ are slightly deviated from the GUI solver results, with up to 0.3844° of difference.

Based on the calculated angular outputs of the GUI and NX Motion analyses results, it can be stated that the user interface solver provides reliable values to the user. Since the GUI-estimated link lengths are directly being used as NX CAD model inputs, no comparison of link lengths is necessary.

7.3 Discussion on Free Parameter Choices

The primary step of this study was to derive a set of equations for the kinematic synthesis of the planar and spatial mechanisms employing the D-H convention and the exponential matrices. While the goal has been achieved, it is noteworthy that several joint variables and link parameters have been treated as free parameters to facilitate the synthesis tasks. Some of these parameters are structural design restrictions regarding the second ground joint that originate from the fuselage design. Another set of free parameters, s_3^0 and s_3^2 is dependent on the product catalogs. However, most of the free parameters are up to the design of the landing gear itself. A brief classification of the free parameters for three-position synthesis of the retraction mechanisms is provided in Table 7.2.

Table 7.2 Free Parameter Classification for the Three-Position Synthesis

| Linkage Type | Synthesis Task with | Fuselage Parameters | LG Design Parameters | Free Choices for the User |
|---------------------|-------------------------------------|----------------------------|-------------------------------|----------------------------------|
| RRPR (planar) | Prescribed Ground Joint Positions | $ AA' , A'D' , D'D $ | $ AP , R_0, R_1, R_2$ | $ AB $ |
| | Unprescribed Ground Joint Positions | N/A | $ AP , R_0, R_1, R_2$ | $s_3^0, s_3^2, AB , BC $ |
| RRRR (planar) | Prescribed Ground Joint Positions | $ AA' , A'E' , E'E $ | $ AP , R_0, R_1, R_2$ | $ AB $ |
| | Unprescribed Ground Joint Positions | N/A | $ AP , R_0, R_1, R_2$ | $ AB , BC $ |
| SSRR (spatial) | Prescribed Ground Joint Positions | $ OO' , O'D' , D'D $ | $ AP' , PP' , R_0, R_1, R_2$ | $ AB $ |
| | Unprescribed Ground Joint Positions | $ O'D' $ | $ AP' , PP' , R_0, R_1, R_2$ | $ AB , BC $ |

CHAPTER 8

CONCLUSION

The principal objective of this study was to develop a computer program that performs landing gear retraction four-link mechanism synthesis, which provides a ready-to-use tool for the landing gear system designers. The program allows users to easily conduct multiple design iterations, resulting in a reduction in the time and effort required during the conceptual design phase of projects.

Since planar four-link mechanisms are being dominantly utilized for most of the retraction tasks, RRPR and RRRR mechanisms are selected as the linkage types to be used on the program. Nonetheless, there are instances where a single-axis retraction may be insufficient to accommodate the retracted configuration of the landing gear within the designated stowage volume. In such scenarios, the rotation of the shock absorber around its axis is introduced to the system as a secondary motion by using SSRR linkages. During this process, the capability of state-of-the-art planar mechanism synthesis programs is enhanced by extending the system into three-dimensional space.

The necessary path generation synthesis equations are derived by using D-H convention and exponential rotation matrices for the positional loop closure equations and geometrical constraint equations written for several positions of the mechanism. Even though it is cumbersome to use this approach for the planar systems, exponential rotation matrices, together with the D-H convention, are preferred for all synthesis tasks to effectively incorporate joint offsets within the kinematic synthesis procedure. The derived set of equations for the kinematic synthesis of both planar and spatial mechanisms are transformed into individual

functions for each synthesis task. Using these functions, a user interface is constructed within the MATLAB R2019a environment.

The computer program successfully provides expression files as outputs of the synthesis process. These expression files are called into the NX Open journal files to autonomously update the master geometry models, referred to as “stick diagrams” of the 3D CAD models of the landing gear. For each synthesis task, an individual CAD model on NX, which undergoes automatic updates without any additional user intervention. Each CAD model is managed by its dedicated NX journal. Upon the execution of the journal, a simplified helicopter-level assembly model that encompasses multiple instances of retracting motion for both MLGs is initiated and systematically updated. For each synthesis task, the resulting link and position parameters are compared with the direct measurements on the NX models. It is seen that the GUI outputs are consistent with the CAD models for all cases.

The computer software, integrated with Siemens NX, enables users to visualize the resulting mechanism and evaluate its design and manufacturability aspects effectively.

The given CAD models include solely the retraction of the main landing gear; however, they can easily be used to retract the nose landing gears. The major difference between the two systems is the axis of the axle and wheel centers. When the axles of the parametric landing gear models are rotated 90° , they essentially transform into configurations suitable for the nose landing gear. The guided user interface is ready-to-use for the nose landing gears with no modification.

Each selected mechanism type incorporates its own limitations. For the RRPR mechanism, if the actuator link does not provide enough clearance for the overtravel, the actuator may bottom out, resulting in damage to or complete separation of the actuator. Therefore, overtravel length must be checked after the determination of minimum and maximum strokes. Conversely, with the RRRR mechanism, the mechanism is always at its dead-center at its initial position. To ensure that the coupler link initiates its motion in the desired direction, guiding elements such as

preloaded springs must be introduced into the system. For the SSRR mechanism, it is essential to consider the angular mobility limits mechanism, which imposes constraints on the design options.

The original goal was to execute the entire system as a single-step process; however, the user interface lacks the capability to operate the NX CAD models automatically. To perform updates on the CAD models, the journal file must be executed individually within the NX environment. To combine this two-step process into a unified one-step approach, software redevelopment can be pursued utilizing the Python programming language. Furthermore, it is also noted that the free parameter choices outlined for the user in Table 7.2 provide an opportunity to perform consecutive runs on the program to obtain optimal design solutions.

REFERENCES

- [1] J. Roskam, “Airplane Design, Part IV:Layout design of landing gear,” *DAR Corp.*, pp. 303–370, 1989.
- [2] R. K. Schmidt, *The Design of Aircraft Landing Gear*. 2021.
- [3] H. G. Conway, “The Kinematics of Undercarriage Retraction,” *J. R. Aeronaut. Soc.*, vol. 52, no. 446, pp. 125–137, 1948, doi: 10.1017/s0001924000097001.
- [4] A. Svboda, *Computing Mechanisms and Linkages*, 1st Editio. New York, N.Y.,: McGraw-Hill Book Company, Inc., 1948.
- [5] J. H. Allen Strickland, *Kinematics and Linkage Design*. Englewood Cliffs: Prentice-Hall, INC, 1961.
- [6] Ferdinand Freudenstein, “Design of Four-link Mechanisms,” Columbia University, 1954.
- [7] Ferdinand Freudenstein, “Approximate Synthesis of Four Bar Linkages,” *Mech. Eng.*, vol. Vol.76, no. December, 1954.
- [8] S. Mather and A. Erdman, “Reformulation of Theories of Kinematic Synthesis for Planar Dyads and Triads,” *Robotics*, vol. 12, no. 1, p. 22, Feb. 2023, doi: 10.3390/robotics12010022.
- [9] K. Erener, “Developing A Four-Bar Mechanism Synthesis Program in CAD Environment,” 2011.
- [10] Q. J. Zhao, P.; Ge, X.; Zi, B.; Ge, “Planar linkage synthesis for mixed exact and approximated motion realization via kinematic mapping,” *J. Mech. Robot.*, vol. 8, 2016.
- [11] M. Polat, “Computer Aided Synthesis of Planar Mechanisms,” Middle East Technical University, 1985.

- [12] S. Sezen, “Development Of An Interactive Visual Planar Mechanism Synthesis And Analysis Program By Using Delphi Object Oriented Programming Environment,” Middle East Technical University, 2001.
- [13] E. Demir, “Kinematic Design of Mechanism In a Computer Aided Design Environment,” Middle East Technical University, 2005.
- [14] C. H. Suh and C. W. Radcliffe, *Kinematics and Mechanism Design*. New York, NY: Wiley, 1978.
- [15] C. H. Suh, “Design of space mechanisms for function generation,” *J. Manuf. Sci. Eng. Trans. ASME*, vol. 90, no. 3, pp. 507–512, 1968, doi: 10.1115/1.3604678.
- [16] K. Russell and R. S. Sodhi, “Kinematic synthesis of RRSS mechanisms for multi-phase motion generation with tolerances,” *Mech. Mach. Theory*, vol. 37, no. 3, pp. 279–294, 2002, doi: 10.1016/S0094-114X(01)00064-7.
- [17] K. Russell and R. S. Sodhi, “Kinematic synthesis of adjustable RRSS mechanisms for multi-phase motion generation,” *Mech. Mach. Theory*, vol. 36, no. 8, pp. 939–952, Aug. 2001, doi: 10.1016/S0094-114X(01)00028-3.
- [18] K. W. Lee and Y. S. Yoon, “Kinematic Synthesis of RRSS Spatial Motion Generators using Euler Parameters and Quaternion Algebra,” *Proc. Inst. Mech. Eng. Part C J. Mech. Eng. Sci.*, vol. 207, no. 5, pp. 355–359, 1993, doi: 10.1243/PIME_PROC_1993_207_139_02.
- [19] M. Rotzoll, M. H. Regan, M. L. Husty, and M. J. D. Hayes, “Kinematic geometry of spatial RSSR mechanisms,” *Mech. Mach. Theory*, vol. 185, pp. 1–24, 2023, doi: 10.1016/j.mechmachtheory.2023.105335.
- [20] Siemens, “Getting Started with NX Open,” no. February, pp. 1–4, 2016, [Online]. Available: https://docs.plm.automation.siemens.com/data_services/resources/nx/11/nx_api/common/en_US/graphics/fileLibrary/nx/nxopen/nxopen_getting_started_v11.pdf.

- [21] E. Söylemez, *Mechanisms*, 4th ed. METU Publ., 2013.
- [22] S. M. Wharton and Y. P. Singh, “Development of Solid Models and Multimedia Presentations of Kinematic Pairs,” in *ASEE Annual Conference Proceedings*, 2001, pp. 6.381.1-6.381.12, doi: 10.18260/1-2--9134.
- [23] M. K. Ozgoren, *Kinematics of General Spatial Mechanical Systems*. Wiley, 2020.
- [24] F. Soltani, “Kinematic Synthesis of Spatial Mechanisms Using Algebra of Exponential Rotation Matrices,” Middle East Technical University, 2005.
- [25] B. Ren, S. S. Ge, C. Chen, C.-H. Fua, and T. H. Lee, *Modeling, Control and Coordination of Helicopter Systems*. New York, NY: Springer, 2012.
- [26] N. S. Currey, “Aircraft Landing Gear Design: Principles and Practices,” *Aircr. Land. Gear Des. Princ. Pract.*, 1988, doi: 10.2514/4.861468.
- [27] “Landing Gear Structures and Mechanisms,” *Aerosp. Recomm. Pract.*, no. ARP13211 Rev D, 2018.
- [28] H. Su, C. L. Collins, and J. M. McCarthy, “Classification of RRSS linkages,” *Mech. Mach. Theory*, vol. 37, no. 11, pp. 1413–1433, 2002, doi: 10.1016/S0094-114X(02)00060-5.

APPENDICES

NX Journal for Expression Integration on CAD Model

```
' NX 1855
```

```
Imports System
```

```
Imports NXOpen
```

```
Module NXJournal
```

```
Sub Main (ByVal args() As String)
```

```
Dim theSession As NXOpen.Session = NXOpen.Session.GetSession()
```

```
'-----' Menu: File->Open...'
```

```
theSession.Parts.LoadOptions.UsePartialLoading = False
```

```
Dim basePart1 As NXOpen.BasePart
```

```
Dim partLoadStatus1 As NXOpen.PartLoadStatus
```

```
basePart1 = theSession.Parts.OpenBaseDisplay("PARTLOCATION  
\PARTNAME.prt ", partLoadStatus1)
```

```
Dim workPart As NXOpen.Part = theSession.Parts.Work
```

```
Dim displayPart As NXOpen.Part = theSession.Parts.Display
```

```
partLoadStatus1.Dispose()
```

```
Dim markId1 As NXOpen.Session.UndoMarkId
```

```
markId1 = theSession.SetUndoMark(NXOpen.Session.MarkVisibility.Visible,  
"Enter Gateway")
```

```
Dim markId2 As NXOpen.Session.UndoMarkId
```

```

markId2 = theSession.SetUndoMark(NXOpen.Session.MarkVisibility.Visible,
"Enter Modeling")

'-----' Menu: Tools->Expressions...'-----

theSession.Preferences.Modeling.UpdatePending = False

Dim expressionGroups1() As NXOpen.ExpressionGroup
expressionGroups1 =
workPart.ExpressionGroups.GetAllExpressionGroupsInPart()

Dim expressionGroup1 As NXOpen.ExpressionGroup
expressionGroup1 = workPart.ExpressionGroups.Active

Dim expressionGroups2() As NXOpen.ExpressionGroup
expressionGroups2 = expressionGroup1.GetMemberGroups()

Dim expressionGroup2 As NXOpen.ExpressionGroup
expressionGroup2 = workPart.ExpressionGroups.Active
workPart.ExpressionGroups.Active = expressionGroup2

Dim expModified1 As Boolean = Nothing

Dim errorMessages1() As String

workPart.Expressions.ImportFromFile(FILELOCATION \FILENAME.exp,
NXOpen.ExpressionCollection.ImportMode.Replace, expModified1,
errorMessages1)

theSession.Preferences.Modeling.UpdatePending = False

Dim markId3 As NXOpen.Session.UndoMarkId

markId3 = theSession.SetUndoMark(NXOpen.Session.MarkVisibility.Invisible,
"Update Expression Data")

```



```
Dim nErrs1 As Integer

nErrs1 = theSession.UpdateManager.DoUpdate(markId3)

theSession.DeleteUndoMark(markId3, "Update Expression Data")

'-----' Menu: File->Open...'-----

theSession.Parts.LoadOptions.UsePartialLoading = False

Dim basePart2 As NXOpen.BasePart

Dim partLoadStatus2 As NXOpen.PartLoadStatus

basePart2 = theSession.Parts.OpenBaseDisplay("PARTLOCATION
\PARTNAME.prt", partLoadStatus2)

End Sub

End Module
```